The RNA-binding protein NANOS2 is required to maintain murine spermatogonial stem cells

Aiko Sada

DOCTOR OF PHYLOSOPHY

Department of Genetics

School of Life Science

The Graduate University for Advised Studies

2010

Contents

【Abstract】

Spermatogonial stem cells represent a stem cell population in adult testes, and their biological activities provide a base of continuous production of spermatozoa. The stem cell function resides in undifferentiated spermatogonia, consisting of types A_{single}, A_{paired} and $A_{aligned}$. These cells transform into type A_1 differentiating spermatogonia, which subsequently undergo six mitotic and two meiotic divisions to form haploid spermatozoa within 35 days. The entire developmental process from spermatogonia to spermatozoa occurs within seminiferous tubules of testes. In the tubules, all types of spermatogonia are located on the basement membrane, and the subsequent differentiating cell types are arranged in a sequential order towards the lumen. The spermatogenesis is also supported by close interaction of the germ cells with somatic Sertoli cells.

Currently, several factors have been implicated in the regulation of spermatogonial stem cells. For example, a growth factor GDNF (glial cell-line derived neurotrophic factor) is secreted by Sertoli cells and acts as one of the major niche signals for spermatogonial stem cells. A transcription factor PLZF (promyelocytic leukemia zinc finger) is needed in a cell autonomous fashion for the maintenance of the spermatogonial stem cells, since male mice lacking *Plzf* expression exhibit progressive germ cell loss and testis atrophy with age, causing infertility. However, the previous loss of function studies had some limitations in terms of understanding the mechanisms by which stem cells are lost upon the gene deletion, as it could be caused by cell death, a defective proliferation, a premature differentiation, or other mechanisms.

A precise identification of stem cells is another important issue in stem cell biology. According to "A_{single} model", A_{single} spermatogonia represent spermatogonial stem

cells: this type is recognized as single cells without any intercellular connection with others, whereas A_{paired} and $A_{aligned}$ spermatogonia are connected by intercellular cytoplasmic bridges and committed to differentiation. However, the stem cell activity of the A_{single} spermatogonia has not been tested due to a lack of their specific molecular markers.

NANOS, a zinc-finger RNA-binding protein, has been proposed as an evolutionarily conserved factor for germline cell function. Among three NANOS homologs in mice, NANOS2 is essential for the male-type differentiation of embryonic germ cells. In adult testes, NANOS2 is predominantly expressed in the A_{single} and A_{paired} spermatogonia, suggesting that NANOS2 may also be involved in the spermatogonial stem cell function. However, the postnatal function of NANOS2 has not been studied, because the majority of *Nanos2*-null male germ cells undergo apoptosis before birth.

In the first part of my doctoral thesis, I report my findings indicating that the RNA-binding protein NANOS2 is a key regulator for the maintenance of spermatogonial stem cells. First, by lineage-tracing analyses, I revealed that undifferentiated spermatogonia expressing *Nanos2* retained abilities to self-renew and generate the entire spermatogenic cell lineage. Hence, such spermatogonia can be referred to as spermatogonial stem cells. Next, I addressed if NANOS2 plays a role in these stem cells by using a conditional gene knockout system. I showed that conditional disruption of postnatal *Nanos2* led to depletion of spermatogonial stem cell reserves and resulted in the complete depletion of germ cells within a few cycles of spermatogenesis. These results indicate that NANOS2 is expressed in spermatogonial stem cells and is required for the maintenance of these cells.

The current view of the regulation of stem cell state or “stemness” depicts

following cellular processes: (1) cell proliferation to expand stem cell population; (2) maintenance of the undifferentiated state; and (3) cell death/survival. NANOS2 should control these events for maintaining the proper state of spermatogonial stem cells. To further determine the role of NANOS2 in the stem cell maintenance, I generated transgenic mice, which allowed continuous expression of NANOS2 in germ cell lineages. I found that mouse testes in which *Nanos2* had been overexpressed accumulated spermatogonia with undifferentiated, stem cell-like properties. Furthermore, these *Nanos2*-overexpressing cells showed lower proliferation rates and similar levels of apoptosis compared to the control spermatogonia. These results indicate that NANOS2 maintains spermatogonial stem cells by suppressing proliferation and differentiation of these cells.

Studies in diverse stem cell systems indicate that the stem cell regulations are dependent on not only stem cell-intrinsic factors but also extrinsic signals from the microenvironment known as niche signals. However, it remains unclear how extrinsic signals and intrinsic stem cell factors intersect in stem cells to control their cellular state. During murine spermatogenesis, GDNF signals from Sertoli cells and germ cell-intrinsic factor NANOS2 represent key regulators for the maintenance of spermatogonial stem cells. In the second part of my thesis, I examined the possible genetic interaction between NANOS2 and GDNF signal transduction pathway.

First, I conducted conditional knockout of *Gfra1*, a receptor for GDNF, to decipher roles of the GDNF signaling during adult spermatogenesis. The absence of *Gfra1* resulted in rapid loss of spermatogonial stem cells, which might result from deficits in proliferation and/or in the maintenance of undifferentiated state. Next, I asked whether the overexpression of *Nanos2* could negate the stem cell loss phenotype caused by the

Gfra1-deletion. I found that overexpressed *Nanos2* could not support *Gfra1*-mutant stem cells permanently, because proliferation of spermatogonial stem cells was severely impaired by the lack of GDNF signaling. This result indicates that stem cell proliferation is highly dependent on the GDNF-stimulated pathway.

On the other hand, NANOS2 did prevent precocious differentiation of spermatogonial stem cells caused by the *Gfra1*-deficiency, indicating that the stem cell differentiation could be suppressed solely by NANOS2 independent of GDNF signaling. The GDNF-independent NANOS2 function was further assessed by the ectopic expression of *Nanos2* in GFRA1-negative spermatogonia. The results support my idea that NANOS2 is capable of maintaining undifferentiated state of spermatogonial stem cells in the absence of GDNF-signaling pathway. Taken together, I suggest that the stem cell-intrinsic factor NANOS2 and extrinsic GDNF signals coordinately maintain spermatogonial stem cells by acting through different cellular and/or molecular mechanisms. My doctoral studies thus offer a novel insight into understanding how stem cells are maintained during murine spermatogenesis.

【Abbreviations】

A_s: A_{single}

A_{pr}: A_{paired}

A_{al}: $A_{aligned}$

Ngn3: Neurogenin3

E: embryonic day

P: postnatal day

PGC: primordial germ cell

GSC: germline stem cell

TM: tamoxifen

MCM: mutated estrogen receptor (MER)-Cre-MER

R26R: Rosa26-LacZ

CAG: cytomegalovirus (CMV) early enhancer/chicken beta-actin promoter

CAT: chloramphenicol acetyltransferase

(E) GFP: (enhanced) green fluorescence protein

X-gal: 5-bromo-4-chloro-3-indolyl- β -D-galactopyranoside

cKO: conditional knockout

OE: overexpression

Tg: transgene

PI3K: phosphoinositide 3-kinase

PH3: phospho Histone H3

RA: retinoic acid

VAD: vitamin A-deficient

Nos: Nanos

mTORC1: mammalian target of rapamycin complex 1

bp: base pair(s)

kb: kilobase(s)

3'UTR: 3'-untranslated region

PFA: paraformaldehyde

PBS: phosphate-buffered saline

PBS-T: Triton X-100/PBS

H-E: hematoxylin and eosin

RT: room temparature

DAPI: 4',6-diamidino-2-phenylindole

BrdU: 5-bromo-2'-deoxyuridine

RT-PCR: reverse transcriptase polymerase chain reaction

BM: basement membrane

SG_{undif}: undifferentiated spermatogonia

SG_{dif}: differentiating spermatogonia

SC: spermatocytes

ST: spermatids

SZ: spermatozoa

【Gene Symbols】

Gdnf: glial cell-line derived neurotrophic factor

Plzf: promyelocytic leukemia zinc-finger

Gfra1: glial cell line-derived neurotrophic factor family receptor alpha 1

Parp: poly (ADP-ribose) polymerase

Scp3: synaptonemal complex protein 3

Dazl: deleted in azoospermia-like

Stra8: stimulated by retinoic acid gene 8

Cyp26b1: cytochrome P450, family 26, subfamily b, polypeptide 1

Gapdh: glyceraldehyde-3-phosphate dehydrogenase

Chapter 1

Roles of NANOS2 during murine spermatogenesis

【Introduction】

Spermatogonial stem cells represent a stem cell population in the adult testis, and their biological activities provide a base of continuous production of spermatozoa. Spermatogenesis is the intricate and coordinated process, which consists of three distinct phases and takes about 35 days in total [1] (Fig. 1A). In the first proliferative phase, spermatogonia undergo a series of mitotic divisions and differentiate into primary spermatocytes that enter the second phase, or meiotic phase, which forms haploid spermatids. The third phase, termed spermiogenesis, involves the rearrangement of cytoskeletal structure, transforming round germ cells to specialized spermatozoa. The mature spermatozoa are eventually released from the testes through the tubule lumen. The entire developmental process from spermatogonia to spermatozoa occurs within seminiferous tubules of testes (Fig. 1, B and B'). In the tubules, all types of spermatogonia are located on the basement membrane, and the subsequent differentiating cell types are arranged in a sequential order towards the lumen. The spermatogenesis is also supported by close interaction of the germ cells with somatic Sertoli cells.

The basic biological functions of the stem cells are: (1) to preserve tissue homeostasis by providing differentiated cells; while at the same time (2) to undergo self-renewal to ensure a constant supply of new stem cells. Spermatogenesis is thought to be a classic stem cell-dependent system in which external niche stimuli and internal gene expression regulate self-renewal and differentiation of spermatogonial stem cells [2-10]. For example, GDNF (glial cell-line derived neurotrophic factor), a growth factor produced in Sertoli cells is both essential and sufficient for the spermatogonial stem cell self-renewal [7]. A transcription factor PLZF (promyelocytic leukemia zinc finger, also known as

Zfp145) is needed in a cell autonomous fashion for the maintenance of the spermatogonial stem cells, since male mice lacking *Plzf* expression exhibit progressive germ cell loss and testis atrophy with age, causing infertility [3, 5]. However, the previous loss of function studies had some limitations in terms of understanding the mechanisms by which stem cells are lost upon the gene deletion, as it could be caused by cell death, a defective proliferation, a premature differentiation, or other mechanisms.

A precise identification of stem cells is another important issue in stem cell biology [11]. There are up to nine different spermatogonia populations in mice [1, 12-15] (Fig. 1A), of which there are three major subclasses: type A, Intermediate, and type B spermatogonia according to their cellular shape and amount of nuclear heterochromatin. Due to an incomplete cytokinesis, spermatogonia are connected by intercellular cytoplasmic bridges as a chain of 2^n cells. The spermatogonial types A_{single} (A_s; isolated single cells), A_{paired} (A_{pr}; interconnected 2 cells), and $A_{aligned}$ (A_{al}; interconnected 4, 8, 16 or 32 cells) are the most primitive population and are collectively described as undifferentiated spermatogonia. The undifferentiated spermatogonia differentiate into A_1 spermatogonia, which undergo six cell divisions before entering meiosis via A_2, A_3, A_4, Intermediate, and B spermatogonia. A_1 to B spermatogonia together have been called as differentiating spermatogonia. According to "A_s model", A_s spermatogonia represent spermatogonial stem cells: this type is recognized as the most primitive cells and exists as single cells without any intercellular connection with others, whereas A_{pr} and A_{al} spermatogonia are committed to differentiation [16, 17]. Studies using spermatogonial transplantation [18, 19] along with a lineage study [20] have demonstrated that spermatogonial stem cells is highly enriched in the undifferentiated spermatogonia

containing A_s to A_{al}, although an unequivocal identification of the stem cells within the subpopulation of undifferentiated spermatogonia has not been achieved for over the past decade.

It has recently been shown that the undifferentiated spermatogonia are characterized by variable levels of gene expression in addition to their morphological classification [21-23] (Fig. 2A). For example, PLZF have identical expressions in all the A_s, A_{pr}, and A_{al} spermatogonia, which population are negative for KIT (a marker for differentiating spermatogonia). In contrast, two other genes, GFRA1 (glial cell line-derived neurotrophic factor family receptor alpha 1) and *Neurogenin3* (*Ngn3*), were expressed in subpopulations of the PLZF-positive spermatogonia in a reciprocal manner: GFRA1 is expressed in a large subset of A_s and A_{pr}, while many of A_{al} are *Ngn3*-positive. Furthermore, my laboratory discovered that a zinc-finger RNA-binding protein NANOS showed unique expression pattern in adult testes [21]. Among three NANOS homologs in mice, NANOS2 is expressed predominantly in the GFRA1-positive A_s and A_{pr} (Fig. 2, B to D), but was undetectable in majority of *Ngn3*-positive spermatogonia (Fig. 2, E to G), suggesting that NANOS2 might be a novel marker for spermatogonial stem cells [21]. Whereas, the expression level of NANOS3 was no or low in A_s and A_{pr}, but became higher in A_{al} [21]. Although *Ngn3*-positive cells were previously reported to be capable of contributing to the stem cell pool, both in steady-state spermatogenesis as well as in regenerating tissue post-injury [20], the stem cell activity of NANOS2-positive spermatogonia has not been tested. Also, the difference between NANOS2-positive and *Ngn3*-positive spermatogonia remains uncertain.

Originally, NANOS has been proposed as an evolutionarily conserved factor for

germ cell function [24-33]. In *Drosophila*, Nanos forms a complex with another RNA-binding protein Pumilio, and represses the translation of the *hunchback*, *Cyclin B*, and *hid* mRNAs thereby establishing embryonic polarity, mitotic quiescence, and suppression of apoptosis, respectively [34-38]. In mice, my laboratory has proposed that NANOS2 plays a role in recruiting the deadenylation complex to trigger the degradation of NANOS2-interacting mRNAs [39]. During male germ cell development and postnatal spermatogenesis, *Nanos2* mRNA is expressed in a germ cell-specific manner [40] (Fig. 3). Developmentally, spermatogonial stem cells originate from more undifferentiated precursors termed gonocytes, which are derived from primordial germ cells (PGCs) that proliferate and migrate from the extraembryonic region (base of allantois) to the gonad, a precursor of testis or ovary [41] (Fig. 3). PGCs are sexually bi-potential at the migrating stage, and their sex-specific differentiation begins after their colonization to the gonads at around embryonic day (E) 10.5 [41]. Once entered the gonad, female germ cells initiate meiosis at E13.5, whereas male germ cells undergo cell cycle arrest at G1/G0 phase and never enter meiosis during embryogenesis [41]. After birth, the male gonocytes resume proliferation quickly and migrate from their original central position toward the periphery in the seminiferous tubules, and transform into spermatogonia within first 7 days after birth [12, 14, 42]. It has been shown that the transplantable stem cell activity becomes detectable at approximately postnatal day (P) 3 to P4 [43]. During these processes, *Nanos2* mRNA is first detected in gonocytes at around E13.5 and is transiently down-regulated at later embryonic stages, but it is again detected in spermatogonia by P5 (Fig. 3) [40, 44]. When *Nanos2* was disrupted by the gene knockout technology, *Nanos2*-null males showed a complete loss of germ cells due to apoptosis that occurred as early as E15.5 [40]. In

addition, *Nanos2* is implicated in the sexual development of gonocytes by suppressing meiosis and promoting male-type differentiation at embryonic stages [45]. However, the postnatal function of NANOS2 has not been studied, because the targeted disruption of *Nanos2* results in the disappearance of gonocytes before birth [40].

In my current study, I characterize NANOS2-expressing cells by lineage tracing experiments and reveal that these cells act as self-renewing stem cells in vivo. Next, I employ gain and loss of function studies to define a role of *Nanos2* during spermatogenesis. Conditional knockout of postnatal *Nanos2* fails to maintain spermatogonial stem cells, whereas continuous *Nanos2* expression results in an accumulation of undifferentiated spermatogonia. Thus, I propose that NANOS2 is a key stem cell-intrinsic factor during murine spermatogenesis.

【Results】

NANOS2-expressing undifferentiated spermatogonia can self-renew and generate all stages of differentiating spermatogenic cells

To test whether NANOS2-expressing spermatogonia have stem cell properties in vivo, I followed the fate of *Nanos2*-expressing cells using a tamoxifen (TM) inducible Cre/loxP cell lineage tracing system (Fig. 4). For this purpose, I generated transgenic mice that express *MCM* (*MER-Cre-MER*), a TM-inducible version of Cre recombinase [46], under the control of an endogenous *Nanos2* enhancer (Fig. 4A). I then crossed these *Nanos2-MCM* mice with *Rosa26-LacZ* (*R26R*) [47] (Fig. 4B) or *CAG-CAT-EGFP* (Fig. 4C) reporter mice that express *LacZ* or *EGFP* after Cre-mediated removal of the inactivating sequence. The transient treatment of these animals with TM results in the permanent expression of *LacZ* or *EGFP* in the *Nanos2*-expressing spermatogonia and I can thus delineate the fate of all progeny of the labeled spermatogonia. In my current study, 6-week-old adult *Nanos2-MCM*; *R26R* (or *CAG-CAT-EGFP*) mice were subjected to a TM pulse for 5 days, and were sacrificed at 7-, 10-, 18-, 22- and 26- weeks of age (Fig. 4D). In this experimental system, I confirmed that labeled cells were only observed in the surfaces of the seminiferous tubules, which are either A_s, A_{pr} or A_{al} at 7 weeks (Fig. 5, A to D). Use of the *CAG-CAT-EGFP* reporter gene allowed double staining of the GFP-labeled cells with endogenous anti-NANOS2 antibody and revealed that a label was successfully introduced into about 20-25% of the NANOS2-positive undifferentiated spermatogonia by a TM pulse (Fig. 5E).

To analyze their long-term cell fates, I used *Nanos2-MCM*; *R26R* mice subjected to the TM pulse at 6 weeks of age. At 10 weeks (1 month after labeling), a large number of

X-gal positive cells were observed all along the seminiferous tubules (Fig. 6A), which were classified as either differentiating spermatogenic cells (Fig. 6C, asterisks) or spermatogonia (Fig. 6C, arrowheads). Because the completion of spermatogenesis takes ~35 days from the initial step of differentiating spermatogonia [1] (Fig. 1A), these stained cells would reflect stem cell-derived clones and/or transient clones that originated from non-stem cells. At 18 weeks (3 months after labeling), a sufficiently long period for a repeated completion of spermatogenesis, I observed X-gal positive patches that contained all stages of spermatogenic cells (Fig. 6, B and D). These patches persisted for prolonged periods of time (Fig. 6E). This indicates that the labeled spermatogonia continuously give rise to differentiating cells while maintaining their own population over long periods. Therefore, such spermatogonia can be referred to as spermatogonial stem cells.

Previous gene expression studies indicated that NANOS2-expressing cells appear to represent a different subset of undifferentiated spermatogonia from those expressing *Ngn3* [21] (Fig. 2A and Fig. 2, E to G). To test if these two populations have different ability for generating long-lived patches, I compared differences in the cell fates between the *Nanos2*-lineage and the previously reported *Ngn3*-lineage [20]. Similar to my experiments, in the *Ngn3*-lineage, the labeled undifferentiated spermatogonia formed persistent patches at 3 months after labeling [20], indicating that *Ngn3*-positive spermatogonia did contain spermatogonial stem cells. However, the average number of patches in the *Ngn3*-lineage was 6.1 $\pm$ 0.7 per testis [20], which was more than 10-fold smaller than that of the *Nanos2*-lineage (Fig. 6E). This difference was not due to the higher efficiency of my pulse-labeling system, because the number of initial labeled spermatogonial clones was similar in both cases: in the *Nanos2*-lineage, total number of

labeled undifferentiated spermatogonia were counted as 9224 clones per testis at 7 days after TM-pulse (which corresponds to 7 weeks of age) (Fig. 5E); while in the *Ngn3*-lineage, the number has been reported to be 9046 clones per testis at the same time point [20]. These results indicate that the NANOS2-expressing spermatogonia contain higher proportion of self-renewing stem cells in comparison to the *Ngn3*-positive population.

Progressive loss of spermatogenesis in mice lacking postnatal *Nanos2*

Because *Nanos2* is important for male germ cell development, I asked if it plays an additional role during adult spermatogenesis. As reported previously, the majority of *Nanos2*-null germ cells die by apoptosis before birth [40]; therefore, I sought to establish a novel system in which function of postnatal *Nanos2* could be studied. I generated a transgenic mouse line that expresses a floxed *3×Flag-tagged Nanos2* transgene under the control of the endogenous *Nanos2* enhancer (Fig. 7A). The expressed tagged protein is functional *in vivo* and can rescue the *Nanos2*-null mouse defects (Fig. 7A and Fig. 8, A to F). By introducing an additional transgene, *Ert2-Cre* that ubiquitously expresses a TM-inducible Cre recombinase, a conditional knockout (cKO) of *Nanos2* after birth became possible (Fig. 7A and Fig. 8G). I performed TM treatments to eliminate *Nanos2* expression in males at 4 weeks of age and dissected testes at indicated time points (Fig. 7B).

Histological analysis of the *Nanos2*-cKO testes revealed a progressive defect in spermatogenesis with age (Fig. 9, A to F). At 6 weeks of age, seminiferous tubules of control and *Nanos2*-cKO mice seemed similar, with multiple layers of germ cells (Fig. 9, A and D). However, at 8 weeks (1 month after TM injection), fewer germ cells were

present in *Nanos2*-cKO testes (Fig. 9, B and E). By 12 weeks after birth (2 months after TM injection), most of these tubules became agametic and contained only Sertoli cells (Fig. 9, C and F). Hence, postnatal deficiency of *Nanos2* resulted in the gradual loss of the germ cell population within a few cycles of spermatogenesis.

I confirmed my histological findings by immunostaining with TRA98, a marker that is expressed in spermatogonia, spermatocytes and round spermatids, and spermatogonial marker PLZF (Fig. 9, G to J). In the 8-week-old *Nanos2*-cKO mice, some tubules showed either a selective loss of PLZF-positive spermatogonia only (Fig. 9J, arrowhead) or a combined loss of meiotic spermatocytes with spermatogonia (Fig. 9J, arrow). Others were devoid of germ cells altogether (Fig. 9J, asterisks). These observations suggest that *Nanos2*-deficiency is permissive of normal spermatogenic differentiation but causes germ cell depletion through an initial loss of spermatogonial cells.

The most primitive spermatogonia were lost by *Nanos2*-deletion

To determine the earliest defect for the spermatogonial cell loss, I studied spermatogonial markers further in detail. First, I examined time course for the spermatogonial cell loss by counting the number of PLZF-positive spermatogonia per seminiferous tubule using the testis cross-sections (Fig. 10A). I found in *Nanos2*-cKO testes that the PLZF-positive cells were quickly declined soon after TM injection and were almost disappeared from their tubules by 8 weeks.

It is reported that PLZF-positive undifferentiated spermatogonia are consist of at least two subpopulations, NANOS2^{+}/GFRA1^{+} and NANOS3^{+}/*Ngn3*$^{+}$ (Fig. 2A). Next, I examined which type of spermatogonia was primary affected by the *Nanos2*-deletion. For

this purpose, I performed whole-mount immunostaining with anti-GFRA1 and anti-NANOS3 antibodies (Fig. 10, B to E). In control, GFRA1 and NANOS3 were expressed in a reciprocal manner: GFRA1 was expressed preferentially in A_s or A_{pr}, while NANOS3 was strongly expressed in A_{al} (Fig. 10, B and C). In the *Nanos2*-cKO testes, the most primitive set of spermatogonia indicated by GFRA1 expression were lost immediately after *Nanos2*-deletion. However, more differentiated types of undifferentiated spermatogonia that express NANOS3 still remained (Fig. 10, D and E). Hence, the germ cell-loss phenotype in *Nanos2*-cKO mice was caused by the depletion of GFRA1-positive spermatogonia, which include stem cell population that produce differentiating progenies.

Possible causes of spermatogonial depletion in *Nanos2*-cKO mice

The stem cell depletion in *Nanos2*-cKO mice could occur by apoptosis and/or the inability to maintain an undifferentiated state. I examined the former possibility since it has been shown that NANOS has a conserved function in preventing apoptosis of germ cells in a variety of species [27, 32, 37, 40, 48, 49]. I found that the number of apoptotic cells in the PLZF-positive population in the mutants was slightly increased compared with those of controls at the critical time window for spermatogonial reduction, although significant differences were not observed (Fig. 11A). Total number of apoptosis regardless of the cell types did not change in the mutants (Fig. 11B). These results indicate that apoptotic cell death partly contributes to the loss of stem cells by postnatal *Nanos2*-deficiency.

Next, I tested another possibility that *Nanos2*-deficient cells might undergo differentiation. This interpretation is consistent with the results of a loss of function study

in the *Drosophila* ovary, in which the removal of *Nanos* from either germline stem cells (GSCs) or their precursors (PGCs), resulted in the premature differentiation of both cell types into germline cysts [33, 50]. In my study, I visualized *Nanos2*-cKO cells and their progenies by introducing *R26R* reporter in the *Nanos2*-null genetic backgrounds together with *floxed-Nanos2* transgene (Fig. 12A). In order to induce Cre recombination specifically in *Nanos2*-expressing cells, I used *Nanos2-MCM* (Fig. 4A) instead of ubiquitous *Ert2-Cre*. TM injections to 4-week-old *Nanos2*-null mice with triple transgenes (*Nanos2-MCM*, *Nanos2* enhancer-*floxed 3xFlag-tagged Nanos2* and *R26R*) resulted in simultaneous deletion of the *Nanos2* gene and induction of *LacZ* expression (Fig. 12A). Control experiments were performed in *Nanos2*-hetero genetic backgrounds. This experimental system allows us to trace the fates of *Nanos2*-cKO cells and to distinguish the above possibilities whether *Nanos2*-deficient cells proceed to differentiation or apoptosis. One or two months after TM injection, I observed X-gal positive spermatogenic cells in the *Nanos2*-hetero genetic backgrounds as expected (Fig. 12, B and C). Remarkably, X-gal positive cells were present in 8 weeks of transgenic testes even in the *Nanos2*-null backgrounds (Fig. 12D). Most of these X-gal positive cells were eventually disappeared from their testes (Fig. 12E). This result indicates that *Nanos2*-deficient cells, at least in part, might undergo premature differentiation rather than be eliminated by apoptosis.

PLZF-positive cells were accumulated by *Nanos2*-overexpression

It is considered that the maintenance of stem cells might rely on the regulation of several cellular events such as cell cycle, apoptosis, differentiation and so on. NANOS2 should control these events for maintaining the proper state of spermatogonial stem cells.

However, the previous loss of function study cannot clearly distinguish these possibilities. To further determine the role of NANOS2 in the stem cell maintenance, I designed a gain of function strategy. In the normal spermatogenesis, NANOS2 is expressed in the undifferentiated spermatogonia but the expression disappears along with their differentiation [21]. In this experiment, I generated transgenic mice, which allows continuous expression of NANOS2 in germ cell lineages (hereafter referred to as *Nanos2*-overexpression [*Nanos2*-OE]). To achieve this, I crossed *CAG-floxed CAT-3xFlag-Nanos2* transgenic mice [45] (Fig. 13A) with *Nanos3-Cre* mice [49], in which Cre recombinase expression occurs in majority of male gonocytes by E14.5 (Fig. 16). The Cre-expressing cells and their offspring irreversibly expressed *Flag-tagged Nanos2* during embryogenesis and after birth.

The resulting *Nanos2*-overexpressing male mice were infertile, and testis weights were reduced (Fig. 13B). The histology (Fig. 13, C and F) and the expression of germ cell (Fig. 13, D and G) or meiotic markers (Fig. 13, E and H) revealed that most tubules in the *Nanos2*-overexpressing testes retained spermatogonia-like cells on the basement membrane, whereas differentiated germ cells were absent or markedly reduced in number. Rarely observed meiotic cells in *Nanos2*-overexpressing testes possibly due to incomplete recombination by Cre (an efficiency is about 70%), as they showed weaker expression of FLAG-NANOS2 (Fig. 13, I and J).

To characterize the peripheral germ cells in the *Nanos2*-overexpressing testes, I examined spermatogonial markers. In *Nanos2*-overexpressing testes, most FLAG-positive cells on the basement membrane expressed PLZF, a marker of undifferentiated spermatogonia (Fig. 14, A to F). However, they did not express KIT, a marker of

differentiating spermatogonia, although strong and consistent expression of this factor was observed in somatic Leydig cells in both genotypes (Fig. 14, G to L). Based on the immunostaining data, *Nanos2*-overexpressing cells were characterized as undifferentiated spermatogonia rather than differentiating spermatogonia.

On the cross sections, I scored the number of PLZF-positive cells per one seminiferous tubule and found that the number was significantly larger in *Nanos2*-overexpressing testes (Fig. 15A). I speculate that the increased number of PLZF-positive spermatogonia might be caused by: (1) a hyper-proliferation; (2) a reduction in apoptosis; or (3) a blocked differentiation of these cells. To test these possibilities, I counted the number of proliferating cells and apoptotic cells in PLZF-positive spermatogonia. I found that these PLZF-positive cells in *Nanos2*-overexpressing mice had lower proliferation rates (Fig. 15B) and similar levels of apoptosis (Fig. 15C) compared to the control spermatogonia. Taken together, I conclude that the accumulation of undifferentiated spermatogonia observed in *Nanos2*-overexpressing testes is due to the blocked differentiation rather than a hyper-proliferation or a reduction in apoptosis.

Effects of *Nanos2*-overexpression during embryonic or neonatal stages

To induce *Nanos2*-overexpression, I employed *Nanos3-Cre* mice, in which Cre recombinase expression commences during embryonic stages (Fig. 16). Thereby, I suspected that the phenotype I observed in adult *Nanos2*-overexpressing mice might reflect germ cell abnormalities during embryogenesis and/or shortly after birth. I evaluated the effects of *Nanos2*-overexpression on neonatal germ cells by analyzing PLZF and KIT

expression (Fig. 17). Within postnatal day 3, *Nanos2*-overexpressing germ cells migrated from center of the testis cords to the basement membrane of the testis tubules and started to express PLZF as a similar timing that observed in controls (Fig. 17, B and E). Consistent with the results in adult testes, KIT expression was not observed at P5 in the *Nanos2*-overexpressing germ cells, when KIT-positive spermatogonia first appeared in controls (Fig. 17, C and F). These results indicate that NANOS2 might repress spermatogonial differentiation but not affect on germ cell migration during early postnatal periods. However, I found that total number of germ cells (Fig. 18, B and D) and PLZF-positive cells (Fig. 19A) were fewer at the early postnatal stage in *Nanos2*-overexpressing testes although the number of embryonic germ cells was similar (Fig. 18, A and C). This might be caused by a reduced proliferation (Fig. 18E) rather than an increased apoptosis (Fig. 18F) of *Nanos2*-overexpressing cells.

To avoid the influence of *Nanos2*-overexpression on germ cells during embryogenesis and within the first few days after birth, I conducted the similar experiment using *Ngn3-Cre* mouse line, in which *Nanos2* could be induced in spermatogonia around 5 days after birth [51, 52] (Fig. 16). In this induction system, the number of PLZF-positive cells was found to be unchanged during first 2 weeks (Fig. 19B). Eventually in adult stages, I observed an increased number of PLZF-positive cells in the periphery of the tubules (Fig. 19B and Fig. 20, B and E) and a decrease of differentiating germ cells (Fig. 20, A, C, D and F). Therefore, the accumulation of PLZF-positive spermatogonia observed in the adult was not due to the overexpression of *Nanos2* during embryonic or neonatal stages.

***Nanos2*-overexpressing cells show characteristics of the most primitive**

undifferentiated spermatogonia.

To further analyze the outcome of *Nanos2*-overexpression, I performed whole-mount immunostaining of seminiferous tubules, which enables us to study both morphology and gene expression of spermatogonia. First, I stained the control and *Nanos2*-overexpressing testes with anti-PLZF antibody, which covers all types of undifferentiated spermatogonia, and then classified them by their morphology in terms of number of cells connected. In the control tubules, PLZF-positive A_s, A_{pr}, A_{al-4}, and A_{al-8} spermatogonia were observed at comparatively similar proportions (Fig. 21A), whereas the proportion of A_s and A_{pr} spermatogonia was higher in *Nanos2*-overexpressing tubules and A_{al} spermatogonia in chains of more than 8 cells were rarely observed (Fig. 21B). Hence, *Nanos2*-overexpressing cells were morphologically identified as primitive sets of undifferentiated spermatogonia.

Subsequently, I characterized the protein expression patterns of these cells with several molecular markers representing distinct populations of undifferentiated spermatogonia (Fig. 2A). In control testes, PLZF expression was observed in most of undifferentiated spermatogonia (Fig. 22, A to C), whereas GFRA1 was expressed preferentially in A_s and A_{pr} spermatogonia, in which endogenous NANOS2 was co-expressed (Fig. 22, G to I). Conversely, *Ngn3*-EGFP expression was generally found in the longer chained cells (Fig. 23, A to C). For example, some A_s and A_{pr} spermatogonia expressed only NANOS2, others co-expressed both NANOS2 and *Ngn3*-EGFP, while A_{al} were generally expressed *Ngn3*-EGFP with either no or lower expression of NANOS2. Similar to *Ngn3*-EGFP, NANOS3 was also found to be expressed largely in undifferentiated spermatogonia except for some A_s and A_{pr} spermatogonia (Fig. 23, G to I).

Using the combination of these protein expression patterns as a reference, I characterized *Nanos2*-overexpressing cells. I found in the *Nanos2*-overexpressing testes that most of FLAG-NANOS2 positive cells expressed PLZF (Fig. 22, D to F) and GFRA1 (Fig. 22, J to L), but exhibited no or lower levels of *Ngn3*-EGFP (Fig. 23, D to F) or NANOS3 (Fig. 23, J to L) expression. Hence, the *Nanos2*-overexpressing cells had properties similar to the most primitive set of undifferentiated spermatogonia. Therefore, I conclude that NANOS2 is a cell-intrinsic factor to maintain the unique, undifferentiated state of spermatogonial stem cells.

【Discussion】

Stem cells during murine spermatogenesis

My current long-term lineage tracing analysis showed that NANOS2-expressing spermatogonia indeed acted as spermatogonial stem cells in vivo (Fig. 6). Furthermore, *Nanos2*-expressing spermatogonia appeared to have the higher probability of generating long-lived patches, while the *Ngn3*-positive spermatogonia might be primed for differentiation (Fig. 6E compared with [20]). However, my study and following recent reports indicate that the spermatogonial stem cells might not be simply defined by their expression of NANOS2$^+$/GFRA1$^+$, and that NANOS3$^+$/*Ngn3*$^+$ state might not be the irreversible commitment to differentiation: (1) My lineage tracing experiments can not distinguish NANOS2-positive spermatogonia that serve as self-renewing stem cells from those lacking the ability; (2) there is some heterogeneity within NANOS2-positive spermatogonia both in their morphology (there are A_s, A_{pr} and some A_{al}) and gene expression profiles regarding GFRA1 and *Ngn3* expression [21], although the biological meaning is unclear; (3) *Ngn3*-positive spermatogonia are also capable of switching own state to a GFRA1$^+$ (probably NANOS2$^+$) state through cyst fragmentation and a change in gene expression, and contributing to the self-renewing stem cells [20, 53]; (4) spermatogonial stem cells are proposed not to be a long-lived, rather they are continuously lost and subsequently replaced by their neighboring cells, on average within 2 weeks [54]. Collectively, these findings suggest that spermatogenesis are supported by a pool of undifferentiated spermatogonia including both NANOS2$^+$/GFRA1$^+$ and NANOS3$^+$/*Ngn3*$^+$ populations, and are dependent on complex mechanisms more than expected. However, I still think that there are some critical cellular and molecular differences between

NANOS2^{+}/GFRA1^{+} and NANOS3^{+}/*Ngn3*$^{+}$ state, and the regulatory mechanisms of their cellular status are key points in my study. Thus, I like to define hereafter NANOS2^{+}/GFRA1^{+} undifferentiated spermatogonia as spermatogonial stem cells, and up-regulation of NANOS3 and/or *Ngn3* as spermatogonial stem cell differentiation.

Essential role of NANOS2 in the maintenance of spermatogonial stem cells

In this Chapter 1, I found that *Nanos2*-cKO mice lost their spermatogonial stem cells, whereas *Nanos2*-overexpression led to an accumulation of stem cell-like cells (summarized in Fig. 39). Although my current study has clearly shown the central role of NANOS2 in the maintenance of spermatogonial stem cells, many important questions related to NANOS2 functions remain to be addressed: (1) What are the critical target mRNAs of NANOS2 protein in murine spermatogonial stem cells; (2) how NANOS2 expression is induced and maintained in spermatogonial stem cells, and turned off in differentiating progenies. I discuss these points in Chapter 2.

Other interesting question is whether NANOS2 and a key extrinsic factor GDNF interact each other for the regulation of several cellular events in the spermatogonial stem cells e.g. apoptosis, proliferation and differentiation. I investigate this point in Chapter 2.

Chapter 2

Relationship between NANOS2 and GDNF signaling

【Introduction】

Spermatogonial stem cells represent a stem cell population in adult testes, and their proper biological activities ensure a continuous production of spermatozoa. The stem cell function resides in the undifferentiated spermatogonia, consisting of types A_{single} (A_s; isolated single cells), A_{paired} (A_{pr}; interconnected 2 cells) and $A_{aligned}$ (A_{al}; interconnected 4, 8, 16 or 32 cells) [1, 12-15]. The undifferentiated spermatogonia transform into type A_1 differentiating spermatogonia, which subsequently undergo six mitotic and two meiotic divisions to form haploid spermatozoa [1]. In addition to the morphological classification, undifferentiated spermatogonia are also characterized by the expressions of various marker genes [21-23, 53] (Fig. 24A): PLZF (promyelocytic leukemia zinc finger) is expressed in the entire undifferentiated spermatogonial pool; NANOS2 and GFRA1 (glial cell line-derived neurotrophic factor family receptor alpha 1) are expressed in large subsets of A_s and A_{pr}, which are capable of steady-state self-renewal; NANOS3 and *Neurogenin3* (*Ngn3*) are known as markers for A_{al} spermatogonia which are in a more mature state.

During murine spermatogenesis, external niche stimuli and internal gene expression regulate self-renewal and differentiation of spermatogonial stem cells [2-10, 55]. The growth factor GDNF (glial cell-line derived neurotrophic factor), a ligand for GFRA1, is secreted by somatic Sertoli cells and acts as one of the major niche signals for spermatogonial stem cells. GDNF signals via the GFRA1/RET co-receptor through activation of Src family kinases, Ras and PI3K (phosphoinositide 3-kinase)-Akt pathway and subsequently induces several target genes in spermatogonial stem cells [56-64]. Previous study has shown that *Gdnf* haploinsufficiency led to a progressive germ cell loss phenotype and that testicular overexpression of *Gdnf* resulted in an accumulation of

predominantly A_s spermatogonia [7]. Although mice lacking *Gdnf* or its receptors exhibit neonatal lethality, transplanted testes from each of *Gdnf*-, *Gfra1*- and *Ret*-null newborn mice showed severe spermatogonial cell depletion, which might result from deficits in spermatogonial proliferation and/or in their maintenance of an undifferentiated state [8]. It is as yet unclear how GDNF signaling influences adult spermatogenesis, since germ cells are lost by postnatal day (P) 7 in the testes of null mutants of *Gdnf* or its receptors [8].

An RNA-binding protein NANOS2 is an intrinsic factor required for the maintenance of spermatogonial stem cells (see Chapter 1 and [55]). In the first part of my thesis, I showed that the removal of *Nanos2* gene in adult testes resulted in the depletion of spermatogonial stem cells, which was evidenced by the absence of PLZF and GFRA1 expression (Fig. 9, G to J and Fig. 10, A to E) [55]. In contrast, continuous *Nanos2* expression in the germline caused an accumulation of PLZF-positive spermatogonia (Fig. 14, A to F and Fig. 15A), which were positive for GFRA1 (Fig. 22, G to L), but exhibited no or lower levels of NANOS3 or *Ngn3* expression (Fig. 23) [55]. Furthermore, the *Nanos2*-overexpressing cells showed slower proliferation and wild-type levels of apoptosis (Fig. 15, B and C) [55]. These results indicate that NANOS2 suppresses proliferation and differentiation of spermatogonial stem cells.

Since NANOS2 and GDNF (or its receptors) induced similar phenotypes upon loss of function and overexpression experiments with respect to spermatogonial stem cell maintenance, I examined the relationship between these two factors. By using an inducible Cre-loxP system, I induced overexpression of *Nanos2* in the *Gfra1*-conditional knockout (cKO) genetic background and found that the stem cell loss phenotype of the *Gfra1*-cKO mice was partially rescued. In order to verify this phenotype, I determined which cellular

events were regulated by *Gfra1*-depletion and by *Nanos2*-overexpression. My results indicate that NANOS2 is capable of suppressing differentiation of spermatogonial stem cells even in the absence of GDNF signaling.

【Results】

Conditional knockout of *Gfra1* disrupts adult spermatogenesis

In order to investigate the role of GDNF signaling in the adult stage spermatogenesis, I conditionally deleted *Gfra1* gene using the Cre-loxP system. I used mice carrying a gene cassette composed of floxed *Gfra1* cDNA followed by *EGFP* cDNA [65] (Fig. 24B) crossed with *Ert2-Cre* mice that ubiquitously express a tamoxifen (TM)-inducible Cre recombinase. I injected TM into 4-week-old of (1) $Gfra1^{flox/+}$ (heterozygous for the *Gfra1* floxed allele); *Ert2-Cre* or (2) $Gfra1^{flox/flox}$ (homozygous for the *Gfra1* floxed allele); *Ert2-Cre* mice for 5 consecutive days (Fig. 24D), resulting in the generation of (1) $Gfra1^{\Delta/+}$ (*Gfra1* heterozygous used as control) or (2) $Gfra1^{\Delta/\Delta}$ (*Gfra1*-conditional knockout: *Gfra1*-cKO) mice, respectively. In the *Gfra1* floxed mouse strain, the excision of the floxed *Gfra1* gene results in the expression of a reporter *EGFP* gene, which is inserted into the *Gfra1* locus. This allowed us to mark *Gfra1* enhancer/promoter activated cells that have undergone Cre recombination through monitoring of GFP fluorescence.

At 5 weeks of age (1 week after the first TM injection), I detected GFRA1 expression in GFP (Δfloxed *Gfra1*)-positive cells in control testes, but not in *Gfra1*-cKO testes (Fig. 25, A, B and I), indicating a successful deletion of *Gfra1* upon TM injections. To examine long-term consequences of *Gfra1* ablation during spermatogenesis, I studied testis histology by staining with a germ cell marker TRA98, and a spermatogonial marker PLZF (Fig. 26, A to F). At 5 weeks of age, seminiferous tubules of control and *Gfra1*-cKO mice seemed similar, with multiple layers of germ cells (Fig. 26, A and D). However, at 8 weeks (1 month after TM injection), there was a marked reduction of the PLZF-positive cells in *Gfra1*-cKO testes (Fig. 26, B and E). In addition, some seminiferous tubules in the

mutant mice contained a less number of TRA98-positive germ cells in their inner layers (Fig. 26E). Subsequently, by 12 weeks (2 months after TM injection), all types of germ cells had almost disappeared from the *Gfra1*-cKO testes, revealing Sertoli cell-only phenotypes (Fig. 26, C and F). Hence, I found that *Gfra1*-deficiency in adult testes resulted in the depletion of PLZF-positive spermatogonia that led to a complete loss of spermatogenic germ cells.

Next, to determine the time course of the progressive loss of spermatogonia in *Gfra1*-cKO mice, I quantified the number of PLZF-positive cells per tubule in the mutant and control mice (Fig. 27A, white and blue bars). I found that PLZF-positive spermatogonia rapidly declined and were almost abolished within 1 month after TM injection in the *Gfra1*-cKO mice testes (Fig. 27A, white and blue bars). The time course of depletion of PLZF-positive cells by *Gfra1*-deletion resembled that of *Nanos2*-cKO mice, which I reported previously (Fig. 10A) [55]. This further supports the idea that both the *Gfra1*-mediated GDNF signaling and NANOS2 are essential components in the maintenance of spermatogonial stem cells in adult testes.

Induction of *Nanos2*-overexpression in the *Gfra1*-conditional knockout background

In the *Gfra1*-cKO mice, NANOS2 expression was dramatically decreased in GFP-positive (Δfloxed *Gfra1*) cells (Fig. 25, E, F and J). I next asked whether continuous expression of NANOS2 could negate the stem cell loss phenotype caused by *Gfra1*-deletion. To achieve overexpression of exogenous *Nanos2* simultaneously with the conditional knockout of *Gfra1*, I introduced *CAG-floxed CAT-3xFlag-Nanos2* transgene (hereafter referred to as *Tg-Nanos2*) (Fig. 24C) in the $Gfra1^{flox/+}$; *Ert2-Cre* or $Gfra1^{flox/flox}$; *Ert2-Cre* mouse

backgrounds. Injection of TM to *Gfra1*$^{flox/+}$; *Ert2-Cre*; *Tg-Nanos2* or *Gfra1*$^{flox/flox}$; *Ert2-Cre*; *Tg-Nanos2* mice, resulting in the generation of *Gfra1*$^{\Delta/+}$; *Tg-Nanos2* (*Nanos2*-overexpression in control background) and *Gfra1*$^{\Delta/\Delta}$; *Tg-Nanos2* (*Nanos2*-overexpression in *Gfra1*-cKO background), respectively.

Since *Ert2-Cre* is ubiquitously expressed from *Rosa26* locus, I expected that *Nanos2* expression would be induced in both somatic cells and all stages of germ cells. However, after TM injections, strong NANOS2 expression was predominantly observed in spermatogonia and a part of spermatocyte, while later stages of germ cells or somatic cells were negative for NANOS2 (Fig. 28), which might be due to a higher efficiency of Cre recombinase in mitotic/meiotic cells or a post-transcriptional repression of NANOS2 in later stage germ cells and somatic cells. In spite of differential efficiency of NANOS2 expression among cell types, *Ert2-Cre* successfully induced *Nanos2*-overexpression in GFP-positive spermatogonia in both *Gfra1*$^{\Delta/+}$ and *Gfra1*$^{\Delta/\Delta}$ backgrounds (Fig. 25, C, D, G, H, I and J).

I performed immunostaining using TRA98 and anti-PLZF antibodies to analyze their testis histology (Fig. 26, G to L). At 5 weeks, in both *Gfra1*$^{\Delta/+}$; *Tg-Nanos2* and *Gfra1*$^{\Delta/\Delta}$; *Tg-Nanos2* testes, TRA98-positive germ cells appeared to be slightly less than those of normal testes (Fig. 26, G and J). Thereafter, both testes lost inner layer of differentiating germ cells by as early as 8 weeks, while PLZF-positive spermatogonia were retained on the basement membrane (Fig. 26, H and K). This result indicates that *Ert2-Cre* driven *Nanos2*-overexpression blocked spermatogonial differentiation which is similar to the phenotype observed in *Nanos2*-overexpressing mutants induced by *Nanos3-Cre* (in which Cre recombination occurs in the male gonocytes, precursors of spermatogonial stem

cells by embryonic day 14.5) (Fig. 13, C to H, Fig. 14, A to F and Fig. 16) [55]. However, in the absence of *Gfra1*, *Nanos2*-overexpressing mice eventually lost their germ cells including PLZF-positive spermatogonia by 12 weeks (Fig. 26L). Hence, *Gfra1*-deletion causes spermatogonial cell loss even in the presence of NANOS2.

Partial rescue of *Gfra1*-knockout phenotype by overexpressed *Nanos2*

I further determined the speed in which spermatogonial stem cells are lost upon *Gfra1*-deletion and the extent to which overexpressed *Nanos2* could alleviate this phenotype. For this purpose, I examined the change in numbers of PLZF- and GFP (Δfloxed *Gfra1*)- positive cells in each genotype at 5-, 6-, 8- and 12- weeks of age (Fig. 27). In agreement with the previous studies that PLZF-positive undifferentiated spermatogonia contain both GFRA1-positive and GFRA1-negative population [21, 22, 53] (Fig. 24A), a part of PLZF-positive cells expressed GFP in the control mice (Fig. 29, A and B). In the *Gfra1*-cKO mice, in addition to the overall decrease of PLZF-positive spermatogonia (Fig. 27A, blue bar), there was a severe depletion of GFP-positive spermatogonia (Fig. 27B, blue bar) compared with controls (Fig. 27, A and B, white bars). I could detect GFP-positive cells in the *Gfra1*-cKO testes until 5 weeks of age, but never observed thereafter (Fig. 27B, blue bar). On the contrary, when I induced *Nanos2*-overexpression in the control background, PLZF- (Fig. 27A, gray bar and Fig. 29E) and GFP- (Fig. 27B, gray bar and Fig. 29F) positive spermatogonia were gradually increased. However, when I overexpressed *Nanos2* in the *Gfra1*-cKO background, the number of PLZF- (Fig. 27A, green bar) and GFP- (Fig. 27B, green bar) positive spermatogonia were significantly lower compared with that in the *Gfra1*$^{\Delta/+}$; *Tg-Nanos2* testes (Fig. 27, A and B, gray bars). By 12

weeks, both PLZF- and GFP- positive spermatogonia were almost completely disappeared from the *Gfra1*$^{\Delta/\Delta}$; *Tg-Nanos2* testes (Fig. 27, A and B, green bars). These results are consistent with my histological observations that overexpressed *Nanos2* cannot fully counteract the *Gfra1*-cKO phenotypes. However, if I compared the number of PLZF-positive spermatogonia in *Gfra1*-cKO testes with (Fig. 27A, green bar) or without (Fig. 27A, blue bar) *Tg-Nanos2*, these cells were maintained for a prolong period in the presence of *Tg-Nanos2*. At 8 weeks, I could observe PLZF-positive spermatogonia in *Gfra1*$^{\Delta/\Delta}$; *Tg-Nanos2* testes (Fig. 27A, green bar and Fig. 29G) but not in *Gfra1*$^{\Delta/\Delta}$testes (Fig. 27A, blue bar and Fig. 29C). Consistently, GFP-positive cells were maintained in the 6-week- or 8-week- old *Gfra1*-cKO testes only when the *Tg-Nanos2* was induced (Fig. 27B, green and blue bars; and Fig. 29, D and H). Thus, I found that overexpression of *Nanos2* in the *Gfra1*-cKO testes alleviated the stem cell loss phenotypes of *Gfra1*-cKO mice.

Taken together, I found that: 1) in the absence of GDNF signaling, overexpressed NANOS2 can not maintain spermatogonial stem cells permanently, indicating that the GDNF-dependent mechanism is essential for spermatogonial stem cell maintenance; however 2) a partial or a short-term rescue of the *Gfra1*-cKO phenotype can be achieved by *Nanos2*-overexpression, indicating the existence of GDNF-independent, NANOS2-dependent mechanism(s) in spermatogonial stem cell maintenance.

Apoptotic cell death is not responsible for the loss of spermatogonial stem cells in the *Gfra1*-null testes

Generally, the stem cell state or “stemness” is regulated via the following cellular

processes [66]: (1) cell proliferation to expand the stem cell population; (2) maintenance of the undifferentiated state to ensure the preservation of the stem cell pool while allowing successful generation of differentiated products; and (3) cell death/survival to control their quality and quantity. NANOS2 and GDNF signaling might control these cellular events cooperatively or independently for maintaining the proper state of spermatogonial stem cells. To clarify this point, I asked the reason why NANOS2 alone could not maintain spermatogonial stem cells in the absence of *Gfra1*. I first tested the following possibility: if GDNF signaling suppresses apoptosis of spermatogonial stem cells, the deletion of *Gfra1* may cause an elevated apoptotic cell death of these cells. Since my current study has shown that overexpressed *Nanos2* did not affect the apoptosis of spermatogonia (Fig. 15C) [55], I expected that overexpressed *Nanos2* could not rescue the failure of stem cell maintenance in the *Gfra1*-cKO mice.

To test this possibility, I quantified the apoptosis of GFP-positive (Δfloxed *Gfra1*) cells immediately after the loss of *Gfra1* (Fig. 30A). At 5 weeks of age, apoptotic GFP-positive cells were detected at a very low frequency in the control testes and their numbers were not altered by *Gfra1*-deletion (Fig. 30A and Fig. 31, A and B). In the *Nanos2*-overexpressing testes, regardless of the presence or absence of *Gfra1*, I observed a massive apoptosis in the spermatogonia and spermatocytes (Fig. 31, C and D), indicating that *Nanos2*-overexpression by ubiquitous *Ert2-Cre* may cause inappropriate effects on spermatogenic germ cells. Nevertheless, there were no significant differences in the proportion of cleaved PARP-positive cells within GFP-positive cell population in any comparison I examined (Fig. 30A). I obtained similar results by using 8-weeks of testes (Fig. 33A). Together, these results indicate that apoptotic cell death might not be a major

cause of stem cell loss by *Gfra1*-deficiency.

Opposite effects on stem cell proliferation by GDNF signaling and NANOS2

Given that GDNF signaling is implicated in the proliferation of spermatogonial stem cells [8, 56-58, 61, 67], the loss of *Gfra1* may reduce the proliferation of these cells. If this is the case, I expected that *Nanos2*-overexpression could not rescue the phenotype of *Gfra1*-cKO mice, because *Nanos2* showed a suppressive effect on the spermatogonial proliferation (Fig. 15B) [55].

To test this scenario, I quantified the proliferation of spermatogonial stem cells marked by GFP (Δfloxed *Gfra1*) in the control and mutant testes at 5 weeks of age (Fig. 30B). I used phospho-Histone H3 (PH3) as a marker of cell proliferation, in which mitotic cells from prophase to telophase are labeled. Normally (*i.e.* in *Gfra1*$^{\Delta/+}$ testes), 30.9% of GFP-positive spermatogonia were positive for PH3 (Fig. 30B and Fig. 32, A and B), whereas only 8.7% of *Gfra1*-cKO cells showed the signal (Fig. 30B and Fig. 32, C and D). Hence, I found that the proliferation of spermatogonial stem cells was highly dependent on GDNF-stimulated pathway.

In agreement with my previous results, I found a significant reduction of mitotic GFP-positive cells in *Nanos2*-overexpressing mice even in the presence of a functional *Gfra1* allele (Fig. 30B and Fig. 32, E and F). When I ablated *Gfra1* from the *Nanos2*-overexpressing mice, the proliferation of GFP-positive cells was further declined and they constituted only 1.5% of the total GFP-positive cells (Fig. 30B and Fig. 32, G and H). Similar results were obtained by using testes from 8-week-old mice (Fig. 33B). Hence, the proliferation defects might account for the loss of spermatogonial stem cells through

either *Gfra1*-deletion or *Nanos2*-overexpression. This could be the reason why *Nanos2*-overexpression did not rescue the stem cell loss phenotype of *Gfra1*-cKO mice completely. Collectively, these results suggest that GDNF signaling and NANOS2 have opposite role in spermatogonial stem cell proliferation: GDNF signaling stimulates their proliferation, while NANOS2 might delay cell cycle progression of these cells.

Overexpression of *Nanos2* blocks stem cell differentiation caused by conditional knockout of *Gfra1*

Despite the above, I found that *Nanos2*-overexpression in *Gfra1*-cKO background could sustain PLZF$^+$/GFP (Δfloxed *Gfra1*)$^+$ spermatogonial stem cells for a longer period compared to those in *Gfra1*-cKO alone (Fig. 27, green and blue bars). Therefore, there must be a mechanism to retard the effect of the loss of GDNF signaling by NANOS2. I speculate that the stem cell loss is also caused by the inability of stem cells to maintain an undifferentiated state, which may result in the depletion and ultimate elimination of the self-renewing population through differentiation. Indeed, GDNF signaling is known to suppress differentiation of spermatogonia [7], therefore its deletion might promote their differentiation and result in the depletion of spermatogonial stem cells. If *Nanos2*-overexpression could suppress their differentiation independent of GDNF signaling, it might maintain *Gfra1*-null stem cells in undifferentiated states.

To test this hypothesis, I used NANOS3 as a differentiation marker and performed whole-mount immunofluorescence staining for GFP (Δfloxed *Gfra1*) and NANOS3 (Fig. 34). Although NANOS3 expression was observed at detectable levels in the majority of undifferentiated spermatogonia [21, 68], I found that its expression was

much higher in GFP$^{low\ or\ -}$ spermatogonia (morphologically defined as A_{al}) than in GFP^{+} spermatogonia (morphologically defined as A_s or A_{pr}) (Fig. 34A). This expression pattern might reflect the process of spermatogonial differentiation from GFRA1 (GFP) -positive to a more mature NANOS3-positive state.

By using NANOS3 expression as a reference, I then evaluated the differentiation state of *Gfra1*-deficient cells at 5 weeks and found that most GFP-positive spermatogonia, including A_s or A_{pr} expressed NANOS3 strongly in the *Gfra1*-cKO testes (Fig. 34B). Quantitative analyses revealed that more than 80% of GFP-positive spermatogonial cluster in the *Gfra1*-cKO testes exhibited a strong NANOS3 signal, while 37.0% of GFP-positive cells in the control testes showed the signal (Fig. 34E). These results indicate that, GDNF signaling also acts as a suppressive factor on differentiation of spermatogonial stem cells, in addition to its positive function on spermatogonial proliferation.

On the contrary, *Nanos2*-overexpression decreased the level of NANOS3 expression in spermatogonia (Fig. 34C) as expected from my previous *Nanos2*-overexpression study induce by *Nanos3-Cre* (Fig. 23, G to L) [55]. Notably, the elevated NANOS3 expression caused by *Gfra1*-deletion was suppressed in the cells overexpressing *Nanos2* (Fig. 34D). In both *Gfra1*$^{\Delta/+}$; *Tg-Nanos2* and *Gfra1*$^{\Delta/\Delta}$; *Tg-Nanos2* mice, less than 10% of GFP-positive cells showed the NANOS3 signals (Fig. 34E). Hence, overexpressed *Nanos2* can delay the differentiation progression of spermatogonial stem cells caused by a conditional loss of *Gfra1* through the suppression of NANOS3. This result indicates that NANOS2 could suppress stem cell differentiation independent of GDNF signaling.

Overexpression of *Nanos2* in GFRA1-negative undifferentiated spermatogonia

To further investigate the GDNF signaling-independent NANOS2 function, I utilized *Ngn3-Cre* mice [51] to induce *Nanos2*-overexpression. Since *Ngn3* expression commences around 5 days after birth [51, 52] and becomes restricted in a distinct subpopulation of undifferentiated spermatogonia from GFRA1-positive population [21, 53] (Fig. 24A), I can expect ectopic induction of *Nanos2* in GFRA1-negative population by using this Cre line. To confirm this, I examined PLZF and GFRA1 expressions in the control and *Ngn3-Cre* driven *Nanos2*-overexpressing testes. In the controls, PLZF was expressed in undifferentiated spermatogonia including A_s, A_{pr} and A_{al} (Fig. 35, A to C). While, GFRA1 was expressed predominantly in A_s and A_{pr} spermatogonia, in which endogenous NANOS2 was co-expressed (Fig. 35, G to I). In the *Nanos2*-overexpressing testes, NANOS2-positive cells were abundantly observed on the basement membrane of seminiferous tubules and were positive for PLZF (Fig. 35, D to F), indicating that these cells were undifferentiated spermatogonia. However, only a small portion of the *Nanos2*-overexpressing cells was found to be GFRA1-positive (Fig. 35, J to L). These results suggest that *Nanos2*-overexpression was indeed induced in GFRA1-negative population by using *Ngn3-Cre* and that the ectopically expressed NANOS2 did not have the ability to induce GFRA1 expression in those cells.

NANOS2 suppresses proliferation and differentiation of GFRA1-negative undifferentiated spermatogonia

To further characterize these *Nanos2*-overexpressing cells induced by *Ngn3-Cre*, I examined apoptosis, proliferation and differentiation of these cells. I found that

PLZF-positive cells in *Nanos2*-overexpressing mice showed lower proliferation rates (Fig. 36B and Fig. 37B) and similar levels of apoptosis (Fig. 36A) compared to control spermatogonia, similar to the case in which *Nanos2* was induced via *Nanos3-Cre* [55] or *Ert2-Cre* (Fig. 30). The results suggest that NANOS2 suppresses proliferation, but does not affect apoptosis even in the GFRA1-negative spermatogonia.

Next, I examined differentiation states of the *Ngn3-Cre* driven *Nanos2*-overexpressing cells. As reported previously, I confirmed that *Nanos2*-overexpression resulted in the accumulation of PLZF-positive cells in the periphery of the tubules, while TRA98-positive germ cells in luminal side of the tubules were dramatically reduced [55] (Fig. 20, Fig. 36, C and D and Fig. 37A). This result suggests that ectopic NANOS2 expressed in the GFRA1-negative spermatogonia disturbed the proper production of differentiating germ cells. To further ask the effects of ectopic *Nanos2* on the earlier stages of spermatogonial differentiation, I examined the expression of NANOS3. In control testes, NANOS3 was highly expressed in A_{al} spermatogonia (Fig. 36, E to G). Intriguingly, although the majority of *Nanos2*-overexpressing spermatogonia did not express GFRA1 (Fig. 35, J to L), these cells were negative for NANOS3 (Fig. 36, H to J). Together, these results support my idea that NANOS2 does not act through GDNF signaling pathway to suppress differentiation of spermatogonial stem cells.

【Discussion】

Relationship between NANOS2 and retinoic acid signaling

In my current study, I demonstrated that *Nanos2*-overexpressing cells did not express NANOS3 or *Ngn3* (Fig. 23, Fig. 34, A to D and Fig. 36, E to J), indicating that NANOS2 might suppress spermatogonial differentiation, probably at the transition point from NANOS2^{+}/GFRA1^{+} to NANOS3^{+}/*Ngn3*$^{+}$ state. The next questions are: (1) what are critical downstream targets of NANOS2, which could be determinants of spermatogonial differentiation; (2) whether postnatal NANOS2 control share any target genes with that in the embryonic stage.

During embryogenesis, an RNA-binding protein DAZL (deleted in azoospermia-like), which is expressed by postmigratory germ cells in both male and female embryos, enables those cells to acquire the ability to respond to a meiosis-inducing signal, retinoic acid (RA) (which ability is called as a meiotic competence) [69] (Fig. 38). In female mice, meiosis commences at E13.5, which requires RA signals [70, 71] and its downstream factor STRA8 (stimulated by retinoic acid gene 8) [72]. On the other hand, meiosis is not initiated in male germ cells, since RA-inactivating enzyme CYP26B1 (cytochrome P450, family 26, subfamily b, polypeptide 1) keeps RA levels low in male gonads [70, 71]. After CYP26B1 expression is down-regulated, NANOS2 prevents male germ cells from entering meiosis by suppressing *Stra8* expression [39, 45].

After birth, RA signaling is required for the transition from undifferentiated A_{al} to differentiating A_1 spermatogonia, as it can be disrupted by vitamin A deficiency (VAD) conditions [73]. This result indicates that spermatogonial differentiation in VAD testes is disrupted at the later step than that in *Nanos2*-overexpressing testes (summarized in Fig.

39). Furthermore, it is reported that the suppression of *Stra8* seems not to be enough for blocking spermatogonial differentiation, since *Stra8*-null spermatogonia can differentiate to meiotic phases and showed defects in the progression of meiosis [74, 75]. Hence, it is unlikely that *Stra8* as well as other RA-downstream components are major targets of postnatal NANOS2. Rather, NANOS2 may be required for the upstream events of RA signaling in spermatogonial differentiation, which may be involved in the step acquiring competency to RA signals e. g. down-regulation of *Dazl* or other unknown factors.

Suppressive roles of NANOS2 and GDNF signaling for the differentiation of spermatogonial stem cells

Previous study showed that overexpression of GDNF resulted in the accumulation of A_s undifferentiated spermatogonia [7]. Consistently, conventional knockout of *Gdnf* or its receptors [8] or knockdown of *Gfra1* in culture [67] induced a precocious differentiation of spermatogonia. In cultured spermatogonial stem cells, several genes related to differentiation, for example, *Ngn3*, were up-regulated by GDNF/GFRA1 removal [62]. My current study demonstrated that conditional knockout of *Gfra1* caused up-regulation of NANOS3 in spermatogonial stem cells (Fig. 34, B and E). Therefore, GDNF signaling might act as a suppressive signal for early/initial step of spermatogonial differentiation, probably at the transition point from NANOS2$^+$/GFRA1$^+$ to NANOS3$^+$/*Ngn3*$^+$.

On the other hand, I had shown that NANOS2 also suppressed differentiation step of spermatogonia from NANOS2$^+$/GFRA1$^+$ into NANOS3$^+$/*Ngn3*$^+$ state cell-autonomously, since *Nanos2*-overexpression driven by *Nanos3-Cre* could maintain an undifferentiated state of spermatogonia [55]. However, it has been unclear whether

NANOS2 functions in a GDNF signaling-dependent or -independent manner to suppress stem cell differentiation, because the *Nanos2*-overexpressing cells induced via *Nanos3-Cre* also expressed GFRA1 (Fig. 22, J to L) [55]. In Chapter 2, I demonstrated that overexpressed *Nanos2* did prevent *Gfra1*-null stem cells from entering precocious differentiation (Fig. 34, D and E). I also revealed that *Nanos2*-overexpressing cells induced by *Ngn3-Cre* did prevent expression of differentiation marker NANOS3 in the absence of GFRA1 (Fig. 36, H to J). Thus, although both NANOS2 and GDNF signaling have similar roles in the regulation of stem cell differentiation, they might maintain undifferentiated state of spermatogonial stem cells acting through different or redundant mechanisms/pathways.

Opposite functions of NANOS2 and GDNF signaling for the proliferation of spermatogonial stem cells

The reduced stem cell proliferation rate in *Gfra1*-cKO mice (Fig. 30B), along with previously documented germ cell proliferation defects in *Gdnf*-, *Gfra1*- and *Ret*- null mice [8], as well as the requirement of GDNF and its downstream factors for the growth of spermatogonial stem cells in culture [56-58, 61, 67, 76, 77], demonstrate that proliferation of spermatogonial stem cells is highly dependent on the GDNF-stimulated pathway.

On the other hand, my current and previous studies indicated that *Nanos2*-overexpressing cells showed a lower proliferation rate than that of control spermatogonia [55] (Fig. 30B and Fig. 36B). Hence, one possible mechanism by which NANOS2 maintains the stem cell state is through the regulation of their cell cycle. This idea is supported by previous study in the *Drosophila* embryo, in which *Nanos* represses

the translation of maternal *CyclinB* mRNA in migrating germ cells, which in turn restricts these cells to enter mitosis [34, 35]. Although it has long been postulated that stem cells divide infrequently and are predominantly quiescent in haematopoietic or other adult tissue systems [78, 79], a link between cell division frequency and "stemness" in spermatogonial stem cells remains unclear and should be determined in future works, especially by focusing on the identification of NANOS2 targets in spermatogonial stem cell population.

Regulation of NANOS2 expression

In the adult testes, NANOS2 is preferentially expressed in the most primitive set of spermatogonia, and is down-regulated in their immediate progenies. One of the important remaining questions is the quest in identifying factor(s) that regulates NANOS2 expression during spermatogenesis. In my current study, I examined whether NANOS2 expression was affected by a loss of *Gfra1*. In the *Gfra1*-cKO (GFP-positive, Δfloxed *Gfra1*) cells, NANOS2 expression was decreased (Fig. 25, F and J). This data suggests that GDNF signaling pathway is one of the candidates to induce or maintain NANOS2 expression during spermatogenesis. However, I need further studies to distinguish the following two possibilities: (1) GDNF signaling is involved in the *Nanos2* transcriptional regulation; and (2) GDNF signaling indirectly affects *Nanos2* expression as a result of maintaining proper cellular state of spermatogonial stem cells.

Regulation of competency against niche signals in a germ cell-autonomous manner

Recent report suggests that another stem cell-intrinsic factor PLZF controls stem cell-intrinsic competency against GDNF signals [80]. The authors show that PLZF keeps

mTORC1 (mammalian target of rapamycin complex 1) activity low and allows GDNF-receptor mediated Akt activation. In the absence of PLZF, mTORC1 becomes hyper-activated, followed by down-regulation of the GDNF-receptor components and thus prevents sufficient Akt activation in response to niche-derived GDNF. However, it is still unclear how GFRA1/RET expression is restricted in a small part of PLZF-positive undifferentiated spermatogonia.

In this regard, I noticed that the majority of *Nanos2*-overexpressing cells induced by *Nanos3-Cre* expressed GFRA1 (Fig. 22, J to L) [55]. Based on this result, I initially speculated that NANOS2 might induce/maintain GFRA1 expression directly or indirectly to restrict cell-autonomous responsibility to the GDNF signals. However, in my current study, I revealed that the *Nanos2*-overexpression by *Ngn3-Cre* did not induce ectopic GFRA1 expression (Fig. 35, J to L). Therefore, the mechanism of germ cell-intrinsic regulation against niche signals is still obscure and is an essential future work.

【Conclusion】

Understanding the regulatory mechanisms of stem cells is an important issue in stem cell biology. Despite of progresses in identifying factors essential to maintain these stem cells during murine spermatogenesis, following problems still remained: (1) A precise identification of functional stem cells in intact testes had not been achieved due to a lack of their specific molecular markers; and (2) a loss of function study had some limitation to understand what actually happens in the stem cells upon the gene-deletion. In Chapter 1 of my thesis, I revealed that NANOS2 was expressed in spermatogonial stem cells in intact testes and maintained these cells in an undifferentiated, self-renewing state. Furthermore, in Chapter 2, I showed that NANOS2 and GDNF signaling coordinately regulated stem cell state during murine spermatogenesis. I found that NANOS2 was capable of suppressing differentiation of spermatogonial stem cells in a GDNF signaling-independent manner. In the aspect of stem cell proliferation, NANOS2 and GDNF signaling had opposite functions. These studies thus offer a novel insight into understanding how stem cells are maintained in murine testes.

【Materials and Methods】

Mice

All mice used in this study were maintained in the animal facility in National Institute of Genetics, Japan. The wild-type mice used in this study are MCH (a closed colony established in CLEA, Japan). Mice older than 6 weeks were analyzed as adults.

Generation of transgenic mice

All constructs were digested with restriction enzymes to remove vector sequences and then gel purified. Transgenic mice were generated by microinjection of fertilized eggs. Microinjected eggs were then transferred into the oviducts of pseudopregnant foster females. The genotypes of the offspring were identified by PCR using tail DNA. More than two independent transgenic lines were established for each construct.

Pulse-chase experiments of *Nanos2*-expressing spermatogonia

To construct a TM-inducible version of Cre under the control of an endogenous *Nanos2* enhancer (*Nanos2-MCM*), a DNA fragment containing 8.6 kb of upstream region of the mouse *Nanos2* gene was ligated with a *MER-Cre-MER* sequence (courtesy of Dr. S. Evans) [46] followed by the 3'UTR of the *Nanos2* gene. The *Nanos2-MCM* transgenic mouse lines were subsequently established. I crossed the *Nanos2-MCM* mice with *R26R* [47] or *CAG-CAT-EGFP* (courtesy of Dr. J. Miyazaki) reporter mice. Six-week-old *Nanos2-MCM*; *R26R* or *Nanos2-MCM*; *CAG-CAT-EGFP* mice were intraperitoneally injected with TM (75 mg/kg body weight; Sigma, dissolved in Corn oil [Sigma] at 10 mg/ml) for 5 consecutive days, and their testes were sacrificed at 7-, 8-, 10-, 18-, 22- and

26- weeks of age.

Conditional knockout of postnatal *Nanos2*

The *Nanos2*-null mouse line has been established previously as the *Nanos2 LacZ*-knock-in mouse [40]. For generation of conditional *Nanos2* transgenic construct containing the *floxed 3xFlag-tagged Nanos2* under the control of 8.6 kb of endogenous *Nanos2* enhancer, loxP sequences were inserted in the XbaI and EcoRV sites of the *Nanos2* enhancer-*3xFlag-tagged Nanos2* construct [81]. The transgenic mouse line (*Nanos2* enhancer-*floxed 3xFlag-tagged Nanos2*) were subsequently introduced the *Nanos2*-null genetic backgrounds. The FLAG-tagged NANOS2 protein is functional in vivo and can rescue the *Nanos2*-null mouse defects. To remove a *floxed 3xFlag-tagged Nanos2* sequence, I introduced a transgene, *Ert2-Cre*, a TM-inducible Cre recombinase expressed ubiquitously from *Rosa* locus (Artemis Pharmaceuticals GmbH).

For lineage tracing of *Nanos2*-cKO or control cells, I generated triple transgenic mice, *Nanos2-MCM*; *R26R*; *Nanos2* enhancer-*floxed 3xFlag-tagged Nanos2* in *Nanos2* -null or -hetero backgrounds, respectively.

To induce Cre activity, TM was administrated to 4-week-old mice (75mg/kg body weight) for 5 consecutive days. The testes were dissected at indicated time points.

Nanos2*-overexpression in germ cells by using *Nanos3-Cre* or *Ngn3-Cre

For conditional activation of *Nanos2*, I used the previously established transgenic mice *CAG-floxed CAT-3xFlag-Nanos2* [45]. I intercrossed the transgenic female mice with *Nanos3 Cre* knock-in [49] or the *Ngn3-Cre* (courtesy of Dr. S. Yoshida) [51] male mice

and obtained *CAG-floxed CAT-3xFlag-Nanos2*; *Cre* double transgenic male pups. The littermate *CAG-floxed CAT-3xFlag-Nanos2* transgenic males (without *Cre*) were used as controls.

To analyze *Ngn3* expression in the *Nanos2*-overexpressing mouse backgrounds, I first generated double transgenic females with *Ngn3-EGFP* (courtesy of Dr. S. Yoshida) [51] and the *CAG-floxed CAT-3xFlag-Nanos2*. The *Ngn3-EGFP*; *CAG-floxed CAT-3xFlag-Nanos2* mice were crossed with *Nanos3-Cre*, resulting triple transgenic males were obtained and analyzed.

Gfra1-conditional knockout simultaneously with _Nanos2_-overexpression by a tamoxifen-inducible Cre

To induce conditional inactivation of *Gfra1*, *Gfra1* floxed mice (courtesy of Dr. H. Enomoto) [65] (Fig. 24B) were crossed with *Ert2-Cre* line that ubiquitously expressed a tamoxifen (TM) inducible Cre recombinase (Artemis Pharmaceuticals GmbH). For conditional activation of *Nanos2*, I subsequently introduced transgene, *CAG-floxed CAT-3xFlag-Nanos2* [45] (*Tg-Nanos2*) (Fig. 24C) in the *Gfra1*-cKO background. I generated in a total 4 kinds of mice harboring the following alleles: (1) $Gfra1^{flox/+}$; *Ert2-Cre*, (2) $Gfra1^{flox/flox}$; *Ert2-Cre*, (3) $Gfra1^{flox/+}$; *Ert2-Cre*; *Tg-Nanos2* and (4) $Gfra1^{flox/flox}$; *Ert2-Cre*; *Tg-Nanos2*. Correspondingly, activation of Cre recombinase produces (1) $Gfra1^{\Delta/+}$; *Ert2-Cre* (control), (2) $Gfra1^{\Delta/\Delta}$; *Ert2-Cre* (*Gfra1*-cKO), (3) $Gfra1^{\Delta/+}$; *Ert2-Cre*; *Tg-Nanos2* (*Nanos2*-overexpression), and (4) $Gfra1^{\Delta/\Delta}$; *Ert2-Cre*; *Tg-Nanos2* (*Nanos2*-overexpression in the *Gfra1*-cKO background). Cre activity was induced by intraperitoneal injection of TM (75 mg/kg body weight; Sigma, dissolved in

Corn oil [Sigma]) into 4-week-old mice for 5 consecutive days. The testes from each genotype of mice were dissected at indicated time points (Fig. 24D).

Genotyping

Genomic DNA was isolated from tails and mouse genotypes were determined by PCR. The primers used were as follows:

MCM-F (5'-CCATATCCGGCACATGAGTAACAAAA-3')

N2-3'U-R2 (5'-CCGAGAAGTCATCACCAG-3')

for the *Nanos2-MCM* transgene;

Rosa#2 (5'-GCGAAGAGTTTGTCCTCAACC-3')

Rosa#4 (5'-AAAGTCGCTCTGAGTTGTTAT-3')

for the *Rosa26 reporter* targeted allele;

Rosa#2 (5'-GCGAAGAGTTTGTCCTCAACC-3')

Rosa#3 (5'-GGAGCGGGAGAAATGGATATG-3')

for the *Rosa26 reporter* wild-type allele;

EGFP-F (5'- TACGGCAAGCTGACCCTGAA-3')

EGFP-R (5'- CATGTGATCGCGCTTCTCGT-3')

for the *EGFP* transgenes;

3'lacZ-1 (5'-GGAGCCCGTCAGTATCGGCGGAATT-3')

N2-LA-R1 (5'-TCCCAGTCAGACGACTTG-3')

for the *Nanos2 LacZ*-knock-in allele;

N2-F (suzu) (5'-GGCAGAGAAGAATGCCAGTT-3')

N2-R (suzu) (5'-TGTTCCCAGTCAGACGACTT-3')

for the *Nanos2* wild-type allele;

3FLAG-F1 (5'-CTACAAAGACCATGACGGTG-3')

N2-3'U-R2 (5'-CCGAGAAGTCATCACCAG-3')

for the *Flag-tagged Nanos2* transgenes used for both *Nanos2* -cKO and -overexpression study;

Cre1 (5'-GGACATGTTCAGGGATCGCCAGGCG-3')

Cre2 (5'-GCATAACCAGTGAAACAGCATTGCTG-3')

for the *Cre* allele;

Ert2-Cre SA-F1 (5'-TGTTGCAATACCTTTCTGGGAGTTC-3')

Ert2-Cre LA-R1 (5'-AGAAGGAGCGGGAGAAATGGATATG-3')

for the *Ert2-Cre* wild-type allele;

GFRa1 P1 (5'-CTTCCAGGTTGGGTCGGAACTGAACCC-3')

GFRa1 M202 (5'-TGGCAGCACGAAGTACAGAGTGGCTAGGAACAT-3')

for the floxed *Gfra1* targeted or wild-type allele, which were determined by the presence of 310 and 280 bp fragments, respectively; and

GFRa1 P1 (5'-CTTCCAGGTTGGGTCGGAACTGAACCC-3')

GFRa1 P3 (5'-TTTACGTCGCCGTCCAGCTCGA-3').

for the *Gfra1 EGFP*-knock-in alleles.

X-gal staining

For X-gal staining, the testes were removed from the tunica albuginea and were untangled before fixation. The seminiferous tubules were subsequently fixed in a PBS solution containing 2% PFA, 0.2% glutaraldehyde and 0.02% NP-40 at 4°C for 20 min. Then,

samples were stained for the detection of β-galactosidase activity at 37°C in PBS containing 1 mg/ml X-gal, 5 mM $K_3(CN)_6$, 5 mM $K_4Fe(CN)_6$, and 2 mM $MgCl_2$. The stained specimens were photographed and then embedded in paraffin and sectioned.

Histological methods

For hematoxylin-eosin (H-E) staining, testes were fixed in Bouin's solution for overnight at room temperature (RT) and embedded in paraffin. Six micron sections were deparaffinized, dehydrated, and stained with Mayer's Hematoxylin (Wako) followed by staining with Eosin D (Merck). The stained sections were mounted with Mount-Quick (Daido Sangyo) and were examined using an Olympus BX51 microscope and digitally imaged using a AxioCam HRC camera (Zeiss).

For immunofluorescence analysis, testes and embryonic gonads were directly embedded in OCT compound (Tissue Tek, Sakura) or fixed in 4% PFA for overnight at 4°C and embedded in paraffin. The frozen sections (8 μm) were fixed with 4% PFA for 10 min at 4°C. After blocking with PBS containing 3% skim milk (Yukijirushi) for 1 hour at RT, sections were rinsed and incubated overnight with primary antibodies at 4°C. The following day, the sections were washed in PBS and were incubated for 1 hour with secondary antibodies at RT. After washing, these sections were then counterstained with DAPI (Sigma) and mounted with Gel/Mount (Biomeda). Preparations were examined using an Olympus BX61 microscope and digitally imaged using a Hamamatsu C4742-98 CCD camera.

For paraffin-embedded samples, sections (6 μm) were autoclaved at 105°C for 15 minutes in antigen unmasking solution (Vector Laboratories) after deparaffinization and

hydration. After blocking with PBS containing 3% skim milk for 1 hour at RT, sections were rinsed and incubated overnight with primary antibodies at 4°C. The following day, the sections were washed in PBS and incubated with secondary antibodies for 1 hour at RT. After washing, these sections were counterstained with DAPI (Sigma) and enclosed.

Primary antibodies were used at the following dilutions: rabbit anti-NANOS2 [81] (1:100), rat TRA98 (1:5000, a gift from Dr. Y. Nishimune), rabbit anti-PLZF (1:500, Santa Cruz), rabbit anti-SCP3 (1:500, a gift from Drs., S. Chuma and N. Nakatsuji), mouse anti-FLAG (1:5000, Sigma), rat anti-KIT (1:20, Chemicon), armenian hamster anti-KIT (1:500, a gift from Dr. T. Hirata), mouse anti-cleaved PARP (1:200, Cell Signaling), rabbit anti-phspho Histone H3 (1:500, Millipore), rabbit anti-cleaved CASPASE-3 (1:200, Cell Signaling) and chick anti-GFP (1:500, MBL). All secondary antibodies were used at a 1:250 dilution: anti-rabbit, anti-mouse, anti-rat or anti-chick IgG antibodies conjugated with either Alexa-488 or Alexa-594 (Molecular Probes) and anti-armenian hamster IgG conjugated with Cy3 (Jackson ImmunoResearch).

BrdU staining

Mice were injected intraperitoneally with BrdU (100 mg/kg body weight; Sigma, dissolved in saline at 10 mg/ml) 3 hours before sacrifice. Testes were fixed in 4% PFA, and embedded in paraffin. After deparaffinization and hydration, the sections (6 μm) were autoclaved at 105°C for 15 minutes in antigen unmasking solution. After blocking with 3% skim milk for 1 hour, the sections were incubated overnight at 4°C with rabbit anti-PLZF (1:500) antibody. The following day, the sections were washed in PBS and were incubated with secondary antibodies for 1 hour at RT. Then, the stained specimens were postfixed

with 4% PFA for 20 minutes at 4°C. After that, the section were treated with 2 N hydrochloric acid for 20 minutes at RT and then with 0.1% Trypsin (Sigma)/PBS for 30 minutes at 37℃. After washing, the specimens were subsequently stained with mouse anti-BrdU antibody (1:500, Sigma) at 4°C overnight. The following procedures are the same as the immunostaining method described above.

Whole-mount immunohistochemistry

After removing from the tunica albuginea, the seminiferous tubules were digested with 1mg/ml of collagenase typeⅡ (Sigma)/PBS or were untangled physically. The tubules were rinsed by PBS and subsequently fixed with 4% paraformaldehyde (PFA) for 2 hours at 4°C. After washing with PBS-T (0.3% TritonX-100/PBS), the specimens were incubated with 3% skim milk/PBS-T for 1 hour at room temperature (RT). Then they were rinsed with PBS-T and incubated with primary antibodies at RT overnight. The following day, the tubules were washed with PBS-T and were incubated with secondary antibodies at 4°C overnight. After that, they were washed with PBS-T before mounting. The specimens were examined using a confocal laser scanning microscope (Zeiss LSM510).

Primary antibodies were used at the following dilutions: rabbit anti-NANOS2 [81] (1:500), goat anti-GFRA1 (1:200, R&D Systems), rat anti-GFP (1:500, Nacalai Tesque), rabbit anti-NANOS3 [81] (1:500), mouse anti-FLAG (1:5000, Sigma) and rabbit anti-PLZF (1:1000, Santa Cruz). All secondary antibodies were used at a 1:250 dilution: anti-rabbit, anti-goat, anti-rat or anti-mouse IgG antibodies conjugated with either Alexa-488 or Alexa-594.

Statistics

All statistical analyses in this study were performed using the Student's *t*-test. Statistical significance was defined as $P<0.05$.

RT-PCR

Total RNAs were isolated from 5-week-old control and *Nanos2*-cKO testes prepared by using RNeasy (Qiagen) and used for reverse-transcription by Super script III (Invitrogen). The primers used were as follows:

mNos2-F4 (5'-ACAGCAGTCAGTCAGTCTC-3')

N2-3'U-R2 (5'- CCGAGAAGTCATCACCAG -3')

for *Nanos2* mRNA; and

Gapdh-F (5'-ACCACAGTCCATGCCATCAC-3')

Gapdh-R (5'-TCCACCACCCTGTTGCTGTA-3')

for *Gapdh* mRNA.

【Acknowledgements】

I am grateful to Dr. Y. Saga for supervising my entire research. I thank all members of Mammalian Development Laboratory for valuable suggestions and supporting this work; the members of Progress Report Committee, Drs., N. Sakai, Y. Hiromi, M. Asaoka, K. Nonomura, H. Sasaki, M. Okada for critical advices and discussions; Dr. S. Yoshida for the *Ngn3*-EGFP and *Ngn3-Cre* transgenic mice; Dr. Y. Nishimune for the TRA98 antibody; Dr. S. Evans for the *MER-Cre-MER* construct; Dr. J. Miyazaki for *CAG-CAT-EGFP* transgenic mice; Drs., S. Chuma and N. Nakatsuji for the anti-SCP3 antibody; Dr. H. Enomoto for the *Gfra1* floxed mice; and Dr, T. Hirata for the anti-Kit antibody.

This study was supported in part by Research Fellowships of the Japan Society for the Promotion of Science Young Scientists and by 1st Presidential Award FY2010 (SOKENDAI University).

【References】

1. Russell L, Ettlin, R., Sinha Hikim, A., and Clegg, E. Histological and Histopathological Evaluation of the Testis. Clearwater, FL: Cache River Press 1990.
2. Atchison FW, Means AR. Spermatogonial depletion in adult Pin1-deficient mice. Biol Reprod 2003; 69: 1989-1997.
3. Buaas FW, Kirsh AL, Sharma M, McLean DJ, Morris JL, Griswold MD, de Rooij DG, Braun RE. Plzf is required in adult male germ cells for stem cell self-renewal. Nat Genet 2004; 36: 647-652.
4. Chen C, Ouyang W, Grigura V, Zhou Q, Carnes K, Lim H, Zhao GQ, Arber S, Kurpios N, Murphy TL, Cheng AM, Hassell JA, Chandrashekar V, Hofmann MC, Hess RA, Murphy KM. ERM is required for transcriptional control of the spermatogonial stem cell niche. Nature 2005; 436: 1030-1034.
5. Costoya JA, Hobbs RM, Barna M, Cattoretti G, Manova K, Sukhwani M, Orwig KE, Wolgemuth DJ, Pandolfi PP. Essential role of Plzf in maintenance of spermatogonial stem cells. Nat Genet 2004; 36: 653-659.
6. Falender AE, Freiman RN, Geles KG, Lo KC, Hwang K, Lamb DJ, Morris PL, Tjian R, Richards JS. Maintenance of spermatogenesis requires TAF4b, a gonad-specific subunit of TFIID. Genes Dev 2005; 19: 794-803.
7. Meng X, Lindahl M, Hyvonen ME, Parvinen M, de Rooij DG, Hess MW, Raatikainen-Ahokas A, Sainio K, Rauvala H, Lakso M, Pichel JG, Westphal H, Saarma M, Sariola H. Regulation of cell fate decision of undifferentiated spermatogonia by GDNF. Science 2000; 287: 1489-1493.
8. Naughton CK, Jain S, Strickland AM, Gupta A, Milbrandt J. Glial cell-line derived neurotrophic factor-mediated RET signaling regulates spermatogonial stem cell fate. Biol Reprod 2006; 74: 314-321.
9. Schlesser HN, Simon L, Hofmann MC, Murphy KM, Murphy T, Hess RA, Cooke PS. Effects of ETV5 (ets variant gene 5) on testis and body growth, time course of spermatogonial stem cell loss, and fertility in mice. Biol Reprod 2008; 78: 483-489.
10. Takubo K, Ohmura M, Azuma M, Nagamatsu G, Yamada W, Arai F, Hirao A, Suda T. Stem cell defects in ATM-deficient undifferentiated spermatogonia through DNA damage-induced cell-cycle arrest. Cell Stem Cell 2008; 2: 170-182.
11. Morrison SJ, Spradling AC. Stem cells and niches: mechanisms that promote stem cell maintenance throughout life. Cell 2008; 132: 598-611.

12. de Rooij DG. Stem cells in the testis. Int J Exp Pathol 1998; 79: 67-80.
13. de Rooij DG, Grootegoed JA. Spermatogonial stem cells. Curr Opin Cell Biol 1998; 10: 694-701.
14. de Rooij DG, Russell LD. All you wanted to know about spermatogonia but were afraid to ask. J Androl 2000; 21: 776-798.
15. de Rooij DG. Proliferation and differentiation of spermatogonial stem cells. Reproduction 2001; 121: 347-354.
16. Huckins C. The spermatogonial stem cell population in adult rats. II. A radioautographic analysis of their cell cycle properties. Cell Tissue Kinet 1971; 4: 313-334.
17. Oakberg EF. Spermatogonial stem-cell renewal in the mouse. Anat Rec 1971; 169: 515-531.
18. Oatley JM, Brinster RL. Spermatogonial stem cells. Methods Enzymol 2006; 419: 259-282.
19. Oatley JM, Brinster RL. Regulation of Spermatogonial Stem Cell Self-Renewal in Mammals. Annu Rev Cell Dev Biol 2008; 24: 263-286.
20. Nakagawa T, Nabeshima Y, Yoshida S. Functional identification of the actual and potential stem cell compartments in mouse spermatogenesis. Dev Cell 2007; 12: 195-206.
21. Suzuki H, Sada A, Yoshida S, Saga Y. The heterogeneity of spermatogonia is revealed by their topology and expression of marker proteins including the germ cell-specific proteins Nanos2 and Nanos3. Dev Biol 2009; 336: 222-231.
22. Tokuda M, Kadokawa Y, Kurahashi H, Marunouchi T. CDH1 is a specific marker for undifferentiated spermatogonia in mouse testes. Biol Reprod 2007; 76: 130-141.
23. Zheng K, Wu X, Kaestner KH, Wang PJ. The pluripotency factor LIN28 marks undifferentiated spermatogonia in mouse. BMC Dev Biol 2009; 9: 38.
24. Draper BW, McCallum CM, Moens CB. nanos1 is required to maintain oocyte production in adult zebrafish. Dev Biol 2007; 305: 589-598.
25. Jaruzelska J, Kotecki M, Kusz K, Spik A, Firpo M, Reijo Pera RA. Conservation of a Pumilio-Nanos complex from Drosophila germ plasm to human germ cells. Dev Genes Evol 2003; 213: 120-126.
26. Kobayashi S, Yamada M, Asaoka M, Kitamura T. Essential role of the posterior morphogen nanos for germline development in Drosophila. Nature 1996; 380: 708-711.
27. Koprunner M, Thisse C, Thisse B, Raz E. A zebrafish nanos-related gene is

essential for the development of primordial germ cells. Genes Dev 2001; 15: 2877-2885.

28. Kurokawa H, Aoki Y, Nakamura S, Ebe Y, Kobayashi D, Tanaka M. Time-lapse analysis reveals different modes of primordial germ cell migration in the medaka Oryzias latipes. Dev Growth Differ 2006; 48: 209-221.
29. Mochizuki K, Sano H, Kobayashi S, Nishimiya-Fujisawa C, Fujisawa T. Expression and evolutionary conservation of nanos-related genes in Hydra. Dev Genes Evol 2000; 210: 591-602.
30. Mosquera L, Forristall C, Zhou Y, King ML. A mRNA localized to the vegetal cortex of Xenopus oocytes encodes a protein with a nanos-like zinc finger domain. Development 1993; 117: 377-386.
31. Pilon M, Weisblat DA. A nanos homolog in leech. Development 1997; 124: 1771-1780.
32. Subramaniam K, Seydoux G. nos-1 and nos-2, two genes related to Drosophila nanos, regulate primordial germ cell development and survival in Caenorhabditis elegans. Development 1999; 126: 4861-4871.
33. Wang Z, Lin H. Nanos maintains germline stem cell self-renewal by preventing differentiation. Science 2004; 303: 2016-2019.
34. Asaoka-Taguchi M, Yamada M, Nakamura A, Hanyu K, Kobayashi S. Maternal Pumilio acts together with Nanos in germline development in Drosophila embryos. Nat Cell Biol 1999; 1: 431-437.
35. Kadyrova LY, Habara Y, Lee TH, Wharton RP. Translational control of maternal Cyclin B mRNA by Nanos in the Drosophila germline. Development 2007; 134: 1519-1527.
36. Murata Y, Wharton RP. Binding of pumilio to maternal hunchback mRNA is required for posterior patterning in Drosophila embryos. Cell 1995; 80: 747-756.
37. Sato K, Hayashi Y, Ninomiya Y, Shigenobu S, Arita K, Mukai M, Kobayashi S. Maternal Nanos represses hid/skl-dependent apoptosis to maintain the germ line in Drosophila embryos. Proc Natl Acad Sci U S A 2007; 104: 7455-7460.
38. Sonoda J, Wharton RP. Drosophila Brain Tumor is a translational repressor. Genes Dev 2001; 15: 762-773.
39. Suzuki A, Igarashi K, Aisaki K, Kanno J, Saga Y. NANOS2 interacts with the CCR4-NOT deadenylation complex and leads to suppression of specific RNAs. Proc Natl Acad Sci U S A 2010; 107: 3594-3599.
40. Tsuda M, Sasaoka Y, Kiso M, Abe K, Haraguchi S, Kobayashi S, Saga Y.

Conserved role of nanos proteins in germ cell development. Science 2003; 301: 1239-1241.

41. McLaren A. Primordial germ cells in the mouse. Dev Biol 2003; 262: 1-15.
42. Bellve AR, Cavicchia JC, Millette CF, O'Brien DA, Bhatnagar YM, Dym M. Spermatogenic cells of the prepuberal mouse. Isolation and morphological characterization. J Cell Biol 1977; 74: 68-85.
43. McLean DJ, Friel PJ, Johnston DS, Griswold MD. Characterization of spermatogonial stem cell maturation and differentiation in neonatal mice. Biol Reprod 2003; 69: 2085-2091.
44. Tsuda M, Kiso M, Saga Y. Implication of nanos2-3'UTR in the expression and function of nanos2. Mech Dev 2006; 123: 440-449.
45. Suzuki A, Saga Y. Nanos2 suppresses meiosis and promotes male germ cell differentiation. Genes Dev 2008; 22: 430-435.
46. Laugwitz KL, Moretti A, Lam J, Gruber P, Chen Y, Woodard S, Lin LZ, Cai CL, Lu MM, Reth M, Platoshyn O, Yuan JX, Evans S, Chien KR. Postnatal isl1+ cardioblasts enter fully differentiated cardiomyocyte lineages. Nature 2005; 433: 647-653.
47. Soriano P. Generalized lacZ expression with the ROSA26 Cre reporter strain. . Nat. Genet. 1999; 21: 70-71.
48. Hayashi Y, Hayashi M, Kobayashi S. Nanos suppresses somatic cell fate in Drosophila germ line. Proc Natl Acad Sci U S A 2004; 101: 10338-10342.
49. Suzuki H, Tsuda M, Kiso M, Saga Y. Nanos3 maintains the germ cell lineage in the mouse by suppressing both Bax-dependent and -independent apoptotic pathways. Dev Biol 2008; 318: 133-142.
50. Gilboa L, Lehmann R. Repression of primordial germ cell differentiation parallels germ line stem cell maintenance. Curr Biol 2004; 14: 981-986.
51. Yoshida S, Takakura A, Ohbo K, Abe K, Wakabayashi J, Yamamoto M, Suda T, Nabeshima Y. Neurogenin3 delineates the earliest stages of spermatogenesis in the mouse testis. Dev Biol 2004; 269: 447-458.
52. Yoshida S, Sukeno M, Nakagawa T, Ohbo K, Nagamatsu G, Suda T, Nabeshima Y. The first round of mouse spermatogenesis is a distinctive program that lacks the self-renewing spermatogonia stage. Development 2006; 133: 1495-1505.
53. Nakagawa T, Sharma M, Nabeshima Y, Braun RE, Yoshida S. Functional hierarchy and reversibility within the murine spermatogenic stem cell compartment. Science 2010; 328: 62-67.

54. Klein AM, Nakagawa T, Ichikawa R, Yoshida S, Simons BD. Mouse germ line stem cells undergo rapid and stochastic turnover. Cell Stem Cell 2010; 7: 214-224.
55. Sada A, Suzuki A, Suzuki H, Saga Y. The RNA-binding protein NANOS2 is required to maintain murine spermatogonial stem cells. Science 2009; 325: 1394-1398.
56. Braydich-Stolle L, Kostereva N, Dym M, Hofmann MC. Role of Src family kinases and N-Myc in spermatogonial stem cell proliferation. Dev Biol 2007; 304: 34-45.
57. He Z, Jiang J, Kokkinaki M, Golestaneh N, Hofmann MC, Dym M. Gdnf upregulates c-Fos transcription via the Ras/Erk1/2 pathway to promote mouse spermatogonial stem cell proliferation. Stem Cells 2008; 26: 266-278.
58. Hofmann MC, Braydich-Stolle L, Dym M. Isolation of male germ-line stem cells; influence of GDNF. Dev Biol 2005; 279: 114-124.
59. Hofmann MC. Gdnf signaling pathways within the mammalian spermatogonial stem cell niche. Mol Cell Endocrinol 2008; 288: 95-103.
60. Lee J, Kanatsu-Shinohara M, Inoue K, Ogonuki N, Miki H, Toyokuni S, Kimura T, Nakano T, Ogura A, Shinohara T. Akt mediates self-renewal division of mouse spermatogonial stem cells. Development 2007; 134: 1853-1859.
61. Lee J, Kanatsu-Shinohara M, Morimoto H, Kazuki Y, Takashima S, Oshimura M, Toyokuni S, Shinohara T. Genetic reconstruction of mouse spermatogonial stem cell self-renewal in vitro by Ras-cyclin D2 activation. Cell Stem Cell 2009; 5: 76-86.
62. Oatley JM, Avarbock MR, Telaranta AI, Fearon DT, Brinster RL. Identifying genes important for spermatogonial stem cell self-renewal and survival. Proc Natl Acad Sci U S A 2006; 103: 9524-9529.
63. Oatley JM, Avarbock MR, Brinster RL. Glial cell line-derived neurotrophic factor regulation of genes essential for self-renewal of mouse spermatogonial stem cells is dependent on Src family kinase signaling. J Biol Chem 2007; 282: 25842-25851.
64. Wu X, Oatley JM, Oatley MJ, Kaucher AV, Avarbock MR, Brinster RL. The POU domain transcription factor POU3F1 is an important intrinsic regulator of GDNF-induced survival and self-renewal of mouse spermatogonial stem cells. Biol Reprod 2010; 82: 1103-1111.
65. Uesaka T, Jain S, Yonemura S, Uchiyama Y, Milbrandt J, Enomoto H. Conditional ablation of GFRalpha1 in postmigratory enteric neurons triggers unconventional neuronal death in the colon and causes a Hirschsprung's disease phenotype. Development 2007; 134: 2171-2181.

66. He S, Nakada D, Morrison SJ. Mechanisms of stem cell self-renewal. Annu Rev Cell Dev Biol 2009; 25: 377-406.
67. He Z, Jiang J, Hofmann MC, Dym M. Gfra1 silencing in mouse spermatogonial stem cells results in their differentiation via the inactivation of RET tyrosine kinase. Biol Reprod 2007; 77: 723-733.
68. Yamaji M, Tanaka T, Shigeta M, Chuma S, Saga Y, Saitou M. Functional reconstruction of NANOS3 expression in the germ cell lineage by a novel transgenic reporter reveals distinct subcellular localizations of NANOS3. Reproduction 2009; 139: 381-393.
69. Lin Y, Gill ME, Koubova J, Page DC. Germ cell-intrinsic and -extrinsic factors govern meiotic initiation in mouse embryos. Science 2008; 322: 1685-1687.
70. Bowles J, Knight D, Smith C, Wilhelm D, Richman J, Mamiya S, Yashiro K, Chawengsaksophak K, Wilson MJ, Rossant J, Hamada H, Koopman P. Retinoid signaling determines germ cell fate in mice. Science 2006; 312: 596-600.
71. Koubova J, Menke DB, Zhou Q, Capel B, Griswold MD, Page DC. Retinoic acid regulates sex-specific timing of meiotic initiation in mice. Proc Natl Acad Sci U S A 2006; 103: 2474-2479.
72. Baltus AE, Menke DB, Hu YC, Goodheart ML, Carpenter AE, de Rooij DG, Page DC. In germ cells of mouse embryonic ovaries, the decision to enter meiosis precedes premeiotic DNA replication. Nat Genet 2006; 38: 1430-1434.
73. van Pelt AM, de Rooij DG. Synchronization of the seminiferous epithelium after vitamin A replacement in vitamin A-deficient mice. Biol Reprod 1990; 43: 363-367.
74. Anderson EL, Baltus AE, Roepers-Gajadien HL, Hassold TJ, de Rooij DG, van Pelt AM, Page DC. Stra8 and its inducer, retinoic acid, regulate meiotic initiation in both spermatogenesis and oogenesis in mice. Proc Natl Acad Sci U S A 2008; 105: 14976-14980.
75. Mark M, Jacobs H, Oulad-Abdelghani M, Dennefeld C, Feret B, Vernet N, Codreanu CA, Chambon P, Ghyselinck NB. STRA8-deficient spermatocytes initiate, but fail to complete, meiosis and undergo premature chromosome condensation. J Cell Sci 2008; 121: 3233-3242.
76. Kanatsu-Shinohara M, Ogonuki N, Inoue K, Miki H, Ogura A, Toyokuni S, Shinohara T. Long-term proliferation in culture and germline transmission of mouse male germline stem cells. Biol Reprod 2003; 69: 612-616.
77. Kubota H, Avarbock MR, Brinster RL. Growth factors essential for self-renewal

and expansion of mouse spermatogonial stem cells. Proc Natl Acad Sci U S A 2004; 101: 16489-16494.

78. Fuchs E. The tortoise and the hair: slow-cycling cells in the stem cell race. Cell 2009; 137: 811-819.

79. Orford KW, Scadden DT. Deconstructing stem cell self-renewal: genetic insights into cell-cycle regulation. Nat Rev Genet 2008; 9: 115-128.

80. Hobbs RM, Seandel M, Falciatori I, Rafii S, Pandolfi PP. Plzf regulates germline progenitor self-renewal by opposing mTORC1. Cell 2010; 142: 468-479.

81. Suzuki A, Tsuda M, Saga Y. Functional redundancy among Nanos proteins and a distinct role of Nanos2 during male germ cell development. Development 2007; 134: 77-83.

82. Brinster RL, Zimmermann JW. Spermatogenesis following male germ-cell transplantation. Proc Natl Acad Sci U S A 1994; 91: 11298-11302.

83. Nicholson DW, Ali A, Thornberry NA, Vaillancourt JP, Ding CK, Gallant M, Gareau Y, Griffin PR, Labelle M, Lazebnik YA, et al. Identification and inhibition of the ICE/CED-3 protease necessary for mammalian apoptosis. Nature 1995; 376: 37-43.

84. Tewari M, Quan LT, O'Rourke K, Desnoyers S, Zeng Z, Beidler DR, Poirier GG, Salvesen GS, Dixit VM. Yama/CPP32 beta, a mammalian homolog of CED-3, is a CrmA-inhibitable protease that cleaves the death substrate poly(ADP-ribose) polymerase. Cell 1995; 81: 801-809.

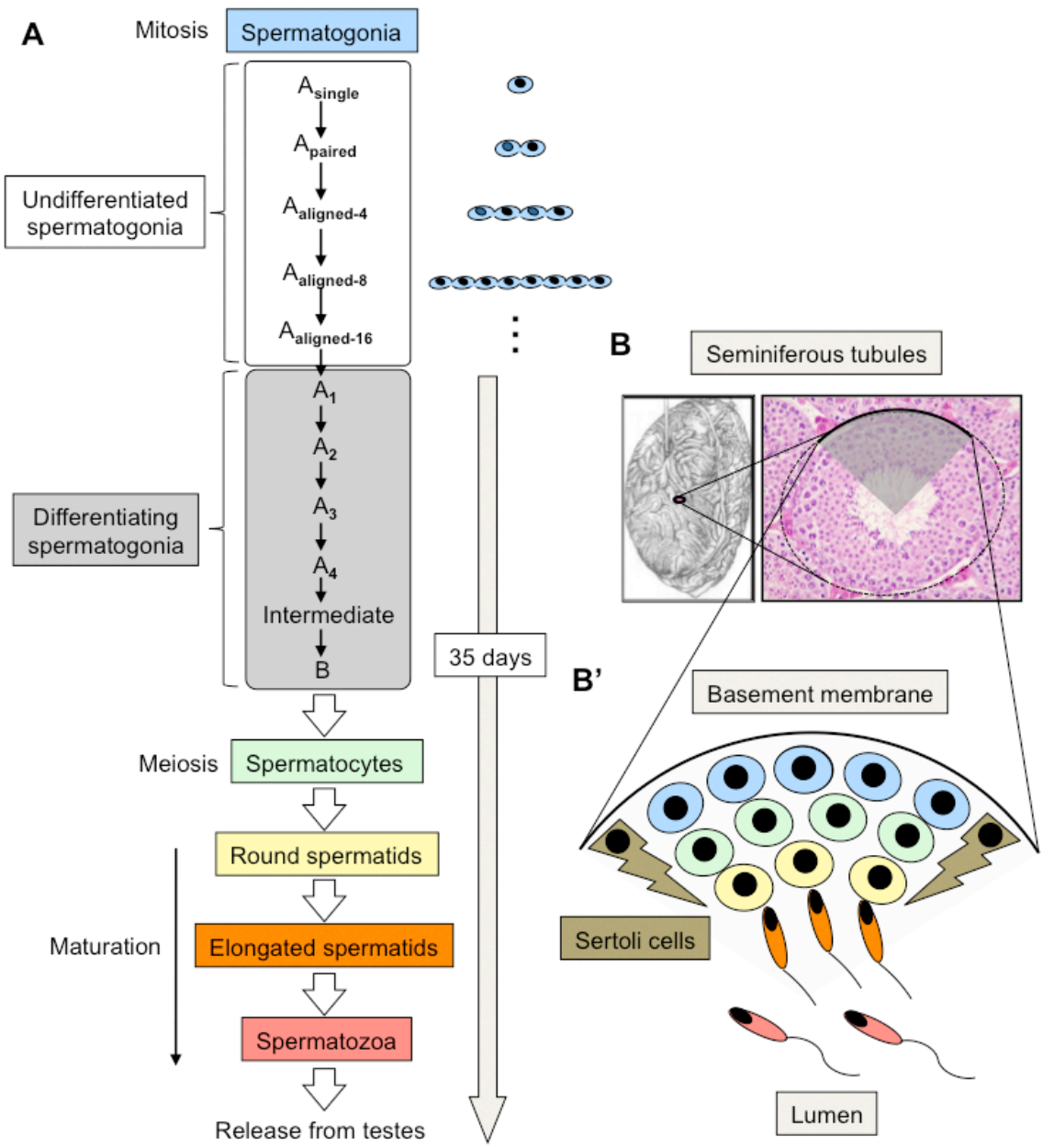

Figure 1. Spermatogenesis in mice. (**A**) A scheme of spermatogonial multiplication and subsequent spermatogenic processes. Spermatogenic cells are interconnected by intercellular bridges, in part are shown in picture (blue cells). (**B**) An adult testis removed from the tunica albuginea (left) (a picture from [82]). A testis is composed of long, coiled tube called seminiferous tubules. The cross section of the testis was stained by hematoxylin and eosin (right). One seminiferous tubule is indicated by a black dotted line. (**B'**) The multi-layered structure in a seminiferous tubule. Color of each cell type corresponds to the color of the cell type shown in (A). Spermatogonia (blue cells) are located on the basement membrane of seminiferous tubules. As germ cells mature, they progressively locate toward the lumen of the tubules (green, yellow, orange and pink cells). The germ cells are enclosed by somatic Sertoli cells (brown cells).

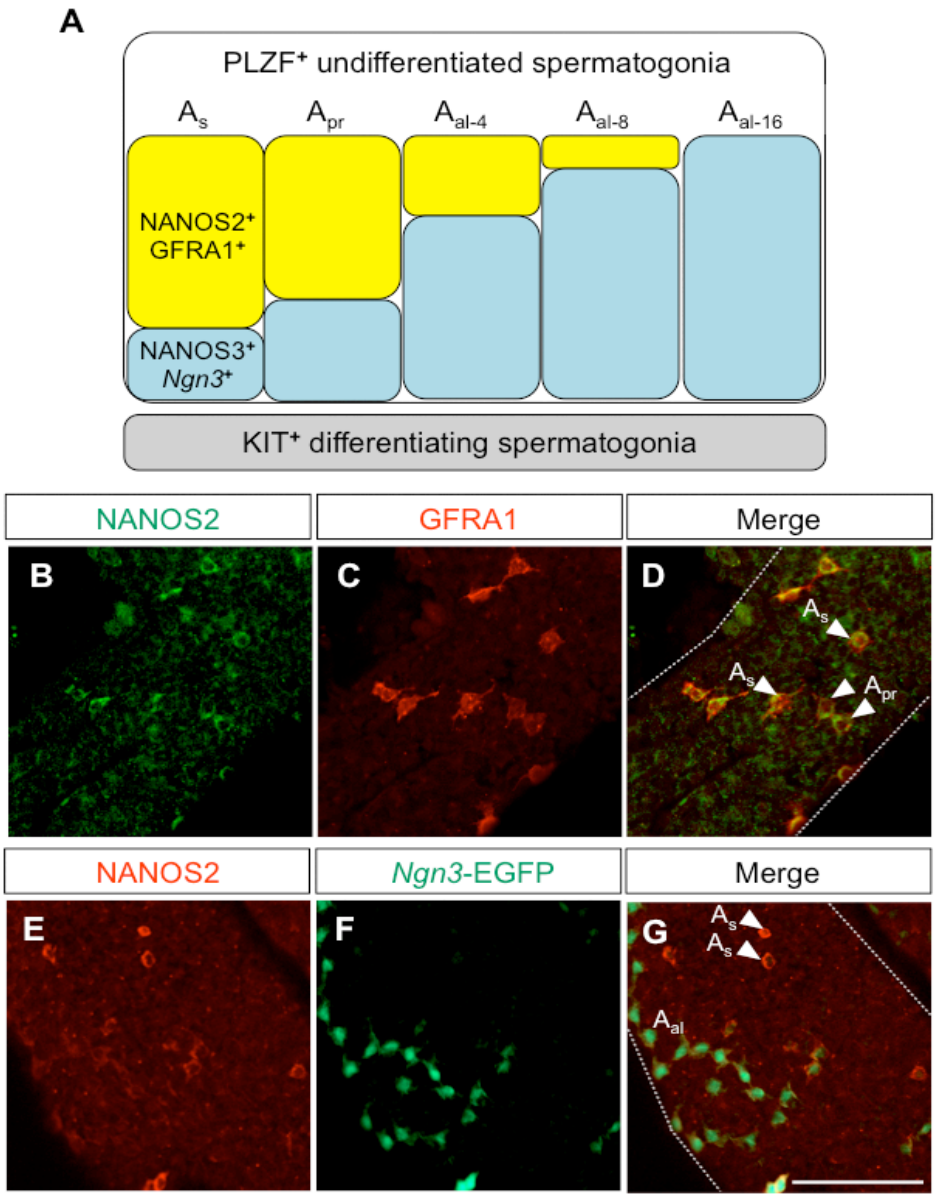

Figure 2. Expression pattern of NANOS2 in adult testes. (**A**) A schematic view of the relationship between the typical morphology and gene expression patterns observed in each group of undifferentiated spermatogonia. PLZF is expressed in all the A_s, A_{pr}, and A_{al} spermatogonia, while other genes depicted here are expressed in subpopulations of them. PLZF$^+$ undifferentiated spermatogonia are differentiated into KIT$^+$ differentiating spermatogonia. (**B** to **D**) Whole-mount immunostaining with anti-NANOS2 (green) and anti-GFRA1 (red) antibodies. NANOS2 was expressed predominantly in A_s and A_{pr} spermatogonia, in which GFRA1 was co-expressed. The dotted lines show outlines of seminiferous tubules. (**E** to **G**) Double-staining using antibodies for NANOS2 (red) and GFP (green) to detect *Ngn3*-EGFP [51]. A_s and A_{pr} spermatogonia have a greater probability of being NANOS2 single-positive, whereas A_{al} tend to be *Ngn3*-EGFP single-positive. Scale bar, 100 μm.

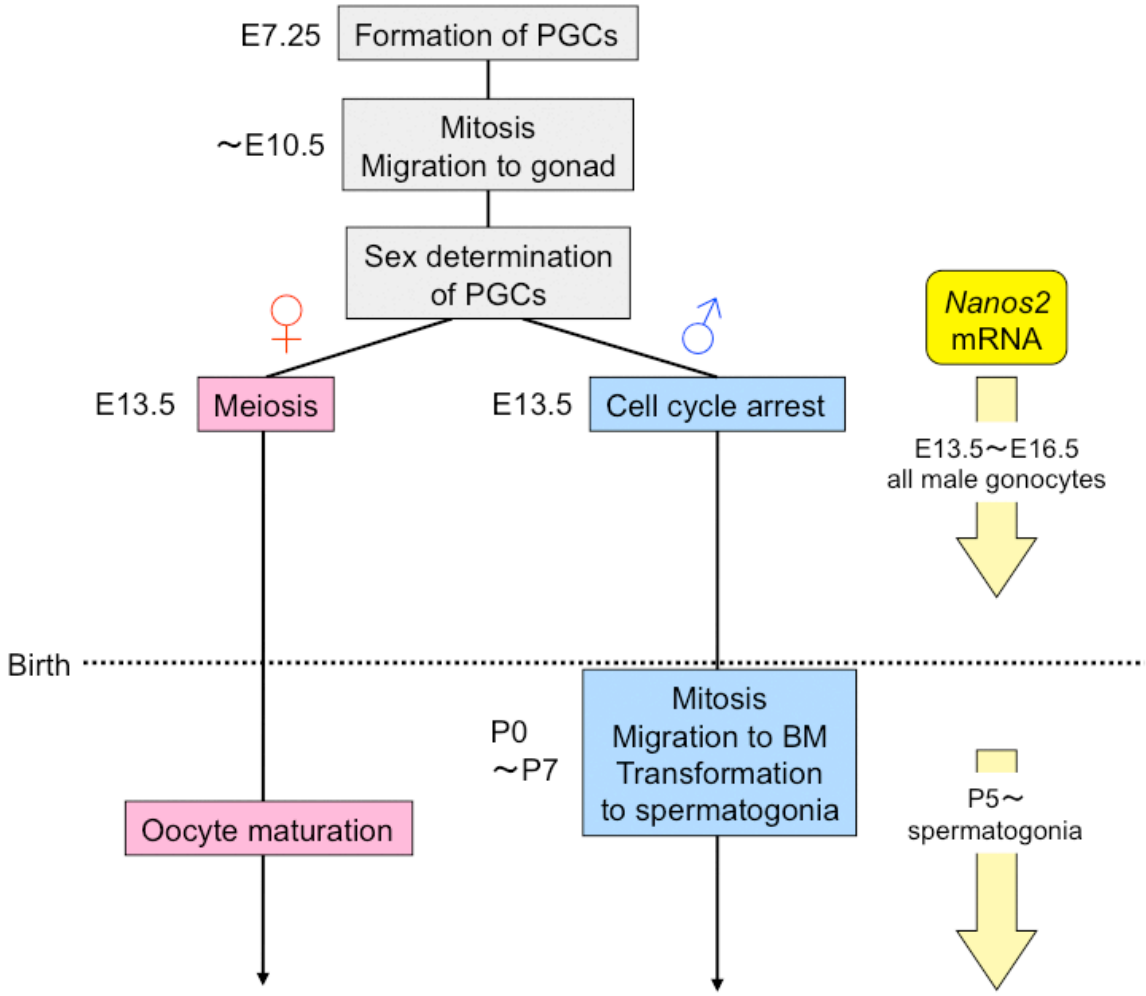

Figure 3. Schematic representation for germ cell development and expression pattern of *Nanos2*. Germ cells are already generated by E7.25, and then proliferate and migrate into the gonad. After colonization to gonad, they start sexual differentiation: female germ cells enter meiosis while male germ cells stop proliferation and stay in mitotic arrest during embryogenesis. After birth, germ cells resume proliferation and migrate to the basement membrane (BM) of seminiferous tubules from the center position. Spermatogonia are developed from these precursor germ cells, called gonocytes. *Nanos2* is expressed in all male gonocytes during E13.5 to E16.5. After birth, *Nanos2* expression is restricted in spermatogonia.

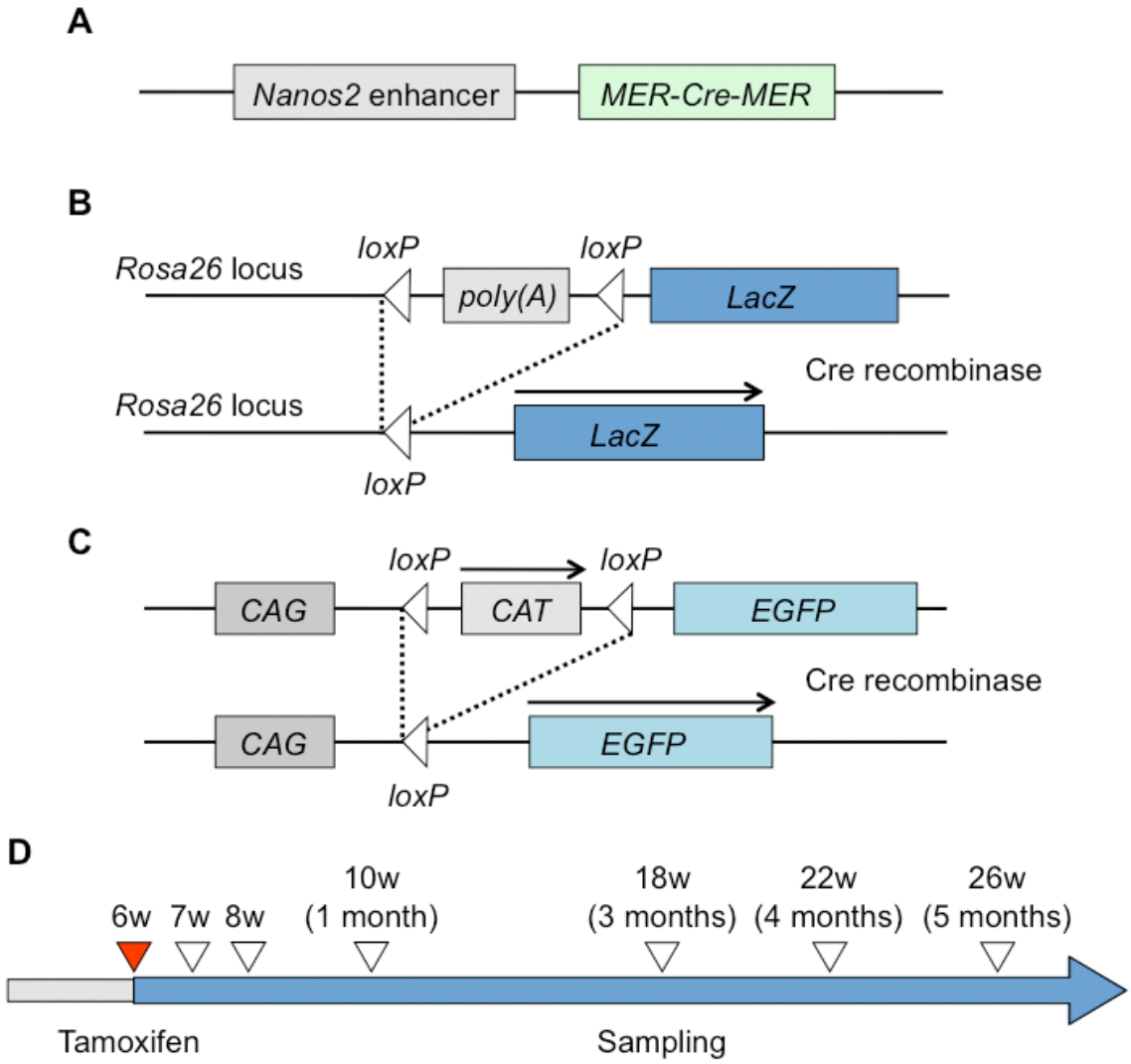

Figure 4. Methods in a pulse-chase study of *Nanos2*-expressing spermatogonia. (**A** to **C**) A schematic representation of the transgenes. I crossed *Nanos2-MCM* mice (A) with *R26R* (B) or *CAG-CAT-EGFP* (C) reporter mice that express *LacZ* (B) or *EGFP* (C) after Cre-mediated removal of the inactivating sequence. Because the recombination is irreversible and inheritable, the progeny of the labeled cells can be traced regardless of their NANOS2 expression status after labeling. (**D**) The experimental schedule. TM was injected at 6 weeks for 5 consecutive days. The mice were sacrificed to dissect testes at indicated time points.

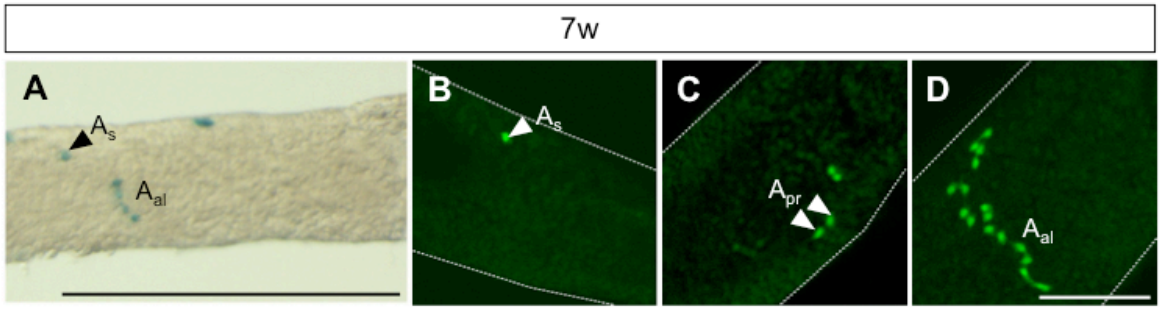

E

Number of chained cells	1 (A_s)	2 (A_{pr})	3	4	5-7	8	9-15	16	more	total
NANOS2 (*N*=4)	**22181**	**10005**	**739**	**3907**	**205**	**1473**	**0**	**43**	**83**	**38636**
Nanos2-lineage 7w (*N*=15)	3522	2123	324	1423	290	1077	164	153	148	9224
Nanos2-lineage 8w (*N*=4)	4565	2002	142	1153	224	889	108	208	117	9408
Nanos2-lineage 10w (*N*=10)	2281	1050	48	735	125	744	69	137	57	5246

Figure 5. Pulse-labeling of the *Nanos2*-expressing spermatogonia. (**A** to **D**) Detection of the labeled cells by either X-gal staining (A, blue) or immunostaining with anti-GFP antibodies (B to D, green) in 7-week-old testes. Undifferentiated spermatogonia were successfully labeled by Cre-mediated recombination under the control of *Nanos2* expression by a TM pulse. The dotted lines show outlines of seminiferous tubules. Scale bars; 500 μm in (A), 100 μm in (D). (**E**) The changes in the composition of *Nanos2*-expressing spermatogonial cell lineage following a TM pulse. To examine fates of the labeled cell shortly after the pulse, 6-week-old *Nanos2-MCM*; *CAG-CAT-EGFP* mice were subjected to the injection of TM for 5 consecutive days and the testes were immunostained with anti-GFP antibody at 7-, 8-, 10- weeks of age. According to the previously described method [20], a number of GFP-positive undifferentiated spermatogonial clones per testis was estimated. A ~5 cm long seminiferous tubule was analyzed for the calculation. The efficiency of pulse-labeling (about 20-25%) was determined by comparison of total number of labeled clones at 7 weeks with the total number of endogenous NANOS2-expressing clones. *N*, the number of experiments conducted independently.

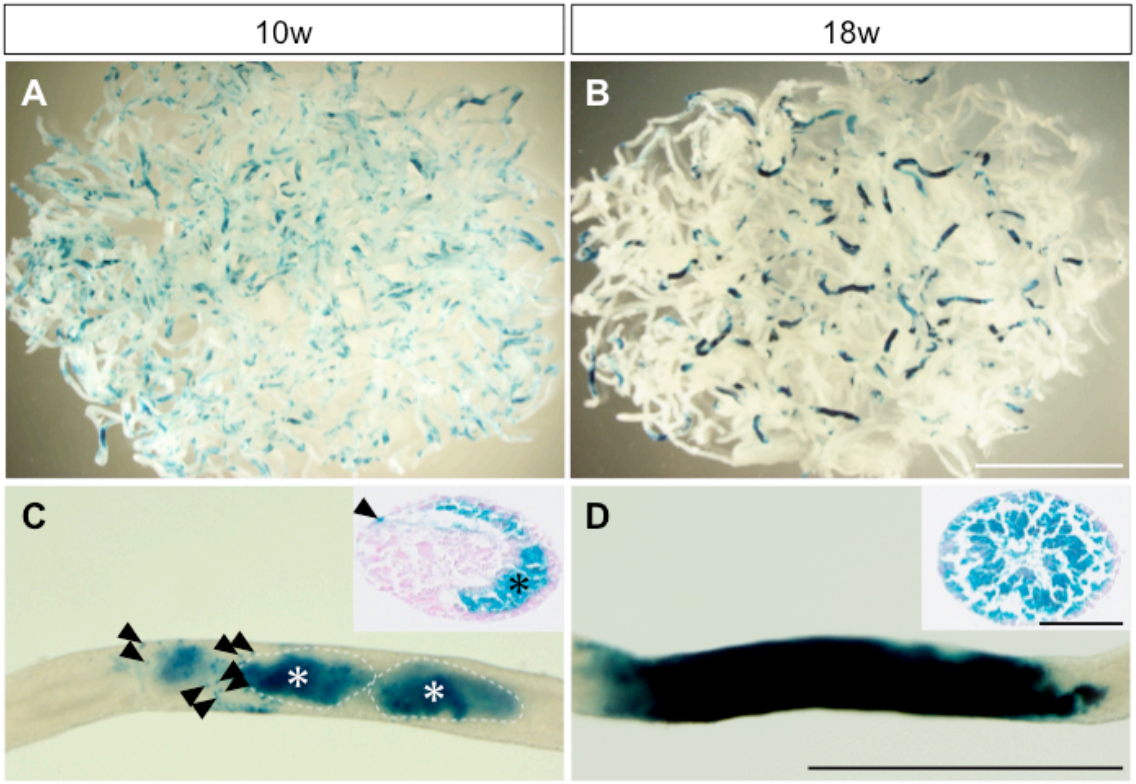

E

Age	18w	22w	26w
Number of X-gal⁺ patches/ testis	86.5 ± 8.1 (*N*=20)	75.3 ± 8.6 (*N*=12)	68.8 ± 3.6 (*N*=4)

Figure 6. Fates of the labeled *Nanos2*-expressing spermatogonia. (**A** to **D**) Detection of the *Nanos2*-expressing cell lineage by X-gal staining (blue). Insets in (C and D) are cross-sections of the representative tubules containing X-gal positive cells. A cytoplasm of cells was counterstained with eosin (C and D insets, red). The stained differentiated spermatogenic cells within the inner layer (asterisks) and spermatogonia on the periphery (arrowheads) are indicated (C). TM was injected at 6 weeks of age. Scale bars; 5 mm in (B), 1 mm in (D), and 100 μm in (D, inset). (**E**) Average number of X-gal positive patches per testis is shown with the standard error. In *Ngn3*-lineage, the number of these patches has been reported to be 6.1 ± 0.7 per testis at 3 months after pulse [20]. *N*, the number of experiments conducted independently.

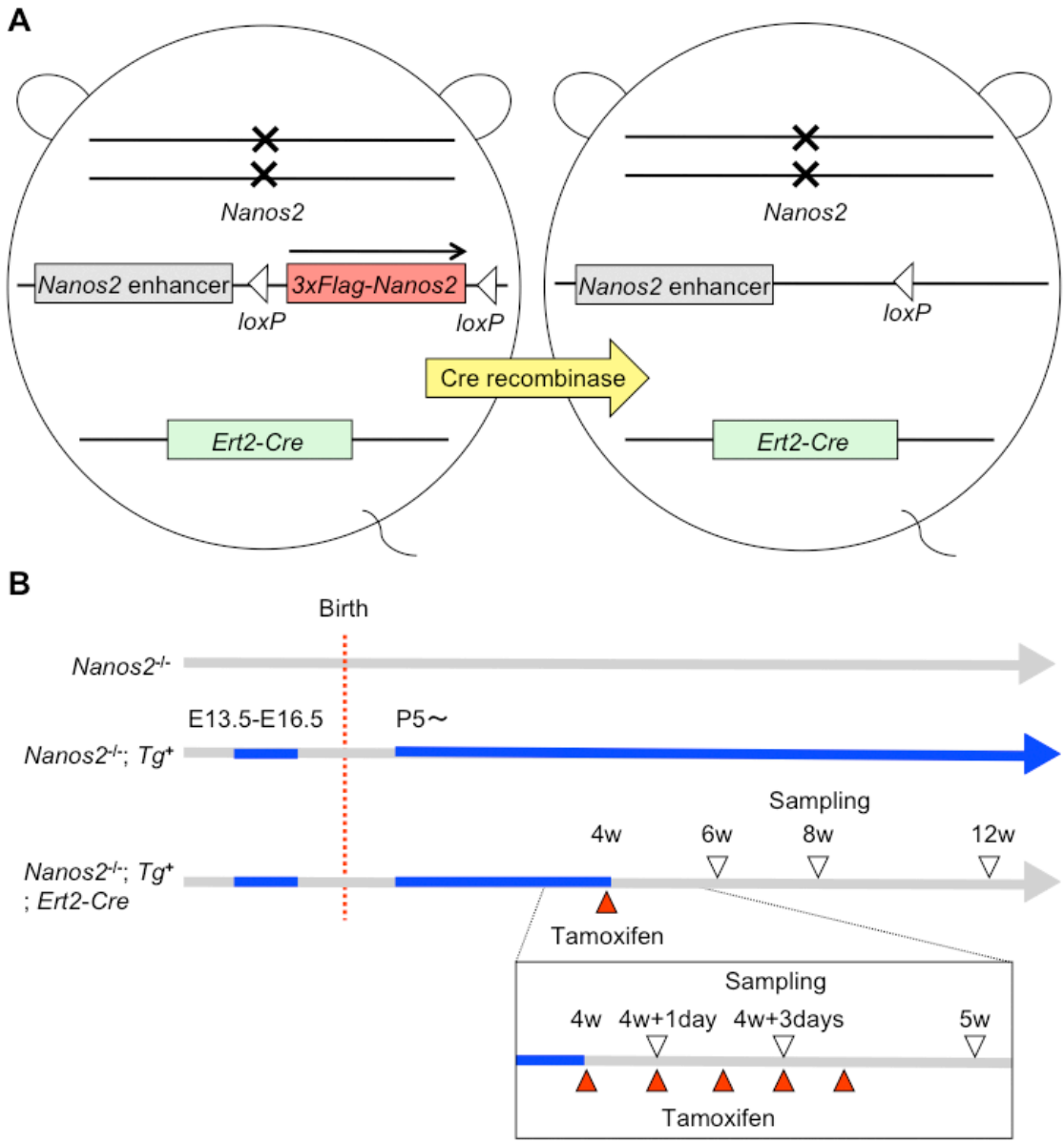

Figure 7. Strategy to generate conditional knockout mouse by the induction and subsequent removal of a *Nanos2* transgene. (**A**) Strategy to generate mice lacking postnatal *Nanos2* expression. By introducing the transgene (*floxed 3xFlag-tagged Nanos2* under the control of a *Nanos2* enhancer) into the *Nanos2*-null backgrounds, the *Nanos2* expression is rescued. For conditional deletion of postnatal *Nanos2*, a TM-inducible *Ert2-Cre* is used. Activation of Cre recombinase by a TM results in a removal of floxed *Nanos2* sequence. (**B**) The experimental schedule. The blue line parts indicate the periods at which male germ cells express *Nanos2*. The transgene is expressed during the appropriate period in the *Nanos2*-null mouse backgrounds (compare *Nanos2*$^{-/-}$ with *Nanos2*$^{-/-}$; *Tg*$^{+}$). For conditional deletion of postnatal *Nanos2*, TM was injected into 4-week-old *Nanos2*$^{-/-}$; *Tg*$^{+}$; *Ert2-Cre* mice for 5 consecutive days and the testes were harvested at the indicated time points.

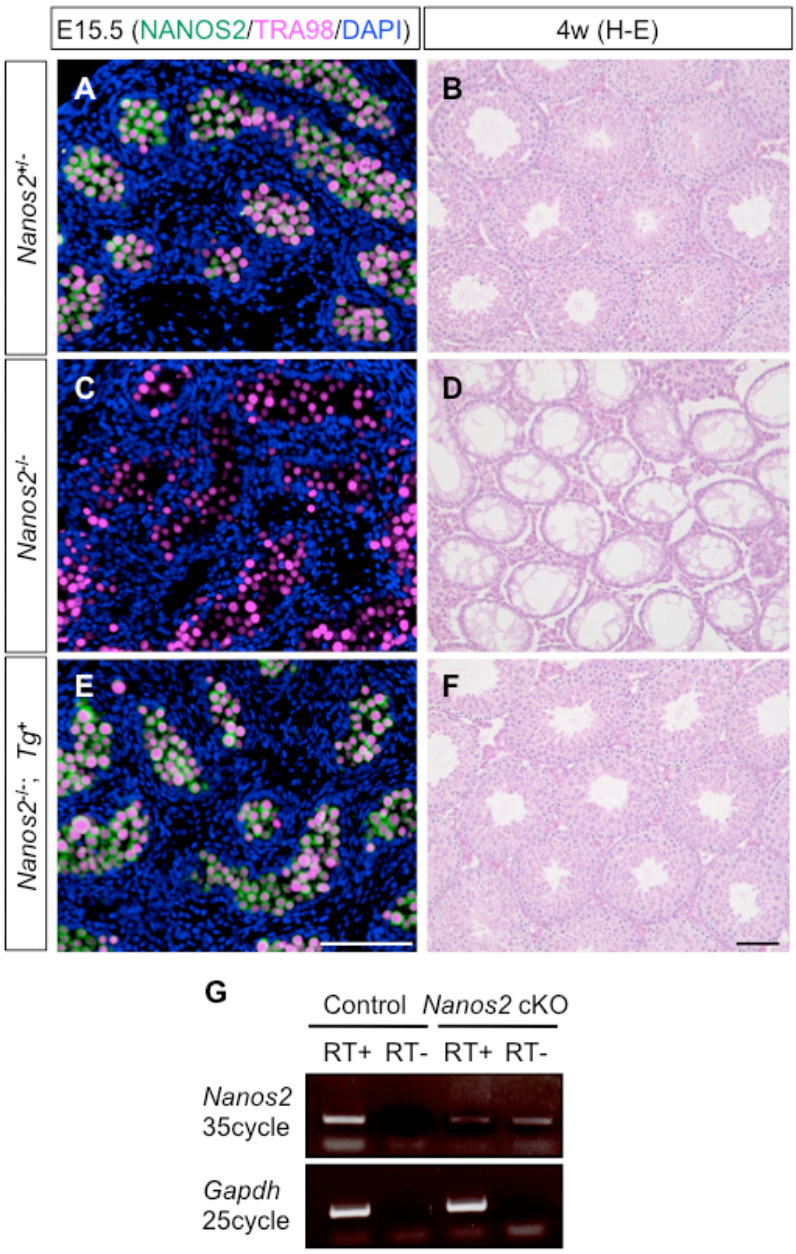

Figure 8. Successful induction and subsequent removal of the floxed *Nanos2* transgene. (**A** to **F**) A rescue of the *Nanos2*-null phenotype by the introduction of the transgene. Testes were prepared from littermates of *Nanos2*$^{+/-}$, *Nanos2*$^{-/-}$ or *Nanos2*$^{-/-}$ mice harboring the transgene at E15.5 (A, C and E) and 4 weeks (B, D and F). Sections of these tissues were stained with anti-NANOS2 (green) and TRA98 (magenta, germ cells) antibodies and counterstained with DAPI (blue) (A, C and E) or hematoxylin and eosin (H-E) (B, D and F). The expression of the FLAG-NANOS2 rescued the germ-less phenotype of the *Nanos2*$^{-/-}$ testes. Scale bars, 100 μm. (**G**) Efficient excision of the transgene by *Ert2-Cre* was achieved upon a TM injection. RT-PCR analysis of *Nanos2* transcription at 5 weeks in control (lanes 1 and 2) and *Nanos2*-cKO (lanes 3 and 4) mouse testes.

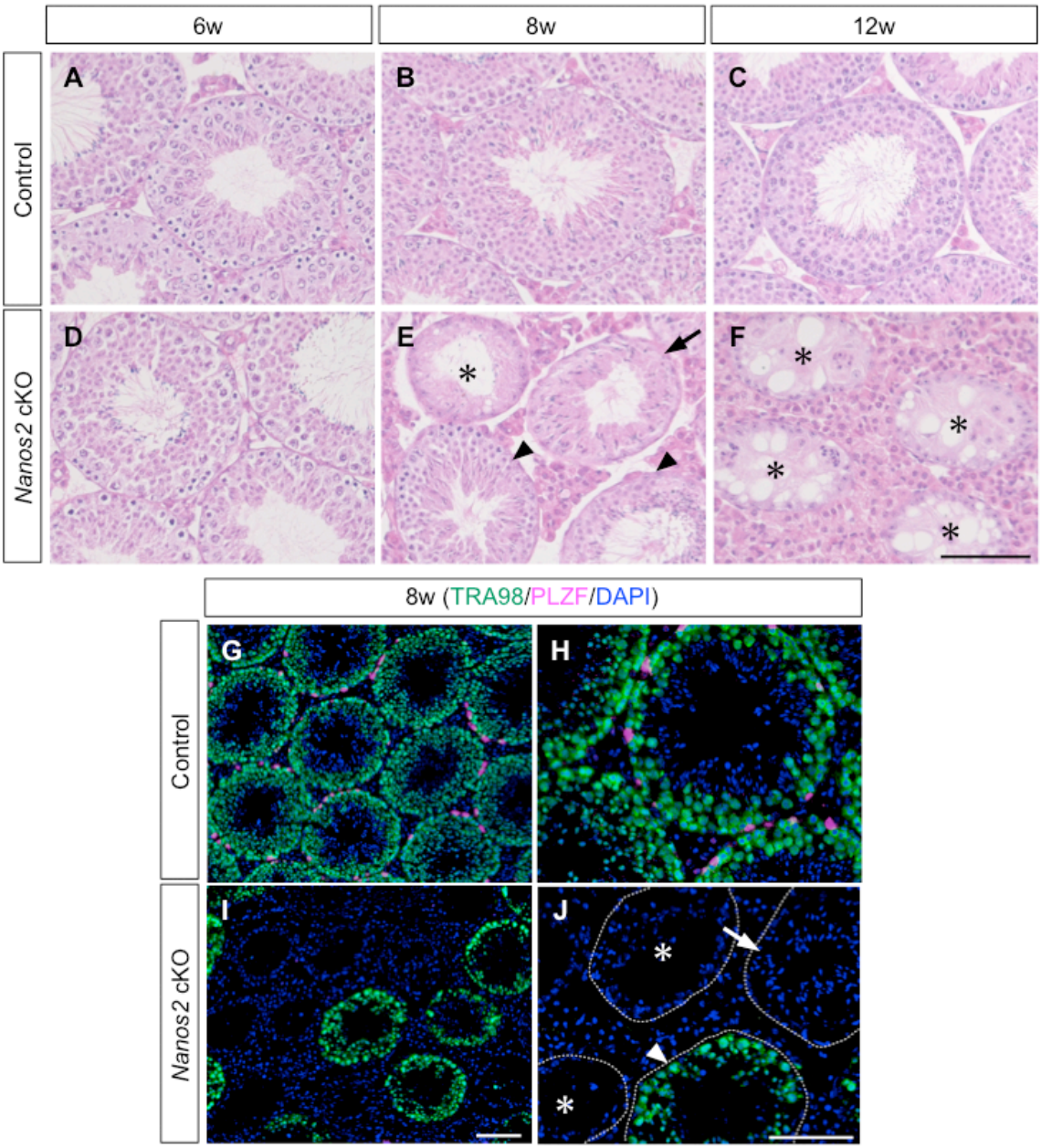

Figure 9. Progressive loss of spermatogenic cells in *Nanos2*-cKO mice. (**A** to **F**) Histology of control and *Nanos2*-cKO testes. In the control, the basal layers of seminiferous tubules contained all stages of spermatogonia; subsequently, spermatocytes relocate toward the lumen as they transform into round, and then elongated, spermatids. In the *Nanos2*-cKO testes, tubules lacking spermatogonia (arrowheads), those with only elongated spermatids (arrows) and those without any germ cells (asterisks) were progressively observed. (**G** to **J**) Immunostaining of 8-week-old testes with TRA98 (green) and anti-PLZF (magenta) antibodies. Nuclear DNA was counterstained with DAPI (blue). The dotted lines show outlines of seminiferous tubules. Scale bars, 100 μm.

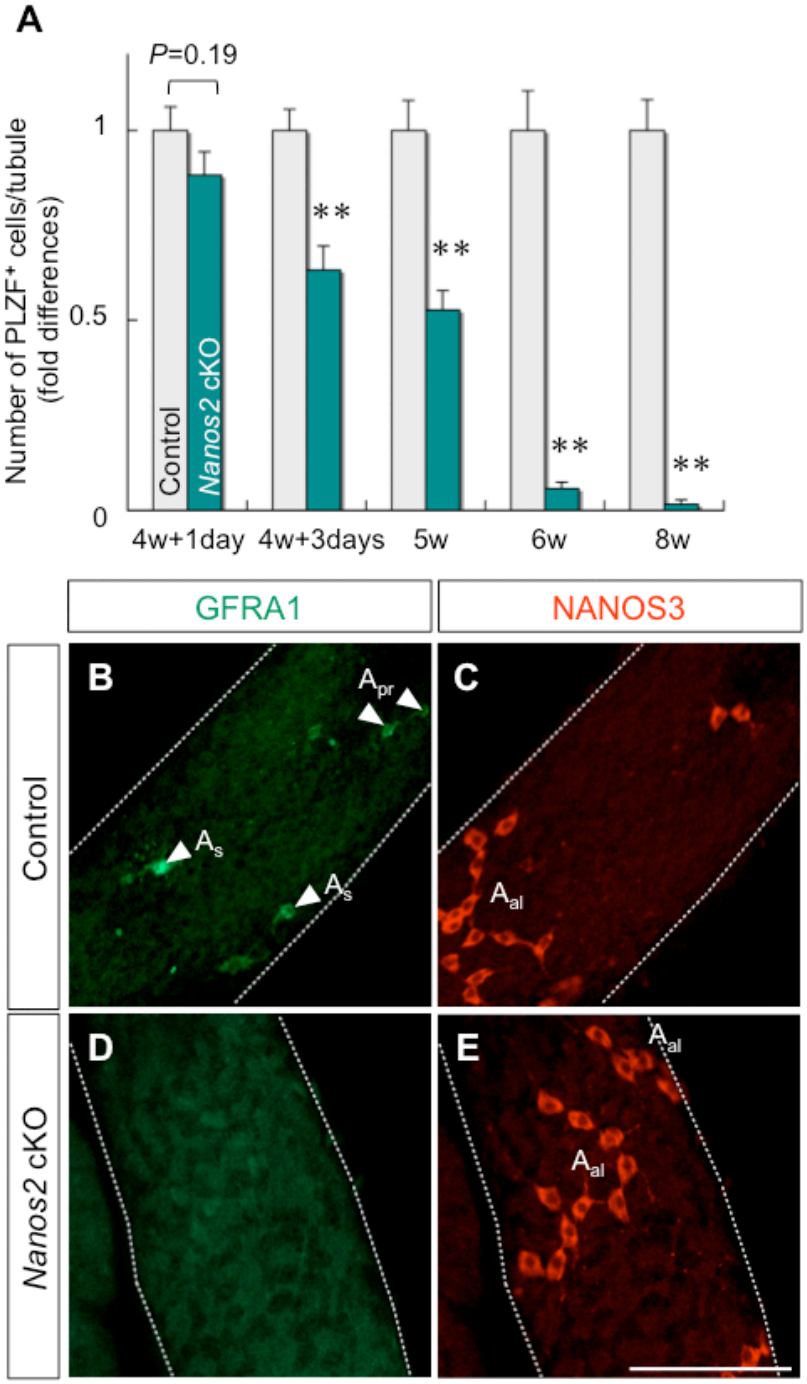

Figure 10. Depletion of PLZF$^+$/GFRA1$^+$ spermatogonia by a *Nanos2*-gene deletion. (**A**) The time course of the reduction in the number of PLZF-positive undifferentiated spermatogonia per seminiferous tubule in sections. More than 100 tubules from 20 independent microscopic fields were scored (N=3). The results were normalized using the control of each stage. Error bars represent the standard error. **; P<0.01. (**B** to **E**) Five-week-old testes of control and *Nanos2*-cKO were examined by whole-mount immunostaining with anti-GFRA1 (green) and anti-NANOS3 (red) antibodies. The dotted lines show outlines of seminiferous tubules. Scale bar, 100 μm.

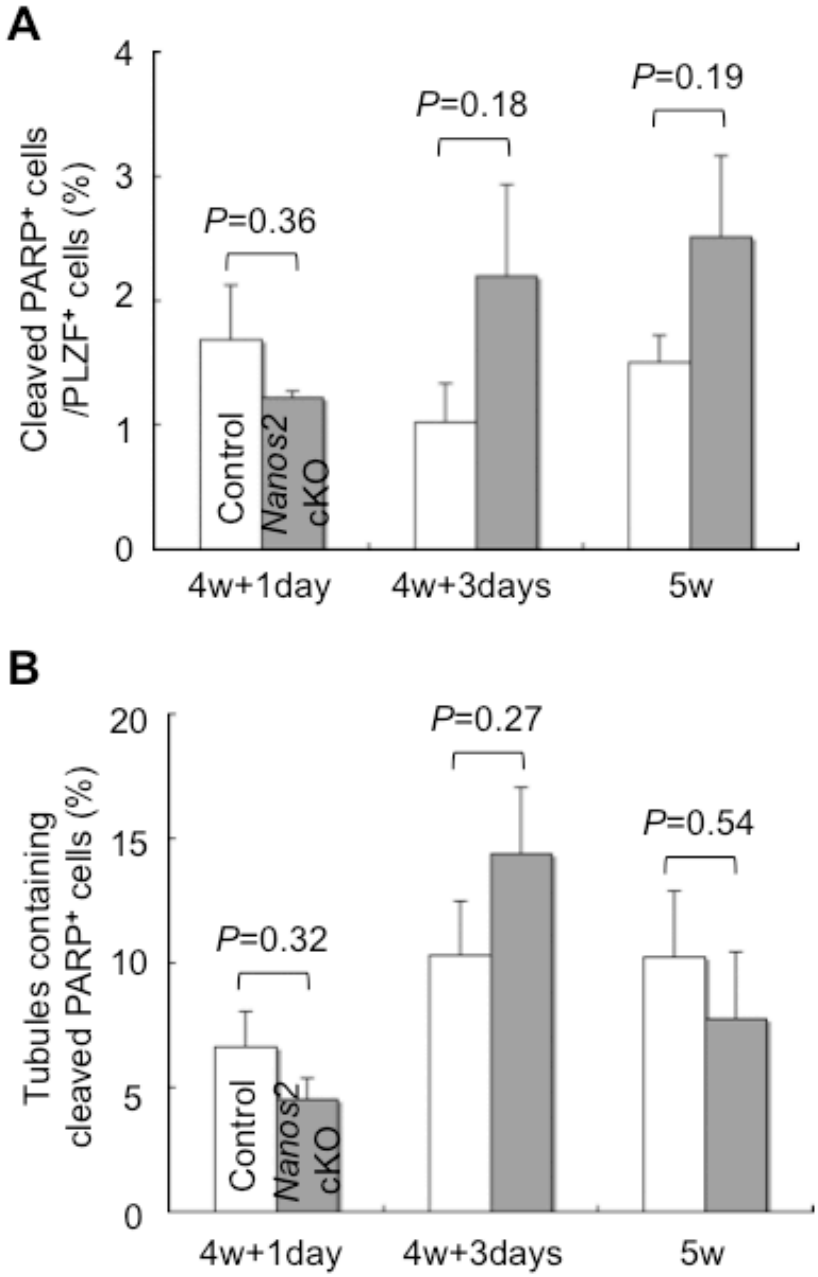

Figure 11. Quantitative analyses of apoptotic cell death in *Nanos2*-cKO testes. (**A**) The ratio of apoptotic cells was determined by double staining of anti-cleaved PARP and anti-PLZF antibodies. PARP is one of the main targets of CASPASE-3, so that the PARP cleavage serves as a marker of cells undergoing apoptosis [83, 84]. Total numbers of counted PLZF-positive cells in each sample are over 800 in both control and *Nanos2*-cKO at 4w+1day (*N*=3), 700 in control and 400 in *Nanos2*-cKO at 4w+3day (*N*=5), 300 in control and 100 in *Nanos2*-cKO at 5w (*N*=4). (**B**) The ratio of tubules containing apoptotic cells was compared between control and *Nanos2*-cKO testes. More than 100 tubules from 10 independent microscopic fields were scored in each sample. The mean values are shown with the standard error.

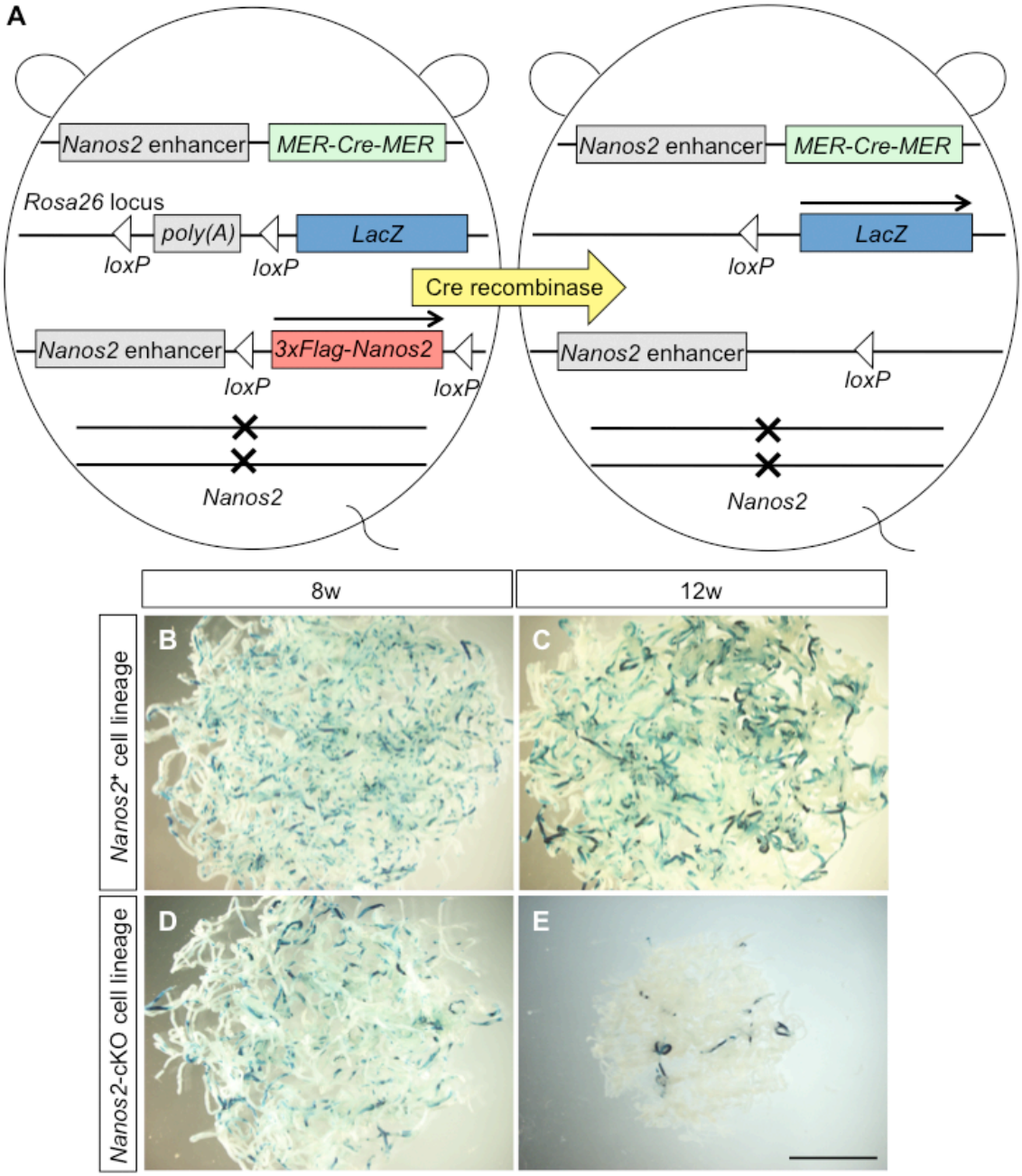

Figure 12. Lineage tracing of *Nanos2*-deficient cells. (**A**) Strategy to follow the fate of *Nanos2*-deficient cells. Three transgenes are introduced in the *Nanos2*-null genetic backgrounds. To induce Cre recombination, I use *Nanos2-MCM* in which the activation of Cre is induced only in the *Nanos2*-expressing cells. A TM injection results in the deletion of the floxed *Nanos2* sequence and induction of *LacZ* expression in the cells. Control experiments are performed in the *Nanos2*-hetero genetic backgrounds. (**B** to **E**) Four-week-old mice were injected with TM and sacrificed at 8- (B and D) and 12- (C and E) weeks of age. *Nanos2*-expressing or *Nanos2*-cKO cell lineages were detected by X-gal staining (blue). X-gal positive cells observed in (E) were likely to be caused by the incomplete removal of the floxed *Nanos2* sequence. Scale bar, 5 mm.

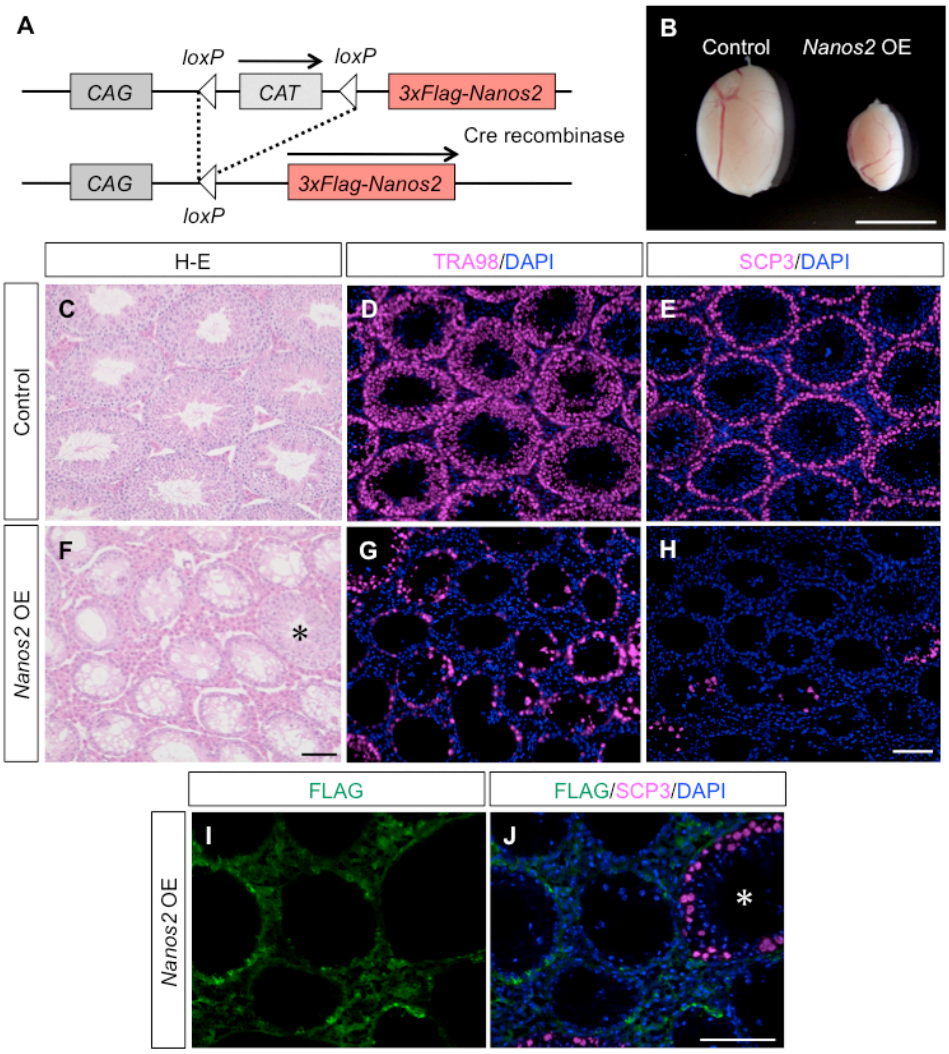

Figure 13. Abnormal spermatogenesis in a *Nanos3-Cre* induced *Nanos2*-overexpressing testis. (**A**) A conditional transgenic mouse line, *CAG-floxed CAT-3xFlag-Nanos2* is capable of expressing *Flag-Nanos2* under the control of the ubiquitous *CAG* promoter after excision of the floxed *CAT* gene by Cre recombinase. (**B**) Testes from 8-week-old control and *Nanos2*-overexpressing (OE) mice. (**C** to **H**) Testes were stained with hematoxylin and eosin (H-E) (C and F), TRA98 antibody (magenta) and DAPI (blue) (D and G), and anti-SCP3 antibody (magenta, meiotic cells) and DAPI (blue) (E and H). In *Nanos2*-overexpressing testes, most germ cells were located on the basement membrane, while SCP3-positive cells were remarkably decreased. (**I** and **J**) Immunostaining of *Nanos2*-overexpressing testes with anti-FLAG (green, FLAG-tagged NANOS2 to detect the transgene-derived NANOS2 expression) and anti-SCP3 (magenta) antibodies. Nuclear DNA was counterstained with DAPI (blue). Rarely observed spermatocytes in *Nanos2*-overexpressing mice (asterisks) are due to an incomplete recombination by Cre, as they did not express FLAG-NANOS2. Scale bars, 5 mm in (B) and 100 μm in (H and J).

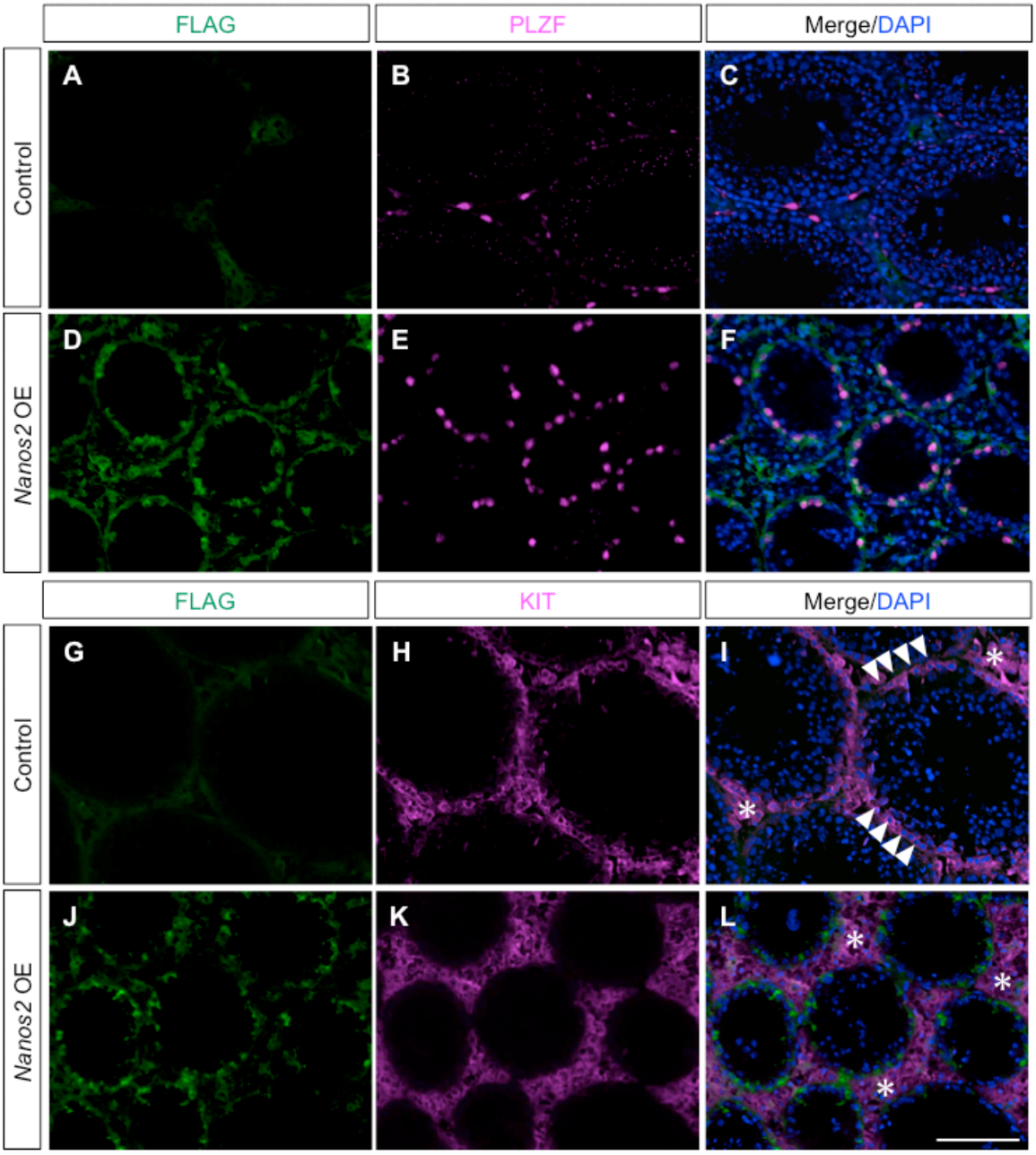

Figure 14. *Nanos2*-overexpressing cells express PLZF but not KIT. (**A** to **F**) Testes were stained with antibody for FLAG (green) and PLZF (magenta). Nuclear DNA was counterstained with DAPI (blue). (**G** to **L**) Testes were stained with antibody against FLAG (green) and KIT (magenta). Nucleus was stained with DAPI (blue). KIT was expressed in differentiating spermatogonia (arrowheads) and somatic Leydig cells (asterisks). Scale bar, 100 μm.

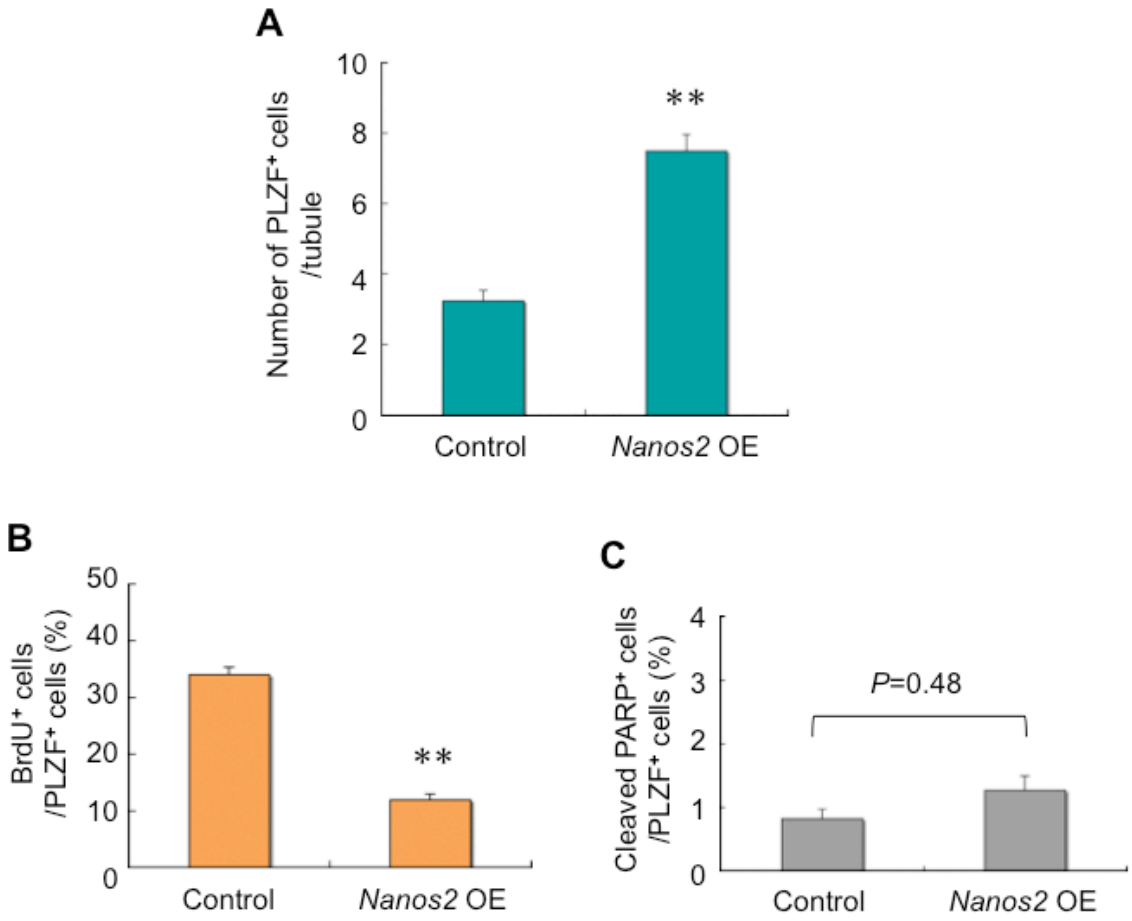

Figure 15. Possible causes for the accumulation of PLZF-positive spermatogonia following *Nanos2*-overexpression. (**A**) Calculation of PLZF-positive cells per seminiferous tubule in 8-week-old mice. (**B** and **C**) Quantification of proliferative (B) and apoptotic (C) spermatogonia in 4-week-old mice. The number of BrdU- and cleaved PARP-positive cells were scored per number of PLZF-positive cells, respectively. More than 15 independent microscopic fields were counted (N=3). The mean values are shown with the standard error. **; P<0.01.

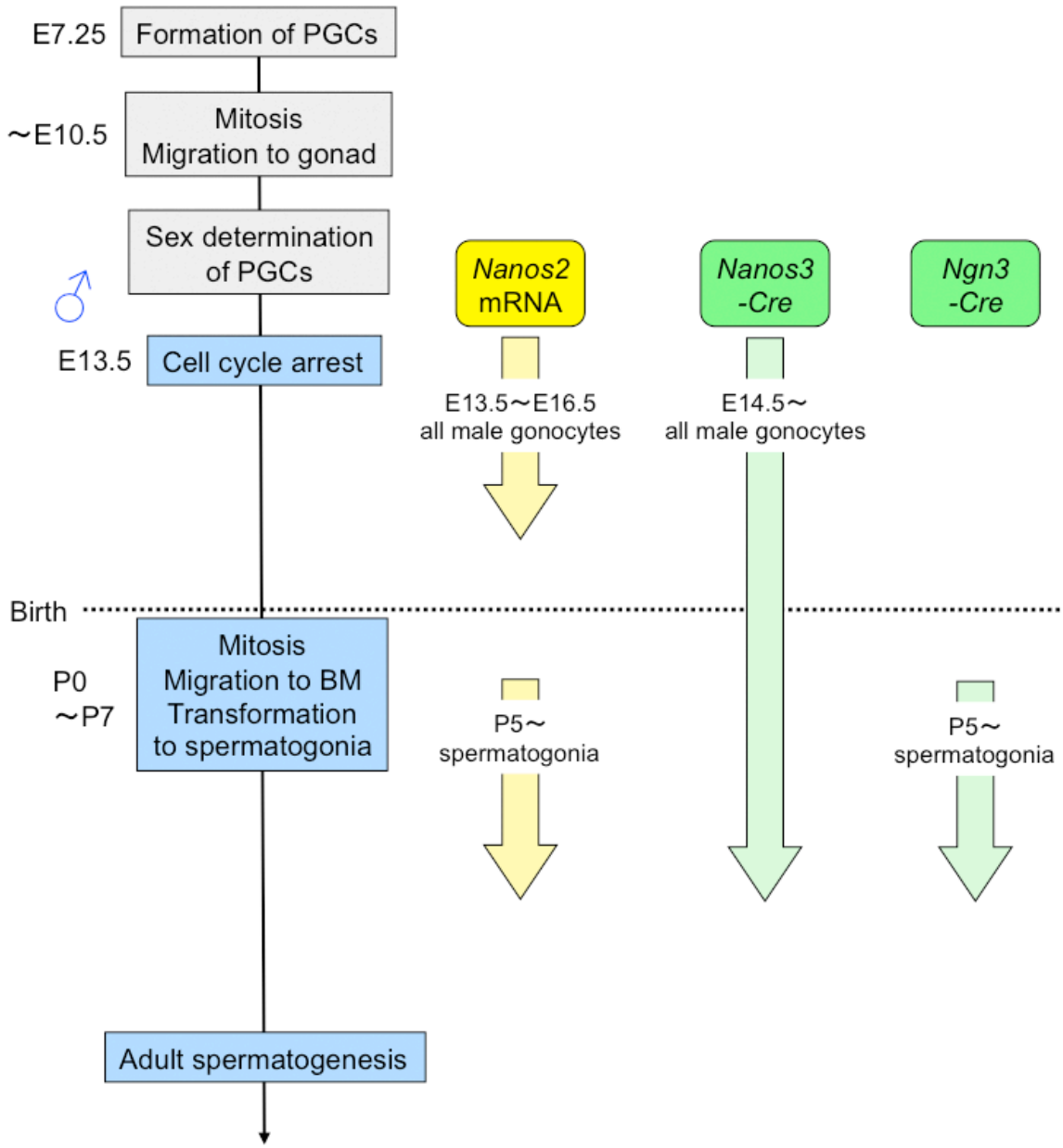

Figure 16. Expression pattern of *Cre* lines used for *Nanos2*-overexpression. The schematic representation of the male germ cell development and expression patterns of *Nanos2* mRNA, *Nanos3-Cre* and *Ngn3-Cre*. Cre recombinase expression in the *Nanos3-Cre* occurs in most of the male gonocytes by E14.5, whereas Cre expression in the *Ngn3-Cre* starts in spermatogonia around P5.

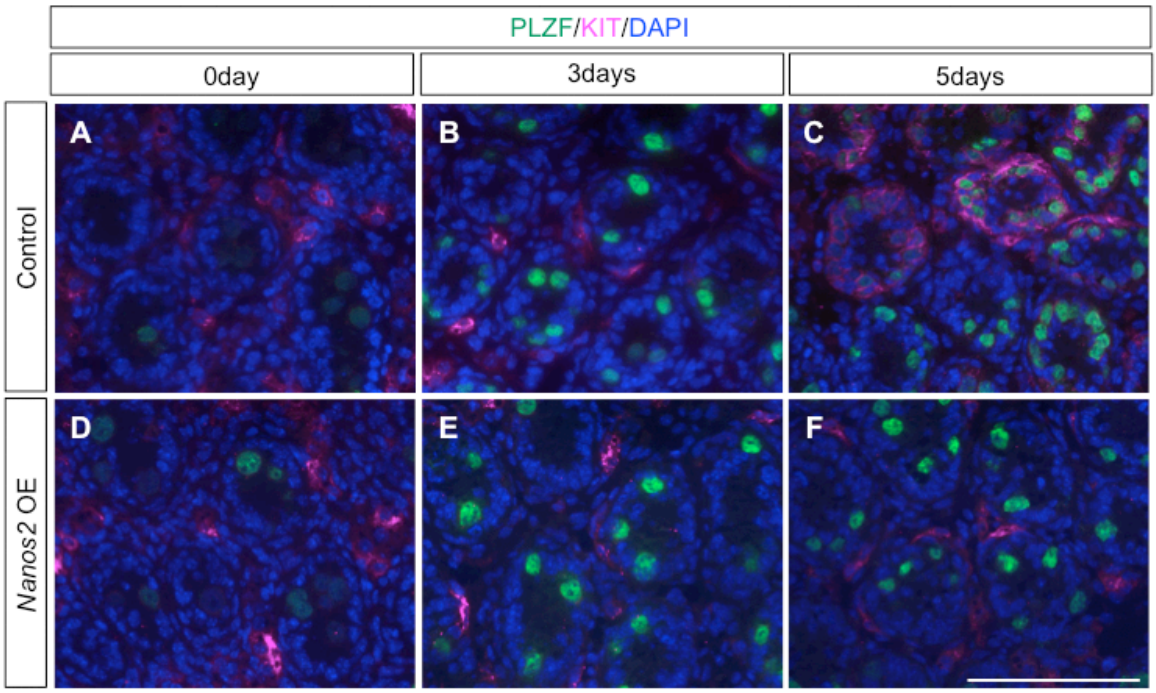

Figure 17. Spermatogonial cell abnormalities in *Nanos2*-overexpressing testes occur during the first postnatal week. (**A** to **F**) Neonatal testes prepared at indicated time points were immonostained with anti-PLZF (green) and anti-KIT (magenta) antibodies. Nuclear DNA was counterstained with DAPI (blue). In *Nanos2*-overexpressing testes, suppression of KIT expression was appeared as early as 5 days after birth. Scale bar, 100 μm.

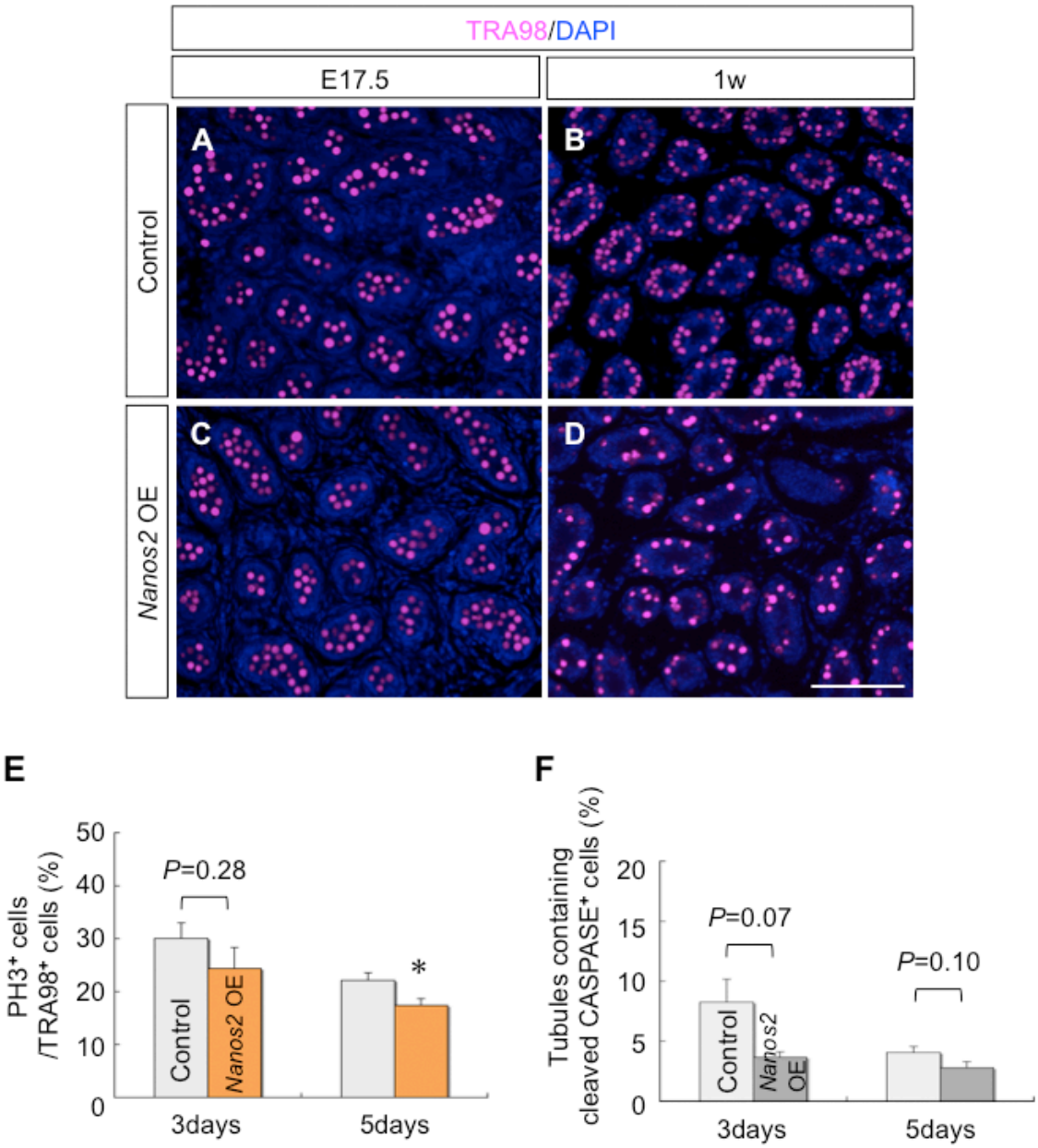

Figure 18. Possible causes of the decreased number in PLZF-positive spermatogonia by *Nanos2*-overexpression at early postnatal stage. (**A** to **D**) Neonatal testes were stained with TRA98 (magenta) antibody and DAPI (blue) at indicated time points. Germ cell number in *Nanos2*-overexpressing testes seemed to be normal during embryogenesis but was decreased after birth. Scale bar, 100 μm. (**E** and **F**) Statistical analysis of proliferation (E) and apoptosis (F). The number of phospho Histone H3 (PH3)-positive cells was scored per number of PLZF-positive cells (E). The ratio of apoptotic cells was determined by the ratio of tubules containing cleaved CASPASE3-positive cells (F). The mean values are shown with the standard error. *; $P<0.05$.

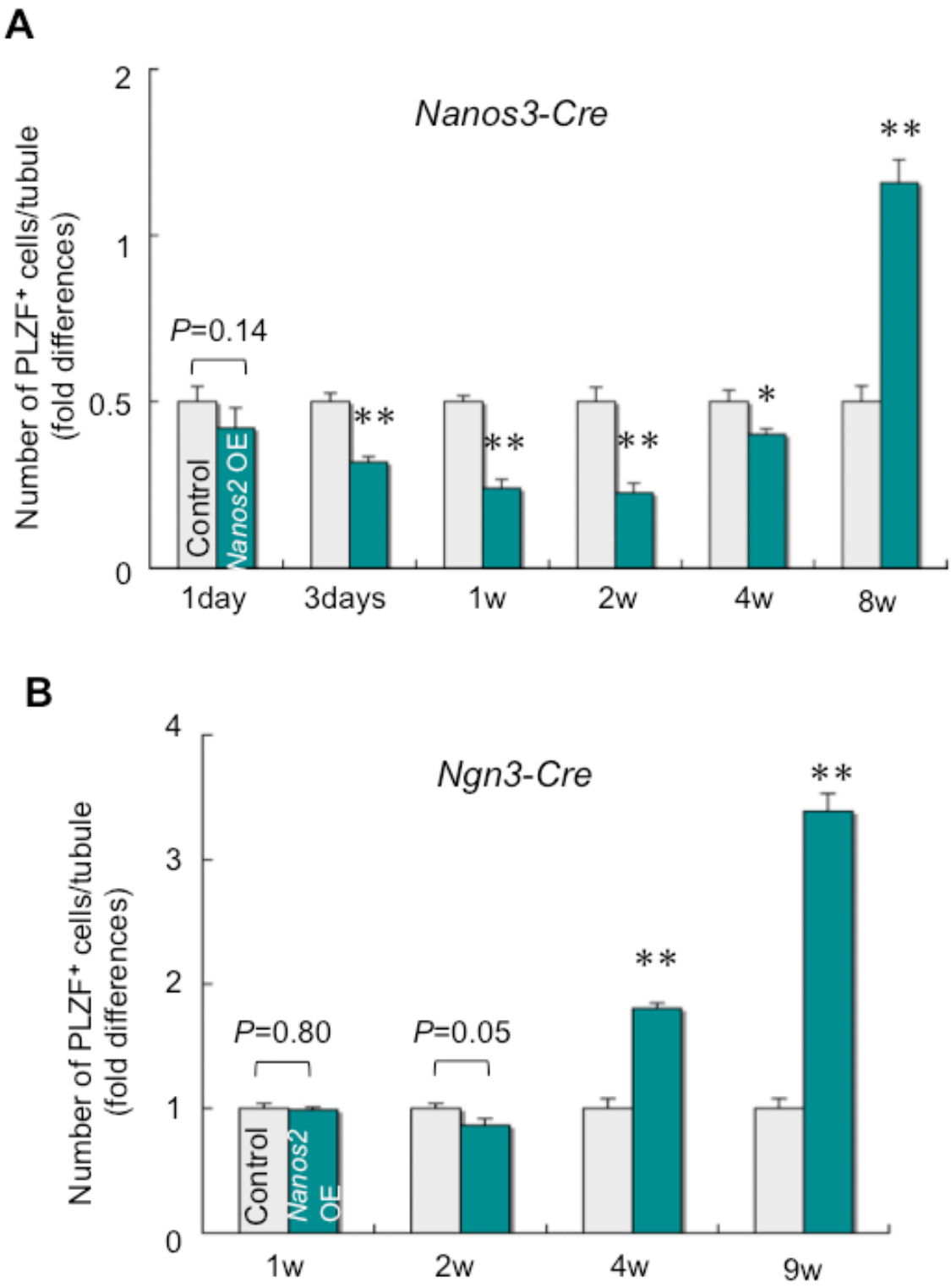

Figure 19. Temporal changes in PLZF-positive spermatogonia in *Nanos2*-overexpressing mutants. (**A** and **B**) The number of PLZF-positive spermatogonia per seminiferous tubule was counted in *Nanos2*-overexpressing testes induced by *Nanos3-Cre* (A) or *Ngn3-Cre* (B). The results were normalized using the control of each stage. Error bars represent the standard error. **; $P<0.01$ and *; $P<0.05$.

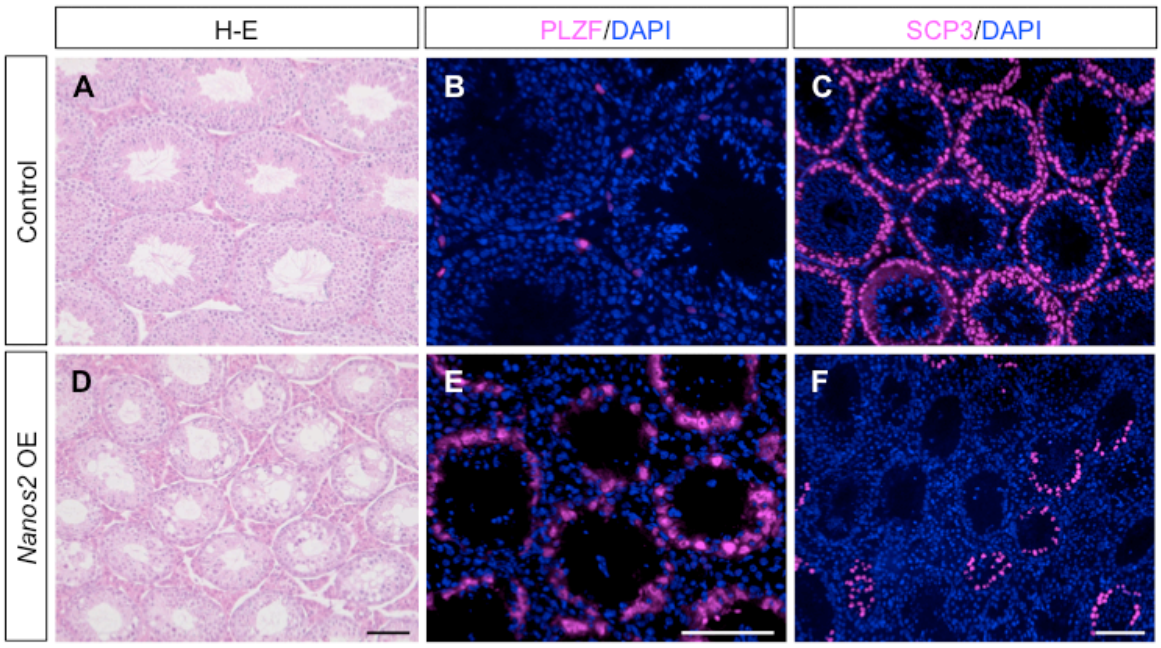

Figure 20. Characterization of spermatogenesis upon *Nanos2*-overexpression induced by *Ngn3-Cre*. (**A** to **F**) Sections of adult testes from control and *Nanos2*-overexpressing mice were subjected to hematoxylin and eosin (H-E) staining (A and D), and immunostaining with anti-PLZF antibodies (B and E, magenta) or anti-SCP3 antibodies (C and F, magenta). Nuclear DNA was counterstained with DAPI (B, C, E and F, blue). Scale bars, 100 μm.

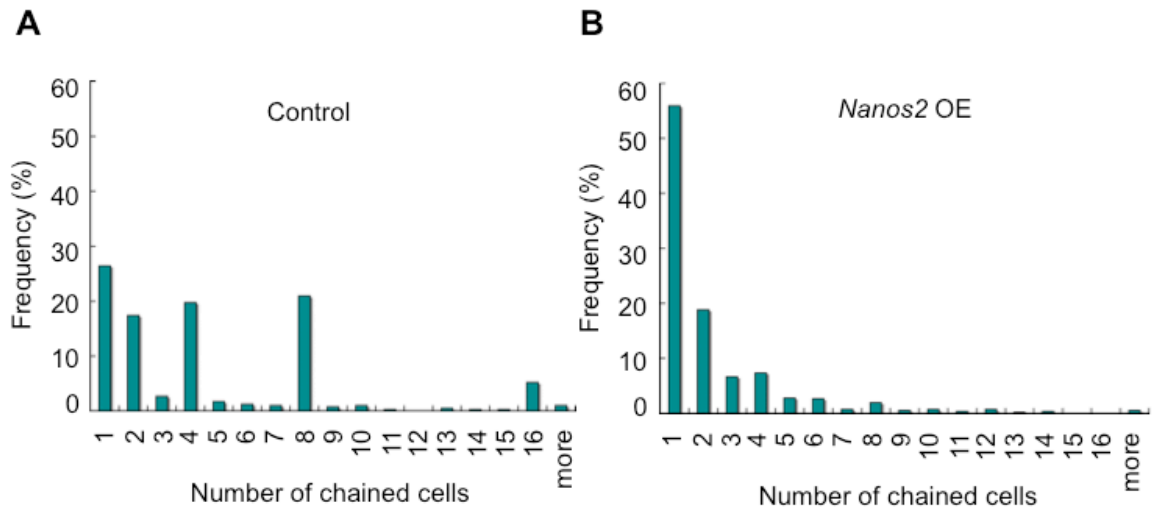

Figure 21. Morphological feature of *Nanos2*-overexpressing cells compared with control spermatogonia. (**A** and **B**) Distributions of PLZF-positive spermatogonia classified by their morphology. The horizontal axis shows a number of cells in a spermatogonial cluster. The vertical axis shows the frequency of spermatogonial cluster harboring the indicated number of cells. A total of 420 (A, control) and 574 (B, *Nanos2*-overexpression) spermatogonial clusters were counted.

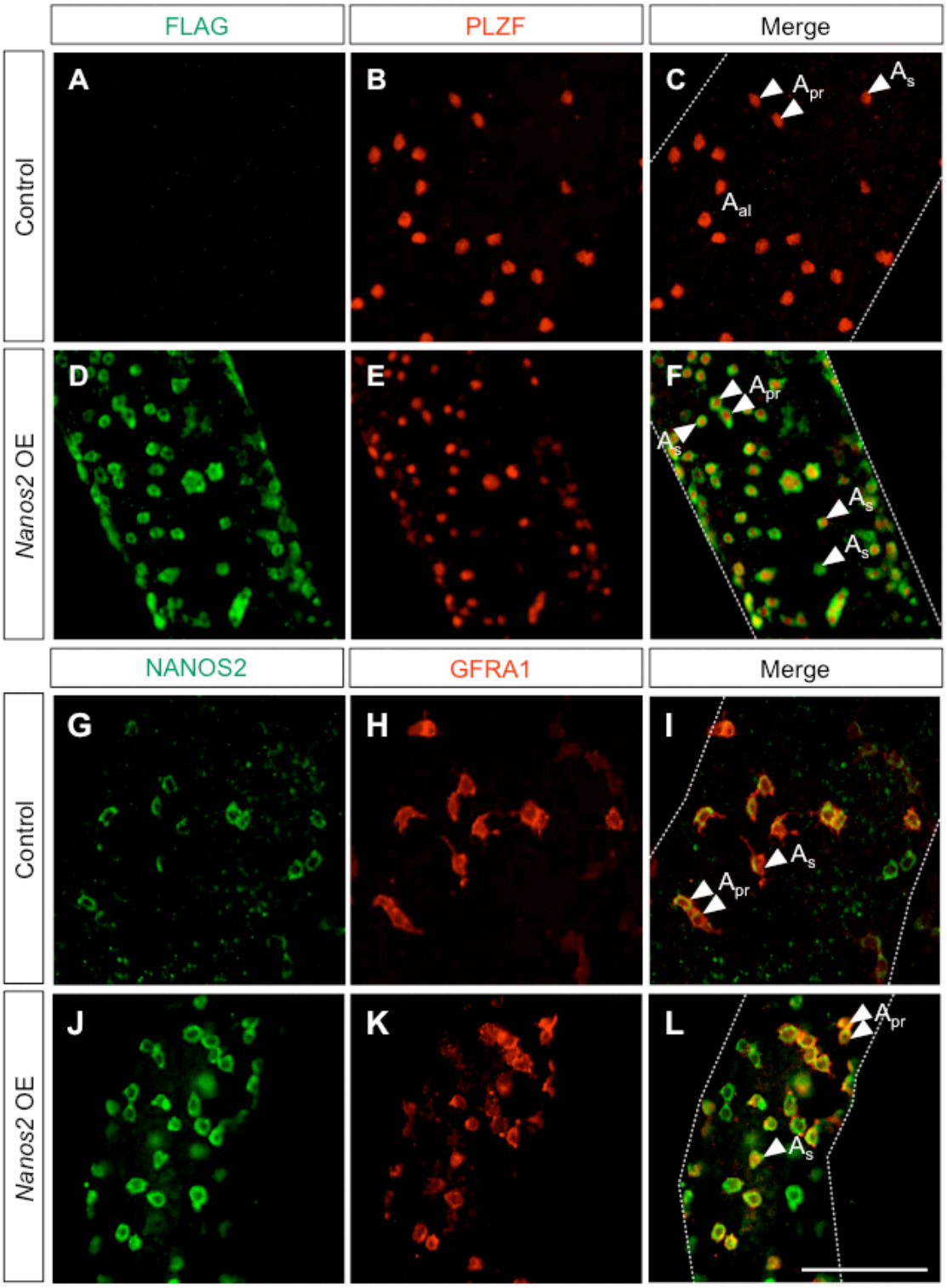

Figure 22. *Nanos2*-overexpressing spermatogonia express PLZF and GFRA1. (**A** to **F**) Whole-mount immunostaining for FLAG-NANOS2 (green) and PLZF (red). PLZF was expressed in undifferentiated spermatogonia in both control and *Nanos2*-overexpressing cells. The dotted lines show outlines of seminiferous tubules. (**G** to **L**) Whole-mount immunostaining with anti-NANOS2 (green) and anti-GFRA1 (red) antibodies. Scale bar, 100 μm.

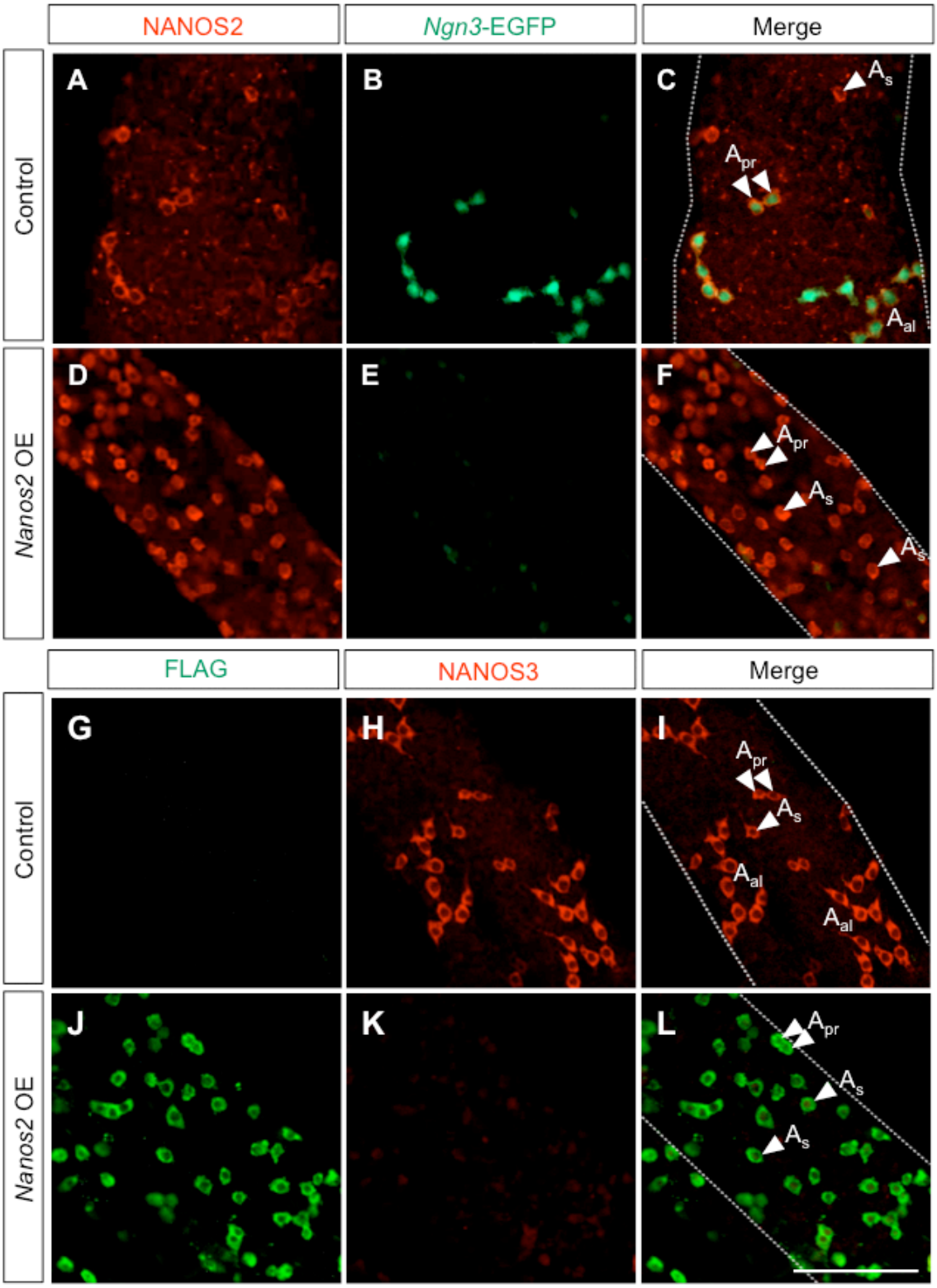

Figure 23. *Ngn3*-EGFP and NANOS3 expression are suppressed by *Nanos2*-overexpression. (**A** to **F**) Double-staining using antibodies for NANOS2 (red) and GFP (green) to detect *Ngn3*-EGFP. The dotted lines show outlines of seminiferous tubules. (**G** to **L**) Whole-mount staining for FLAG-NANOS2 (green) and NANOS3 (red). Scale bar, 100 μm.

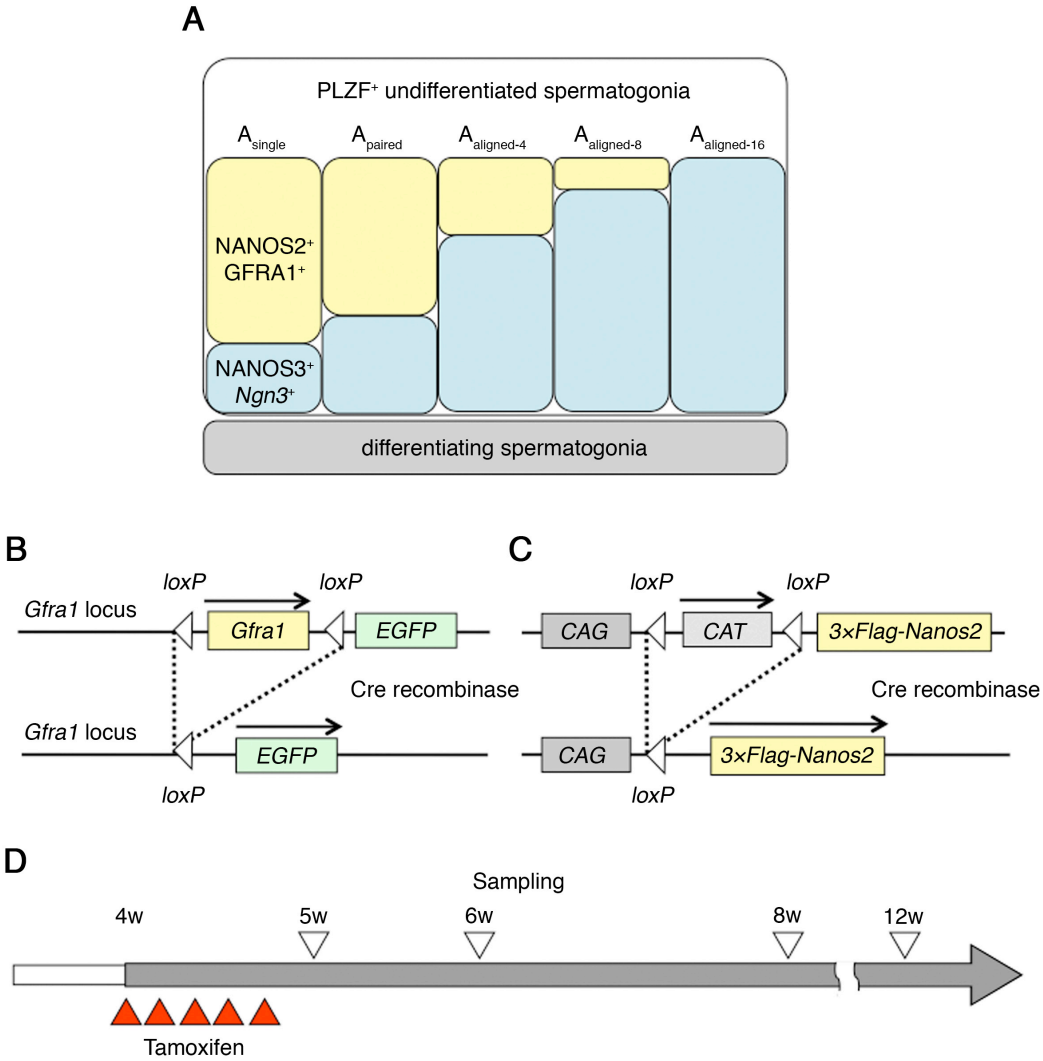

Figure 24. Schematic view of materials and methods used in Chapter 2. (**A**) A schematic drawing of the relationship between the typical morphology and gene expression patterns in PLZF-positive undifferentiated spermatogonia. A_{single} and A_{paired} spermatogonia contain a higher proportion of GFRA1^{+}/NANOS2^{+}, while many of $A_{alinged}$ are NANOS3^{+}/*Ngn3*$^{+}$. The undifferentiated spermatogonia then become differentiating spermatogonia. (**B**) Floxed *Gfra1* allele expresses *Gfra1* cDNA, thereby serving as a functional allele. Activation of Cre recombinase results in a removal of floxed *Gfra1* sequences, simultaneously generating *EGFP* knock-in (*Gfra1* knock-out) allele. (**C**) A conditional transgenic mouse line, *CAG-floxed CAT-3xFlag-Nanos2* (*Tg-Nanos2*) is capable of expressing *Flag tagged-Nanos2* under the control of the ubiquitous *CAG* promoter after excision of the floxed *CAT* gene (an innocent gene) by Cre recombinase. (**D**) The experimental schedule. Cre activity was induced by intraperitoneal injection of TM into 4-week-old mice for 5 consecutive days and the testes were harvested at the indicated time points.

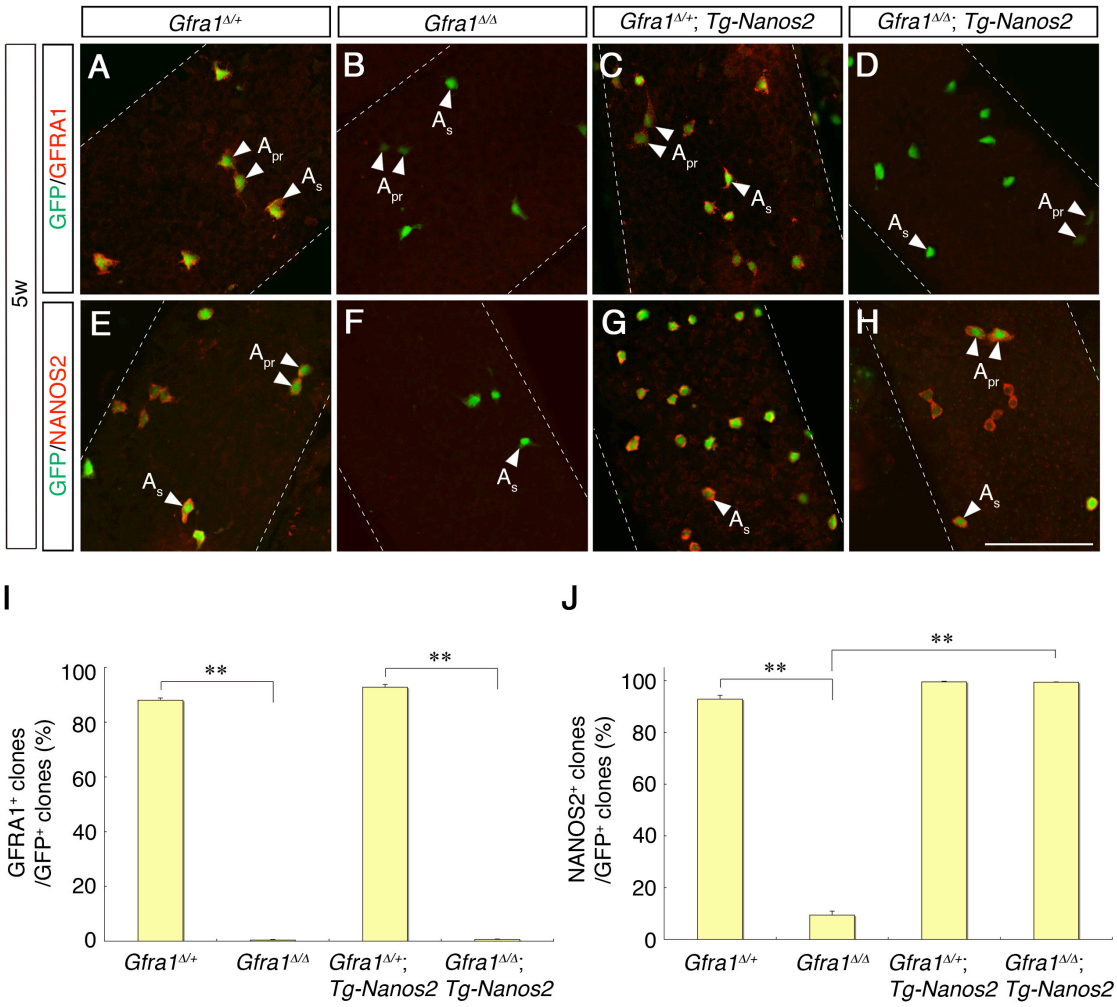

Figure 25. GFRA1 and NANOS2 expression in Δfloxed *Gfra1*-positive spermatogonia. (**A** to **H**) Seminiferous tubules from 5-week-old mice were immunostained with anti-GFP (A to H, green) and anti-GFRA1 (A to D, red) or anti-NANOS2 (E to H, red) antibodies. The dotted lines show outlines of seminiferous tubules. Scale bar, 100 μm. (**I** to **J**) Frequency of GFP-positive spermatogonial clusters (2^n cells: 1, 2, 4, 8, 16) that are either GFRA1-positive (I) or NANOS2-positive (J) were counted (N=3). The mean values are shown with the standard error. **; P<0.01.

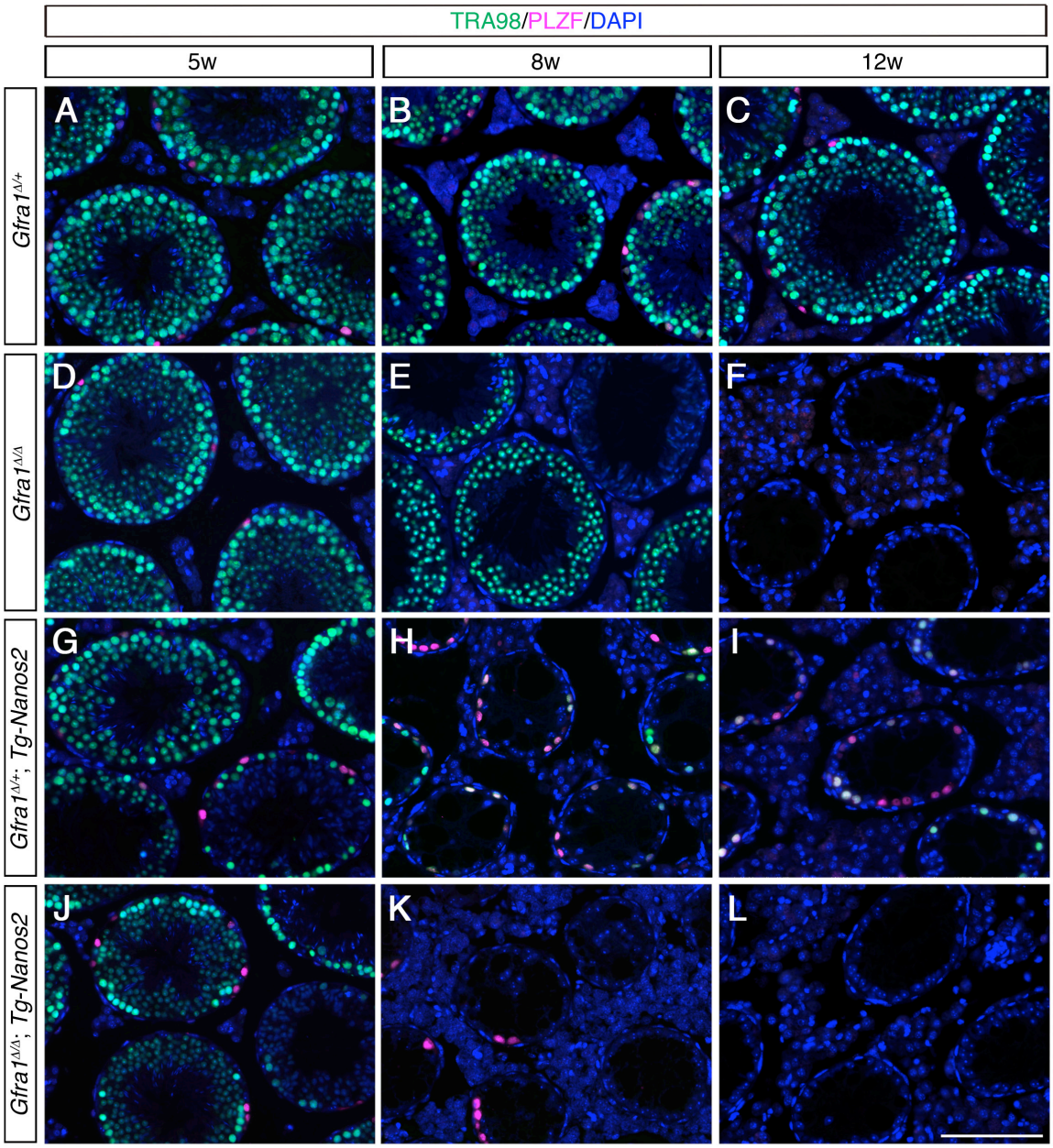

Figure 26. Testicular histology of *Gfra1*-conditional knockout mice with or without overexpressed *Nanos2* transgene. (**A** to **L**) Testes from each mutant were immunostained with TRA98 (green, a marker that is expressed in spermatogonia, spermatocytes and round spermatids) and anti-PLZF (magenta, a marker of undifferentiated spermatogonia) antibodies. Nuclear DNA was counterstained with DAPI (blue). Scale bar, 100 μm.

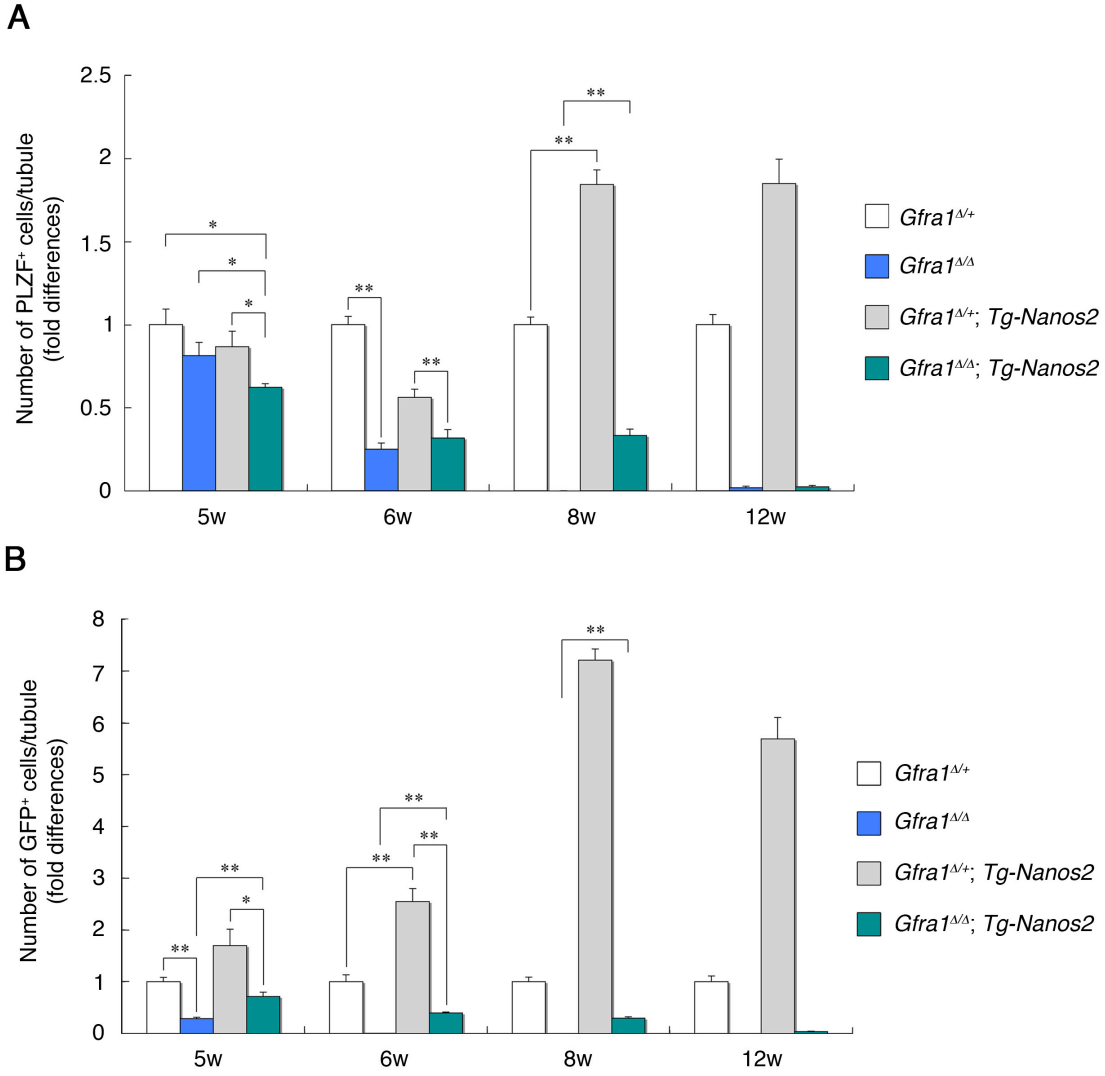

Figure 27. Temporal changes in the number of spermatogonia in each mutant. (**A** and **B**) The numbers of PLZF-positive (A) or GFP-positive (B) cells per seminiferous tubule were counted at the indicated time points. In each genotype, all tubules in two independent testis-cross sections were scored ($N \geqq 3$). The average numbers were normalized using the control of each stage (white bars). Error bars represent the standard error. **; $P<0.01$ and *; $P<0.05$.

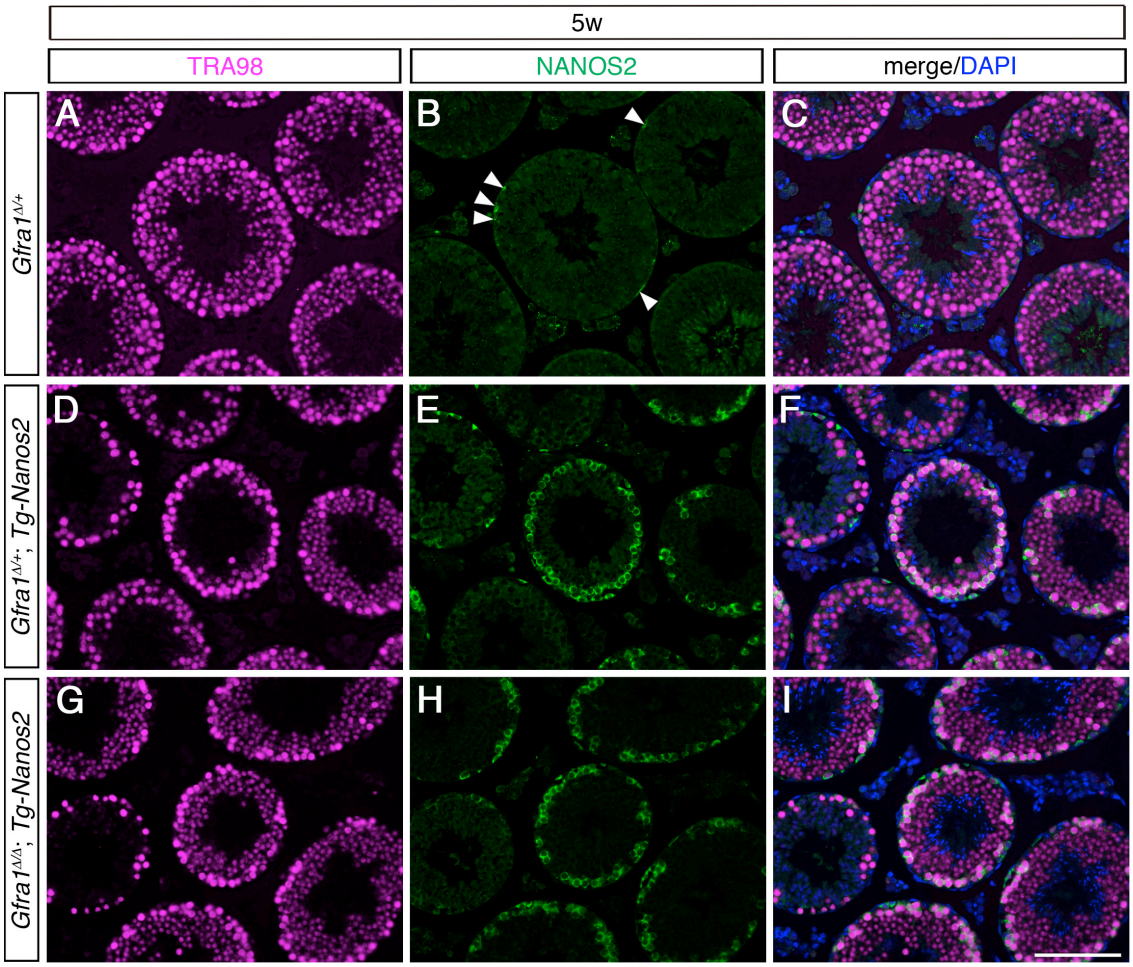

Figure 28. Successful induction of *Nanos2*-overexpression by *Ert2-Cre*. (**A** to **I**) Testes were immunostained with TRA98 (magenta) and anti-NANOS2 (green) antibody. Nuclear DNA was labeled with DAPI (blue). In control *Gfra1*$^{\Delta/+}$ mice, NANOS2 was expressed in a small subset of spermatogonia (arrowheads). In *Gfra1*$^{\Delta/+}$; *Tg-Nanos2* or *Gfra1*$^{\Delta/\Delta}$; *Tg-Nanos2* mice, strong NANOS2 signal were detected in early germ cells located on the basal side of seminiferous tubules. Scale bar, 100 μm.

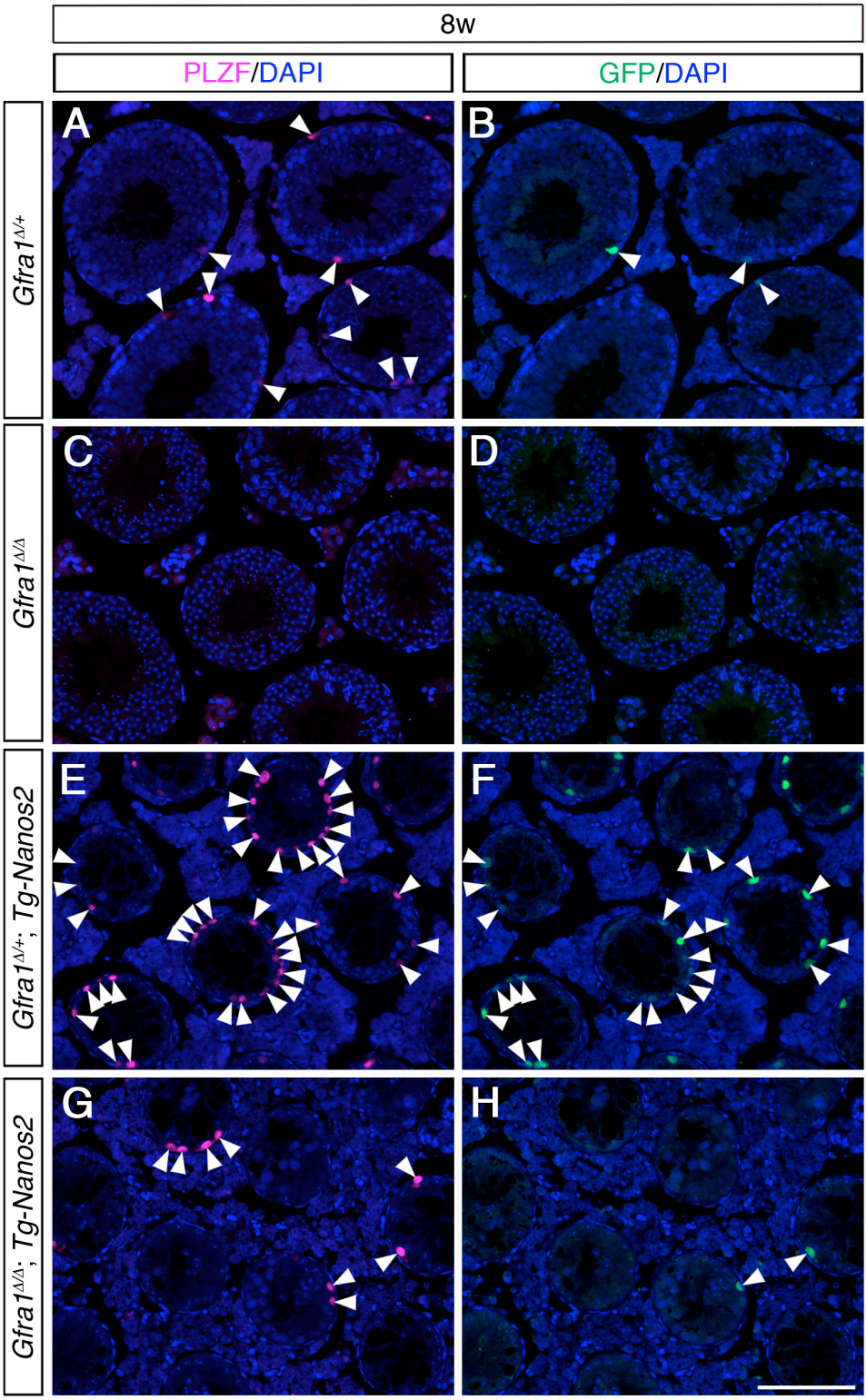

Figure 29. Partial rescue of *Gfra1*-conditional knockout phenotype by overexpressed *Nanos2*. (**A** to **H**) Eight-week-old testes were stained for PLZF (magenta), GFP (green) and DAPI (blue). PLZF- or GFP- positive spermatogonia are indicated by arrowheads. At 8-weeks, both PLZF- and GFP- positive spermatogonia were observed in *Gfra1*$^{\Delta/\Delta}$; *Tg-Nanos2* mice but not in *Gfra1*$^{\Delta/\Delta}$ mice. Scale bar, 100 μm.

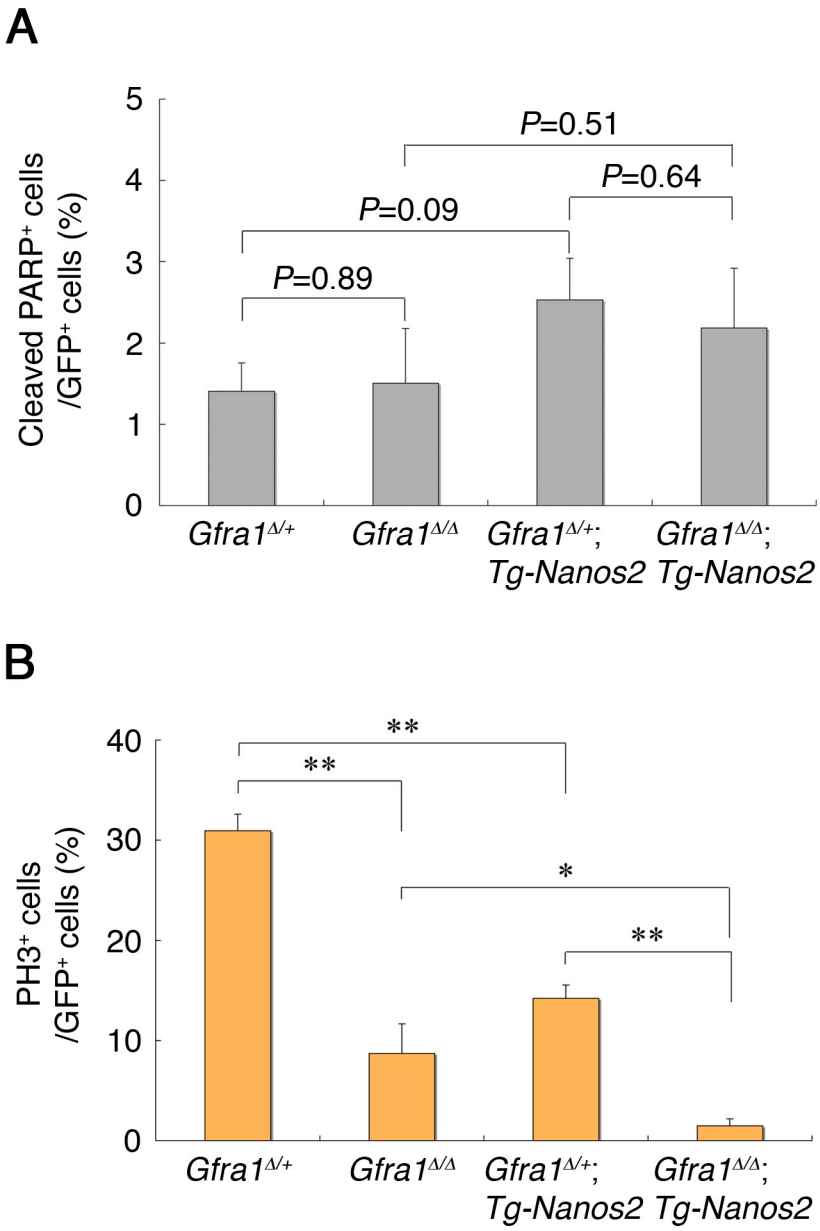

Figure 30. Quantification of proliferation and apoptotic cell death in each mutant. (**A**) The number of cleaved PARP-positive cells was scored per GFP-positive cells in 5-week-old mice. PARP (poly [ADP-ribose] polymerase) is one of the main targets of CASPASE-3, therefore the PARP cleavage serves as a marker of cells undergoing apoptosis. (**B**) Quantification of proliferative spermatogonia in 5-week-old mice. The number of PH3-positive cells was scored per GFP-positive cells. In each genotype, all tubules in two independent testis-cross sections were scored ($N \geqq 5$). The mean values are shown with the standard error. **; $P<0.01$ and *; $P<0.05$.

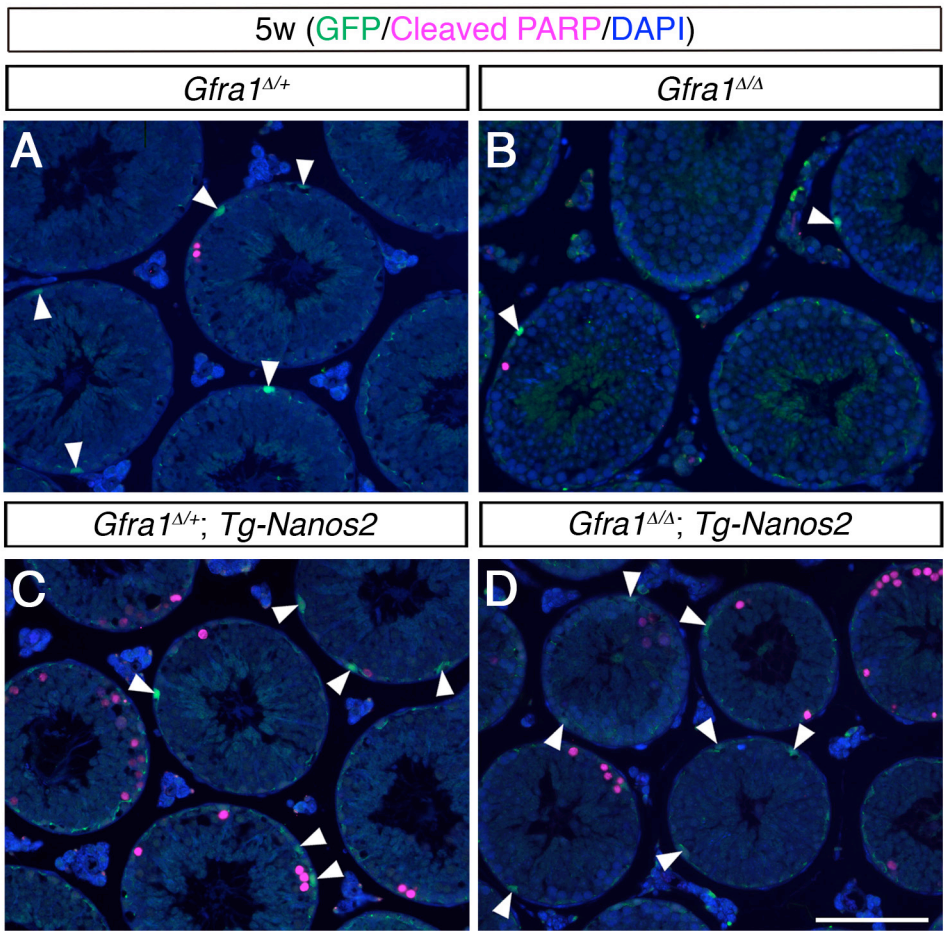

Figure 31. Apoptotic cell death in each mutant. (**A** to **D**) The representative images of double immunostaining with anti-GFP (green) and anti-cleaved PARP (magenta) antibodies at 5 weeks. Nuclear DNA was labeled with DAPI (blue). Arrowheads indicate GFP-positive cells. Many apoptotic signals were observed in *Nanos2*-overexpressing testes, but most of them were GFP-negative. Scale bar, 100 μm.

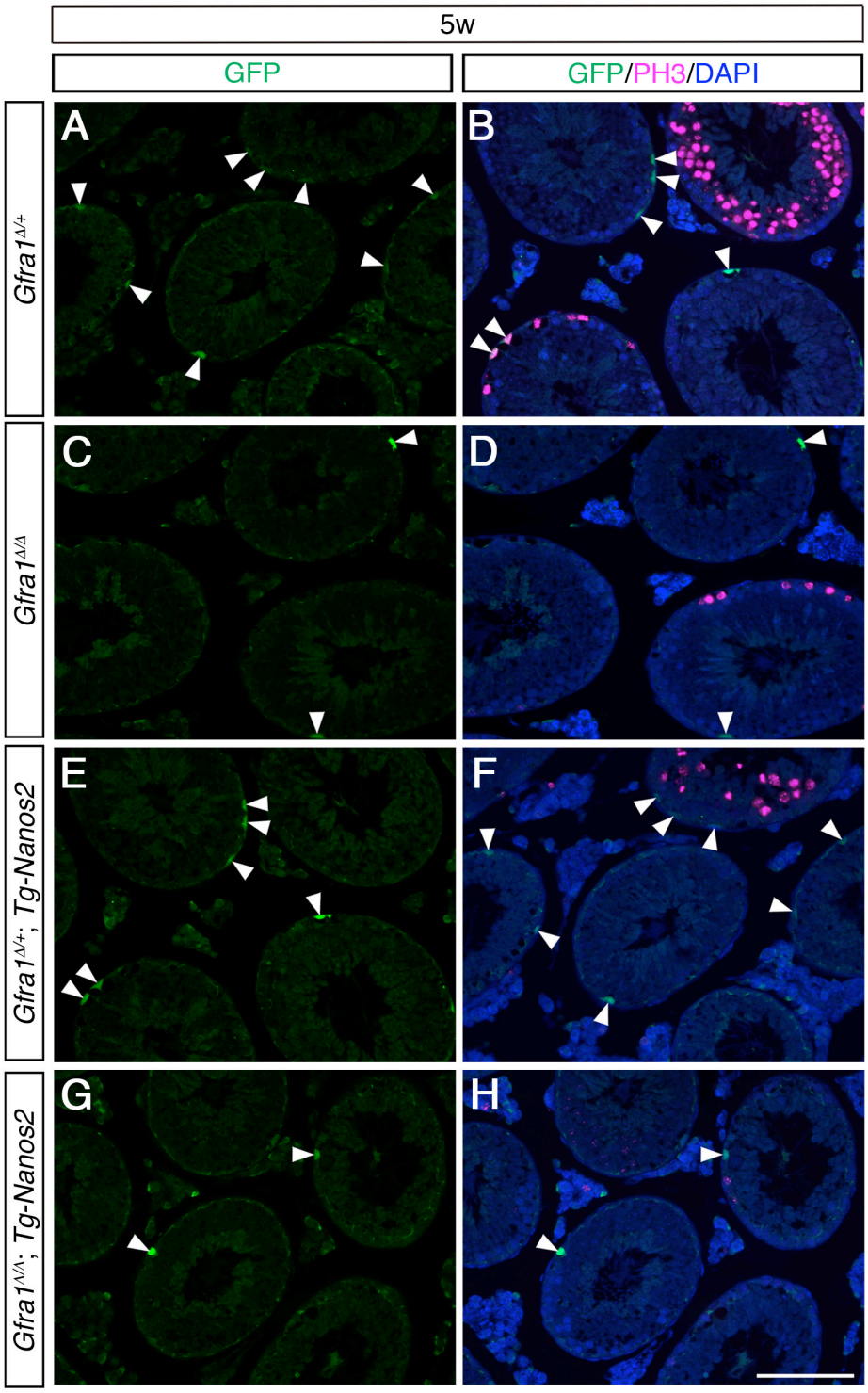

Figure 32. Detection of cell proliferation in *Gfra1*-conditional knockout and *Nanos2*-overexpressing cells. (**A** to **L**) Five-week-old testes from each genotype were immunostained with anti-GFP (green) and anti-PH3 (magenta) antibodies. Nuclear DNA was labeled with DAPI (blue). GFP-positive spermatogonia are indicated by arrowheads. Proliferation of GFP-positive cells was decreased by *Gfra1*-deficiency and by *Nanos2*-overexpression. Scale bar, 100 μm.

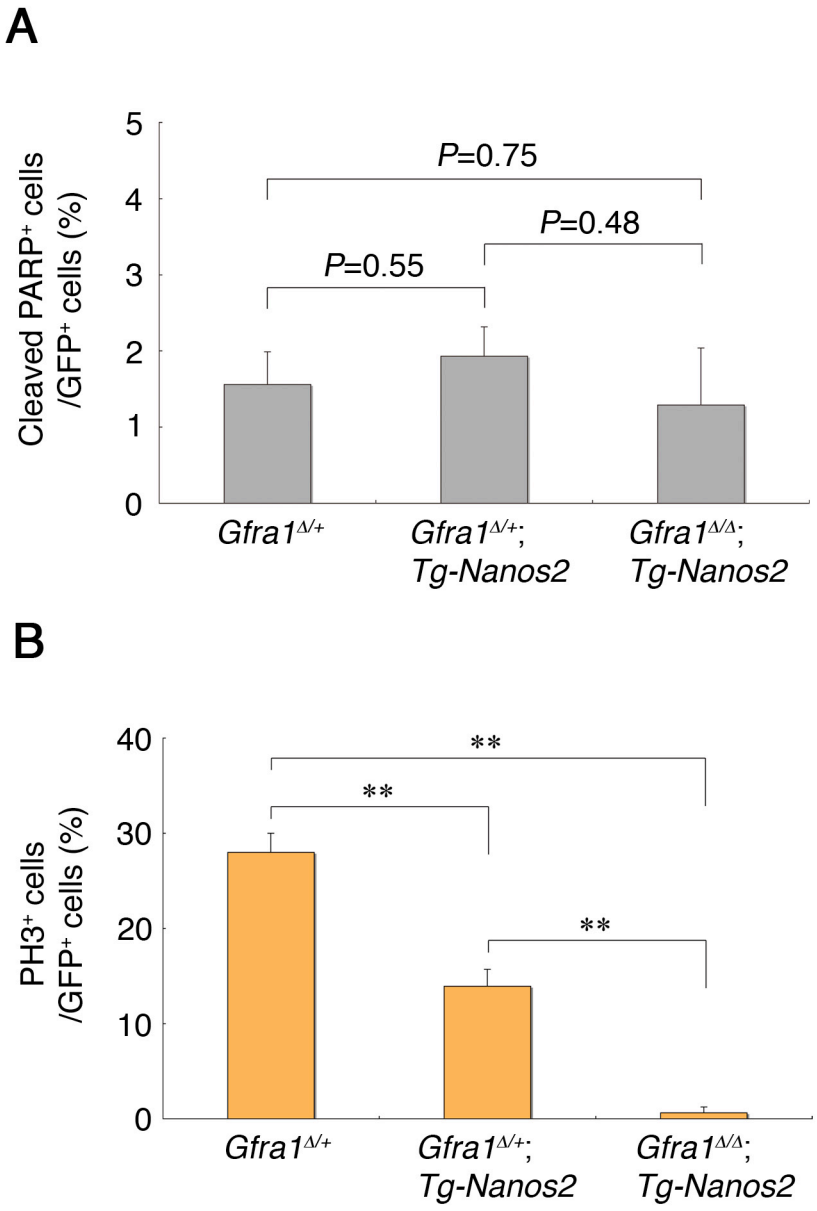

Figure 33. Quantification of proliferation and apoptotic cell death at 8-weeks of age. (**A** and **B**) The number of cleaved PARP-positive, apoptotic cells (A) or PH3-positive proliferative cells (B) was scored per GFP-positive cells in 8-week-old mice. Because *Gfra1*$^{\Delta/\Delta}$ mice have already lost GFP-positive spermatogonia by 8-weeks, I couldn't use this genotype for the experiment. In each genotype, all tubules in two independent testis-cross sections were scored ($N \geqq 4$). The mean values are shown with the standard error. **; $P<0.01$.

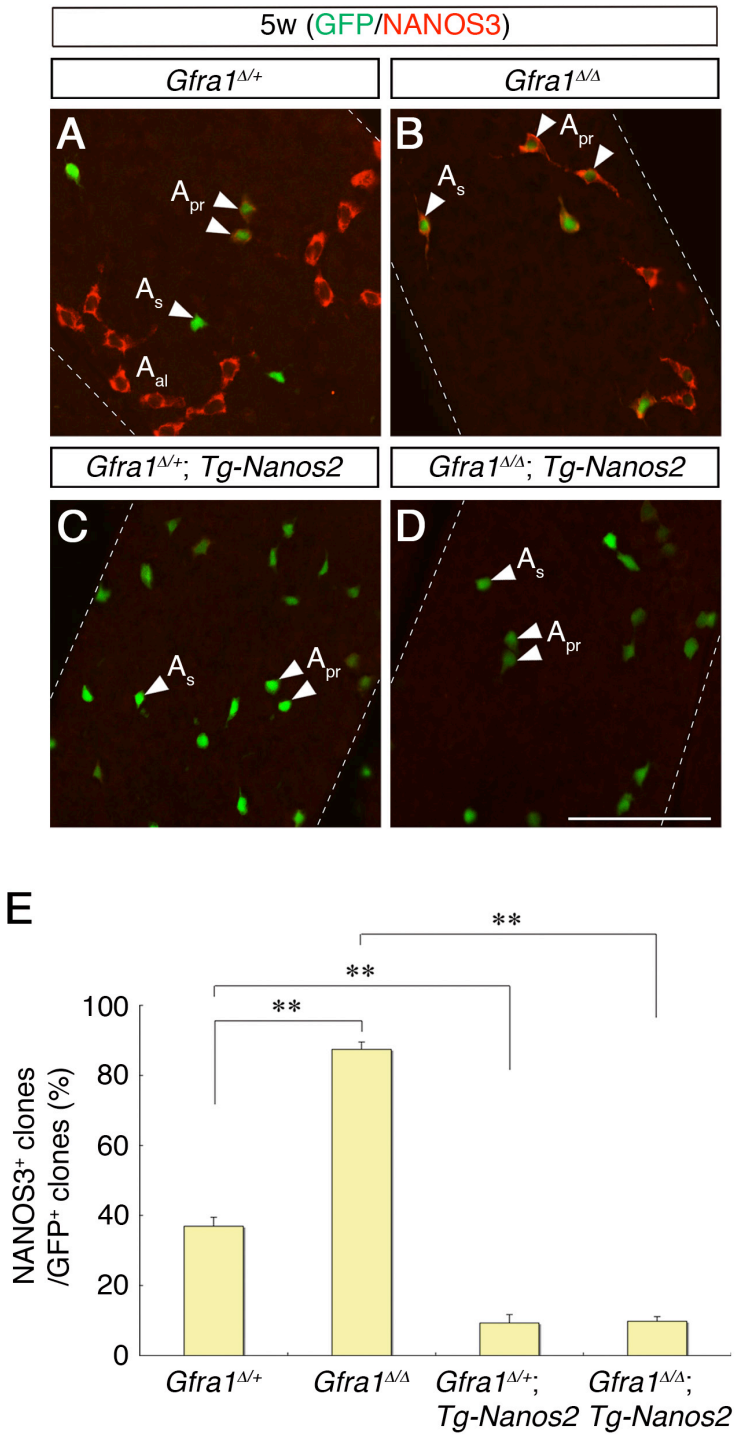

Figure 34. Forced expression of *Nanos2* in *Gfra1*-knockout spermatogonia suppresses their differentiation. (**A** to **D**) Seminiferous tubules from 5-week-old mice were immunostained with anti-GFP (green) and anti-NANOS3 (red) antibodies. The dotted lines show outlines of seminiferous tubules. Scale bar, 100 μm. (**E**) Frequency of NANOS3-positive spermatogonial clusters (2^n cells: 1, 2, 4, 8, 16) in GFP-positive cells was counted by using the stained tubules (N=3). The mean values are shown with the standard error. **; P<0.01.

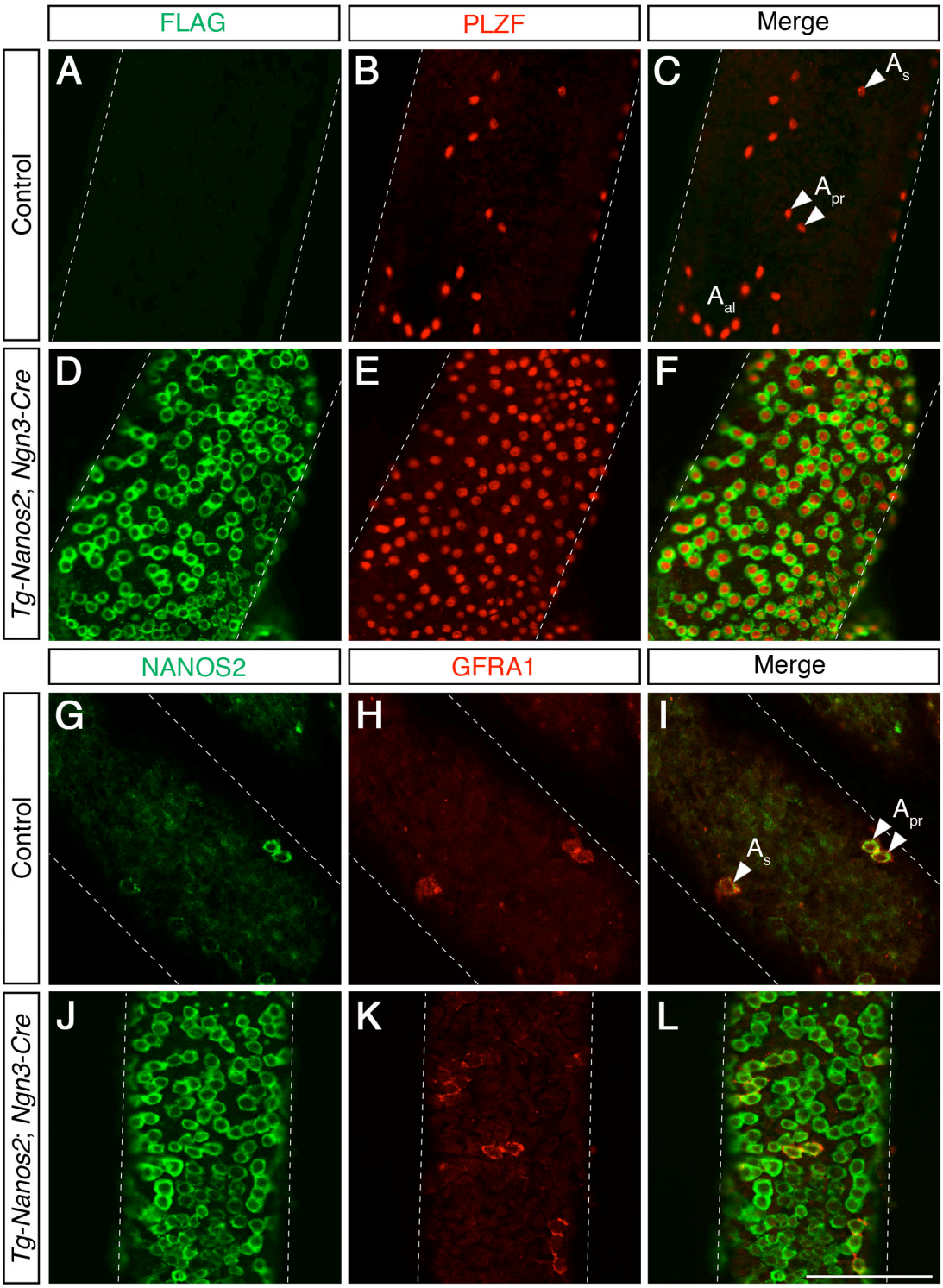

Figure 35. Successful induction of *Nanos2*-overexpression in GFRA1-negative spermatogonia. (**A** to **L**) Six-week-old testes were immunostained with anti-FLAG (green) and anti-PLZF (red) antibodies (A-F); and anti-NANOS2 (green) and anti-GFRA1 (red) antibodies (G-L). The transgene-derived *Nanos2*-overexpression was detected by staining with either anti-FLAG or anti- endogenous NANOS2 antibodies. The dotted lines show outlines of seminiferous tubules. Scale bar, 100 μm.

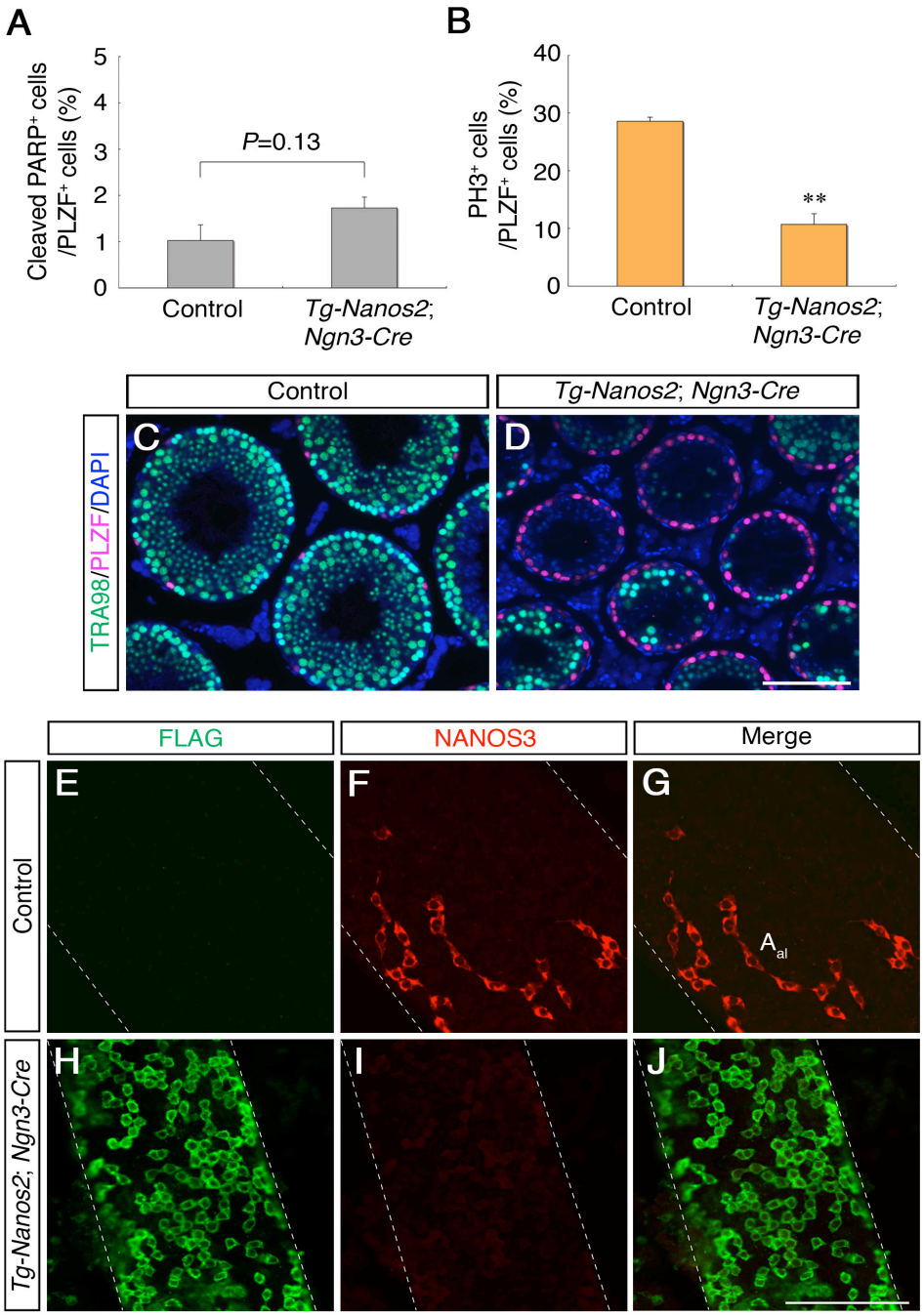

Figure 36. Characterization of *Nanos2*-overexpressing spermatogonia induced by *Ngn3-Cre*. (**A** and **B**) Quantification of apoptotic (A) and proliferative (B) spermatogonia in 6-week-old mice. The number of cleaved PARP- and PH3- positive cells were scored per number of PLZF-positive cells, respectively ($N \geqq 3$). The mean values are shown with the standard error. **; $P<0.01$. (**C** and **D**) Six-week-old testes were stained with TRA98 (green) and anti-PLZF (magenta) antibodies. Nuclear DNA was counterstained with DAPI (blue). (**E** to **J**) Six-week-old testes were immunostained with anti-FLAG (green) and anti-NANOS3 (red) antibodies. The dotted lines show outlines of seminiferous tubules. Scale bars, 100 μm.

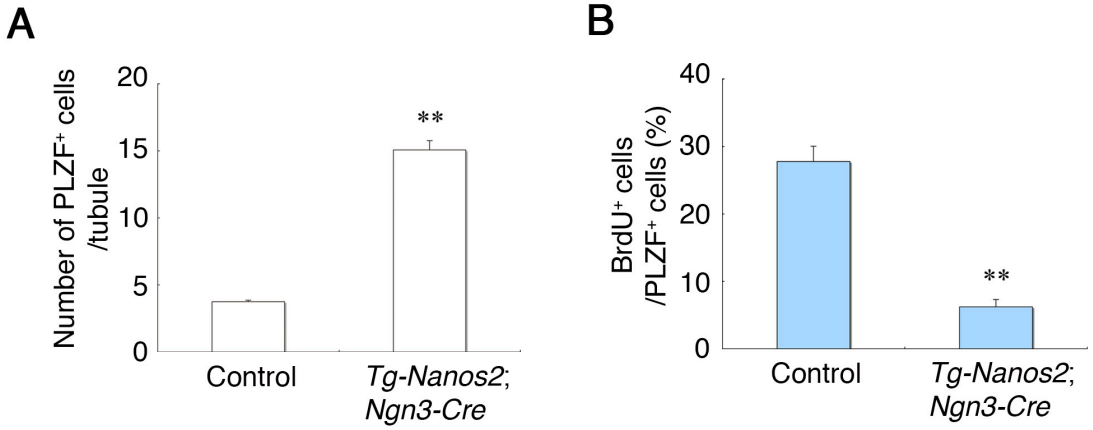

Figure 37. Characterization of *Nanos2*-overexpressing spermatogonia induced by *Ngn3-Cre*. (**A**) Calculation of PLZF-positive cells per seminiferous tubule in 6-week-old mice ($N \geqq 3$). *Nanos2*-overexpression caused a significant increase of PLZF-positive spermatogonia. (**B**) Quantification of proliferative spermatogonia in 6-week-old mice. I examined the number of cells in the S phase of the cell cycle by counting the number that incorporated bromodeoxyuridine (BrdU) after a pulse label ($N \geqq 3$) (see Supplemental Materials and Methods). Consistent with the case of PH3, significantly fewer GFP-positive cells incorporated BrdU in the *Nanos2*-overexpressing spermatogonia than control spermatogonia. The mean values are shown with the standard error. **; $P<0.01$.

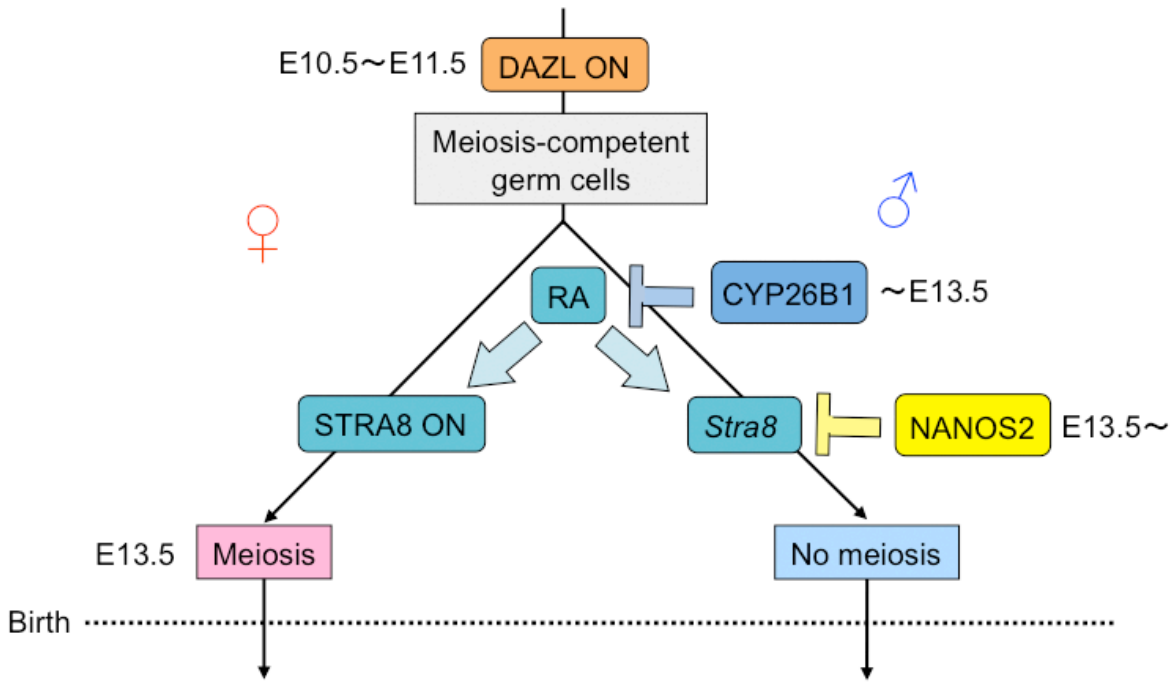

Figure 38. Possible relationship between NANOS2 and RA signaling. Developmental pathways involved in the sexual differentiation of germ cells. A proposed path by which PGCs acquire meiotic competence (in both female and male embryos) and subsequently initiate meiosis (in females) or does not (in males). The difference of RA level between sexes is consequences of differential expression of RA-inactivating enzyme CYP26B1 in embryonic ovaries and testes. NANOS2 begins to be expressed from E13.5 when CYP26B1 is down-regulated, and as a result, *Stra8* is suppressed in male germ cells.

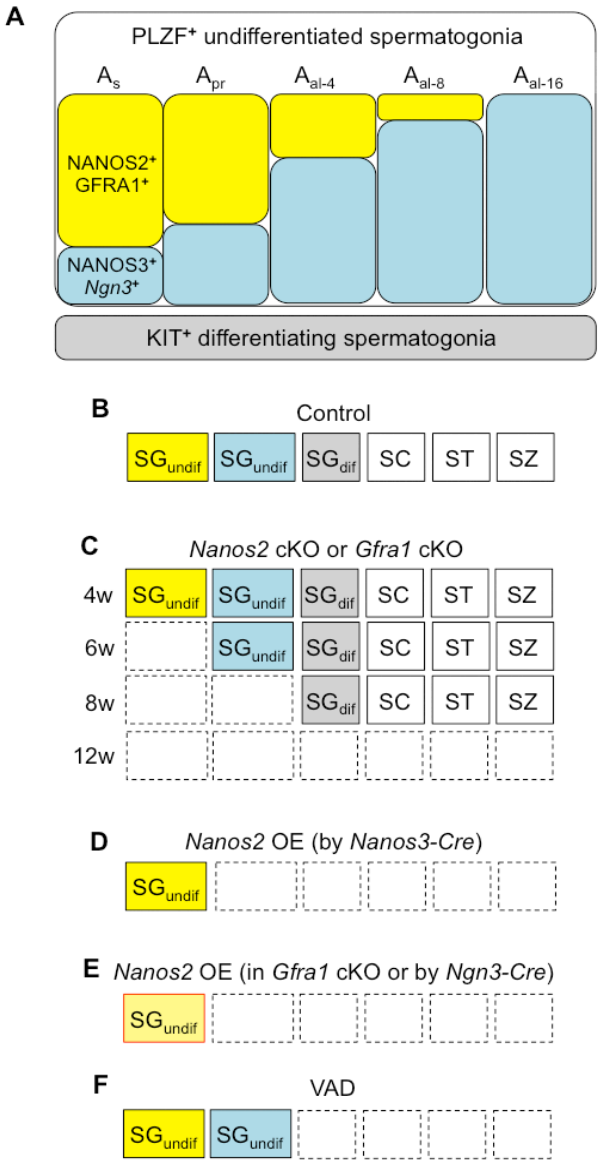

Figure 39. Summary of results. (**A**) A schematic view of the relationship between the typical morphology and gene expression patterns observed in each group of undifferentiated spermatogonia shown in (Fig. 2A). (**B** to **F**) The schematic view of the observed spermatogenic cell types in control or each mutant. *Nanos2*-cKO or *Gfra1*-cKO mice could not maintain spermatogenesis due to a loss of the NANOS2^{+}/GFRA^{+} spermatogonia and a subsequent loss of all types of germ cells (C). Whereas, *Nanos2*-overexpression by *Nanos3-Cre* resulted in the accumulation of the undifferentiated spermatogonia, which are positive for GFRA1 but not NANOS3 or *Ngn3* (D). Without GFRA1 expression, overexpressed *Nanos2* may block the initial steps of spermatogonial differentiation, since it suppresses NANOS3 expression (E). VAD phenotype is not identical to that of *Nanos2*-overexpressing mice (F). Each box indicates $SG_{undif,}$ two distinct subpopulations of undifferentiated spermatogonia shown in (A); SG_{dif}, differentiating spermatogonia; SC, spermatocytes; ST, spermatids; and SZ, spermatozoa.